

# LOW LUMINOSITY COMPANIONS TO WHITE DWARFS

J. Farihi<sup>1,2</sup>, E. E. Becklin<sup>2</sup>, & B. Zuckerman<sup>2</sup>

jfarihi@gemini.edu, becklin@astro.ucla.edu, ben@astro.ucla.edu

## ABSTRACT

This paper presents results of a near-infrared imaging survey for low mass stellar and substellar companions to white dwarfs. A wide field proper motion survey of 261 white dwarfs was capable of directly detecting companions at orbital separations between  $\sim 100$  and 5000 AU with masses as low as  $0.05 M_{\odot}$ , while a deep near field search of 86 white dwarfs was capable of directly detecting companions at separations between  $\sim 50$  and 1100 AU with masses as low as  $0.02 M_{\odot}$ . Additionally, all white dwarf targets were examined for near-infrared excess emission, a technique capable of detecting companions at arbitrarily close separations down to masses of  $0.05 M_{\odot}$ .

No brown dwarf candidates were detected, which implies a brown dwarf companion fraction of  $< 0.5\%$  for white dwarfs. In contrast, the stellar companion fraction of white dwarfs as measured by this survey is 22%, uncorrected for bias. Moreover, most of the known and suspected stellar companions to white dwarfs are low mass stars whose masses are only slightly greater than the masses of brown dwarfs. Twenty previously unknown stellar companions were detected, five of which are confirmed or likely white dwarfs themselves, while fifteen are confirmed or likely low mass stars.

Similar to the distribution of cool field dwarfs as a function of spectral type, the number of cool unevolved dwarf companions peaks at mid-M type. Based on the present work, relative to this peak, field L dwarfs appear to be roughly 2 – 3 times more abundant than companion L dwarfs. Additionally, there is no evidence that the initial companion masses have been altered by post main sequence binary interactions

*Subject headings:* binaries: general — stars: fundamental parameters — stars: low-mass, brown dwarfs — stars: luminosity function, mass function — stars: formation — stars: evolution — white dwarfs

## 1. INTRODUCTION

Until a decade ago and despite many searches, scientists had no definite evidence of astrophysical objects with masses between those of stars and planets. Yet the missing link

---

<sup>1</sup>Gemini Observatory, Northern Operations, 670 North A’ohoku Place, Hilo, HI 96720

<sup>2</sup>Department of Physics & Astronomy, University of California, 430 Portola Plaza, Los Angeles, CA 90095

between these two, dubbed brown dwarfs, are now a field of study unto themselves. There remains much to learn about these failed stars, especially their astrophysical niches, origins and destinies.

Searching for brown dwarfs as companions to stars offers the opportunity to search systems very near to the Sun and requires less time than field and cluster searches covering a relatively large portion of the sky. The very first serious brown dwarf candidate was discovered as a companion to the white dwarf GD 165 (Becklin & Zuckerman 1988). GD 165B ( $M \sim 0.072 M_{\odot}$ ,  $T_{\text{eff}} = 1900$  K) remained unique for a number of years but eventually became the prototype for a new spectral class of cool stars and brown dwarfs, the L dwarfs (Kirkpatrick et al. 1999a,b). The first unambiguous brown dwarf was also discovered as a companion to a star, Gl 229 (Nakajima et al. 1995). Gl 229B ( $M \sim 0.040 M_{\odot}$ ,  $T_{\text{eff}} = 950$  K) became the prototype T dwarf (Marley et al. 1996; Kirkpatrick et al. 1999b), the coolest known spectral class, all of whose members are brown dwarfs.

Precision radial velocity techniques are sensitive to brown dwarfs orbiting within  $\sim 5$  AU but have revealed very few. Butler et al. (2000) estimate the brown dwarf companion frequency to be less than 0.5%. This figure includes the search of several hundred stars and is thus a very good measure for the innermost orbital separations.

Direct imaging searches have also produced a dearth of brown dwarf companions to main sequence stars (relative to stellar companions) at wider separations (Zuckerman & Becklin 1987a, 1992; Henry & McCarthy 1990; Nakajima et al. 1994; Oppenheimer et al. 2001; Schroeder et al. 2000; Hinz et al. 2002; McCarthy & Zuckerman 2004; Farihi 2004b). The separation range corresponding to the peak in the stellar companion distribution for both G and M dwarf primaries is roughly 10 – 100 AU (Duquennoy & Mayor 1991; Fischer & Marcy 1992). This range and beyond has been searched quite extensively by the aforementioned surveys and very few brown dwarfs have been found. The most optimistic estimate for the brown dwarf companion frequency to main sequence stars is a few percent (Lowrance 2001), although most studies conclude that it is less than 1%. The only exception being the case when the primary star is a very low mass star or brown dwarf ( $M \lesssim 0.10 M_{\odot}$ ). For these low mass primaries, the binary fraction is estimated to be  $\sim 20\%$  (Reid et al. 2001; Close et al. 2002; Siegler et al. 2003; Burgasser et al. 2003). Thus it appears that the brown dwarf companion frequency is a strong function of primary mass (Farihi 2004b).

This paper presents the details on 371 white dwarfs which were searched for low luminosity companions using near-infrared imaging arrays at several telescopes over the past 18 years. The particular techniques and analyses used for each camera data are described along with follow up observations. The white dwarf sample is analyzed from a kinematical perspective in order to make an overall age assessment – critical for any calculation of completeness as a function of secondary mass. The measured distribution of low mass companions is presented as a function of spectral type, which is then transformed into mass using existing empirical and theoretical relations. The implications for binary star formation and evolution are discussed.

Within this supplement is a summary of all available data on known companions to the 371 white dwarfs in the sample. Specifically included in this paper are new data and analysis of companions to white dwarfs previously reported in Zuckerman & Becklin (1992) and Schultz et al. (1996). Tables include proper motions,  $UVW$  space velocities, spectral types, and distances for the white dwarf primaries. Data on previously known or newly discovered companions (including candidates) includes optical and near-infrared photometry, low resolution optical spectra, and proper motion measurements.

## 2. THE SEARCH

### 2.1. The Steward Survey

The core of this work was analysis of images obtained at Steward Observatory. Beginning in 1991 and continuing through 2003, a program to image nearby white dwarfs in the near-infrared was conducted on the Bok 2.3 meter telescope at Kitt Peak, Arizona. Images of 273 targets were acquired using the Bok facility near-infrared camera (Rieke et al. 1993). The imaging procedure was to acquire  $J$  band ( $1.2 \mu\text{m}$ ) images in a 5-point dither pattern with 90 seconds integration per dither position for a total exposure time of 7.5 minutes. Each raw science image was dark subtracted, flat fielded, scaled to the central image, registered, shifted and then averaged.

In order to determine the completeness of the Steward Survey, it was necessary to measure the flux of the faintest reliably detectable sources in images taken over the entire length of the study. Figure 1 shows the number of objects detected with signal-to-noise ratio  $(S/N) \geq 3$  as a function of  $J$  magnitude in images representative of each observing run conducted at Steward Observatory. The survey was complete to  $J = 18.0$  mag. It is estimated that 37% of  $J = 18.5$  mag and 57% of  $J = 19.0$  mag objects were missed.

In the last two years of this survey, supplementary data were gathered at Lick Observatory on the Shane 3 meter telescope with the GEMINI camera (McLean et al. 1993). GEMINI sits behind a telescope that is 70% larger than the Bok telescope and employs nearly identical detector technology.  $J$  band data acquired with GEMINI generally went about 1 magnitude deeper, providing greater sensitivity to  $J \sim 19$  mag objects. However, the completeness limit of this survey remains at  $J = 18.0$  mag and all calculations will be restricted to this edge.

The Steward survey was a common proper motion companion search. By imaging the field around a target white dwarf at two epochs separated by a sufficient interval of time, the proper motion of the white dwarf can be measured and compared to any motions exhibited by stars in that field. GEOMAP, a program within the Image Reduction and Analysis Facility (IRAF) was used for this task. This program creates a general transformation between two sets of coordinates corresponding to sources in the same field at two different epochs. Proper motion stars can be identified by their residuals from this map and their motions measured

against the near zero motion of background stars and galaxies, which provide a measure of the standard error.

A typical white dwarf with 5 or more field stars produced a map with a standard deviation in the residuals of approximately 0.2 pixels or  $0.13''$  on the Steward camera. With a typical time baseline of 5 years, proper motions as small as  $0.08'' \text{ yr}^{-1}$  can be measured at the  $3\sigma$  level. These are characteristic values – the actual measurement values and errors depend on the proper motion of a particular white dwarf, the number of field sources with good S/N, the quality of the images at each epoch, and the time baseline between epochs (which varied between 2 and 10 years). Additionally, many proper motions for white dwarf targets and candidate companions were measured using the digitized versions of large sky survey photographic plates, such as the Palomar Observatory Sky Survey I and II. Although the spatial resolution of these scans is lower ( $1.0 - 1.7'' \text{ pixel}^{-1}$ ) than the near-infrared data, the epochs are separated by  $\sim 40$  years and hence provide better measurements and smaller errors.

## 2.2. The Keck Survey

From 1995 to 2001, a program to image nearby white dwarfs at near-infrared wavelengths was conducted on the Keck I 10 meter telescope at Mauna Kea, Hawaii. Images of 91 targets were acquired using NIRC (Matthews & Soifer 1994). These data were not taken in an analogous way to the data collected at Steward. In general, each target was observed at  $J$  and usually one or more of the following bands in order of decreasing usage:  $z$  ( $1.0 \mu\text{m}$ ),  $K$  ( $2.2 \mu\text{m}$ ),  $H$  ( $1.6 \mu\text{m}$ ). A typical total integration time at  $J$  was 60 – 80 seconds times 5 dithers. Data at all wavelengths were reduced in a manner identical to the Steward data.

It is not possible to establish a completeness limit in the same way as for the Steward data (Figure 1) because the relatively small NIRC field of view did not contain sufficient background sources. An analysis was performed on many images representative of each observing run conducted at Keck.  $J$  magnitudes and S/Ns were measured for faint but reliably detected objects in the images. The result being that  $J = 21.0$  mag or brighter objects were consistently detected with  $\text{S/N} > 10$ . Therefore, the NIRC survey is likely complete down to  $J = 21$  mag.

The  $z-J$  and/or  $J-K$  color of point sources in the field of the white dwarf, together with their flux relative to the primary at these wavelengths, were used to filter out uninteresting background stars and discriminate candidate companions. Data were taken at  $z$  &  $J$  for about 75% of the white dwarfs in this survey. For the remainder of the sample, images were obtained at  $K$  for all fields which contained point sources at  $J$ . The  $z - J$  color is the most indicative of low mass stars and brown dwarfs because it is monotonically increasing with decreasing effective temperature, unlike  $J - K$  (Leggett et al. 2002). If a candidate could not be ruled out based on these criteria, then a follow up image was taken at a later epoch in order to perform astrometry and search for common proper motion.

### 2.3. Companion Data & Analysis

For each confirmed or candidate common proper motion companion, optical photometry and spectroscopy, in addition to near-infrared photometry, was performed in order to identify or constrain its temperature and class. Near-infrared *JHK* data were acquired with the same instruments used for the wide field survey, namely the Steward and GEMINI cameras. Images were taken and reduced in a similar manner to the survey observations.

Optical *BVRI* data were obtained at Lick Observatory using the Nickel 1 meter telescope CCD camera. In general, exposures were 1 – 10 minutes depending on conditions and individual target brightness. Images were cleaned of bad pixels in the area of interest, bias subtracted, flat fielded and averaged if there were multiple frames.

Optical spectroscopic data were acquired at Lick Observatory using the Kast dual spectrograph on the Shane 3 meter telescope. The exact setup varied between observing runs but all observations were done at low resolution ( $\sim 500$ ). Additional spectroscopy was performed at Steward Observatory using the Boller & Chivens spectrograph on the Bok 2.3 meter telescope. All optical spectra were reduced using standard IRAF software. The spectral images were bias subtracted, cleaned of bad pixels and cosmic rays, then flat fielded. For each target, two spectra of the sky were extracted, averaged and subtracted from the extracted target spectrum. The resulting spectra were wavelength and flux calibrated by comparison with observed lamp spectra and standard stars. No attempt was made to remove telluric features.

Optical and near-infrared magnitudes and colors were used as the main source of constraints for stellar classification and spectral typing of the discovered companions. Using a circular aperture centered on the target star and an annulus on the surrounding sky, both the flux and S/N were calculated for a range of apertures from one to four full widths at half maximum. The flux measurement was taken at or near the aperture size which produced the largest S/N. In this way the flux of all targets was measured, including photometric standard stars. A fairly large aperture was used for all calibrators, and flux measurements for science targets were corrected to this standard aperture. Optical and near-infrared standard stars were taken from Landolt (1983), Hunt et al. (1998), and Hawarden et al. (2001).

### 2.4. The IRTF Survey

As mentioned in §1, there was a previous phase to the search for substellar companions to white dwarfs that began in late 1986 (Zuckerman & Becklin 1992). Although carried out on several different telescopes and instruments, the majority of those data were obtained at the NASA Infrared Telescope Facility (IRTF). Because some results of the IRTF survey were previously published, the details will not be discussed here. However, those results will be updated below and the white dwarfs surveyed at the IRTF will be included in the overall sample and statistics. Of the over 150 white dwarfs observed during this early phase, 66

were later reobserved at either Keck or Steward Observatory. There were 84 white dwarf targets observed at the IRTF and not elsewhere.

## 2.5. The Search for Near-Infrared Excess

Although data at both  $J$  and  $K$  were taken for about one fourth to one third of the stars surveyed, all 371 white dwarfs in the sample were searched for near-infrared excess emission. A digital finding chart of each white dwarf was overlaid with the 2MASS point source catalog data. The measured  $JHK_s$  values for the the white dwarf were then compared to the model predicted values extrapolated from optical data based on the effective temperature of the star. Stars with excess emission and good S/N at one or more of these near-infrared wavelengths were noted as possible or probable binaries.

# 3. THE SAMPLE

## 3.1. Target Selection

Nearly every target observed for this project can be found in either current or earlier versions of the white dwarf catalog of McCook & Sion (1987, 1999). The catalog is mostly composed of stars selected by one of two criteria: (1) faint proper motion stars or (2) stars with ultraviolet excess. Most of these stars were spectroscopically confirmed to be white dwarfs, but there remains some contamination by nondegenerate stars. Hot subdwarfs, blue horizontal branch stars, BL Lacertae objects, and Population II stars all display one of the characteristics above and can have spectra difficult to differentiate from that of a white dwarf with older photographic techniques.

A sample of nearby hot and massive white dwarfs is ideal to search for substellar companions. Proximity to the Sun is desirable for the ability to partially or totally resolve close companions from the primary star and because flux falls off inversely as the square of the distance. Hot white dwarfs are “recently deceased” and are therefore younger than their cooler counterparts. A typical white dwarf with  $M = 0.6 M_{\odot}$  and  $T_{\text{eff}} = 20,000$  K has been cooling for only 70 Myr (Bergeron et al. 1995b). Most massive white dwarfs ( $M \geq 0.9 M_{\odot}$ ) are thought to descend from main sequence progenitors with masses,  $6 M_{\odot} < M < 8 M_{\odot}$  (Bergeron et al. 1991, 1992; Bragaglia et al. 1995; Weidemann 1987, 1990, 2000; Kalirai et al. 2005). Hence massive white dwarfs have a total age on par with their cooling age because the main sequence lifetime of the progenitor would have been relatively short. Although a large ( $N \sim 100$ ) sample with all three characteristics does not exist, these attributes were guiding principles in selecting stars for the survey.

### 3.2. Kinematics

Proper motion can be an indicator of age relative to the three basic kinematic populations of the Galaxy: young disk ( $\tau \sim 1 - 2$  Gyr), old disk ( $\tau \sim 5 - 10$  Gyr), and halo stars ( $\tau \sim 10 - 15$  Gyr). Ages between  $2 - 5$  Gyr are considered intermediate disk ages. In general, the  $UVW$  space velocities (and perhaps more important, velocity dispersions) of stellar populations increase with increasing age. This is primarily due to gravitational upscattering for disk objects, while the halo is a distinctly separate kinematical group in every sense. Therefore in general, smaller values of  $(U, V, W)$  and  $(\sigma_U, \sigma_V, \sigma_W)$ , for a given kinematical sample, are correlated with younger objects (Wielen 1974; Mihalas & Binney 1981; Leggett 1992; Jahreiß & Wielen 1997; Binney & Merrifield 1998).

Although it is three dimensional space motion that determines kinematic populations and indicates likely membership for an individual star, proper motion is often used as a proxy because the radial velocity ( $v_r$ ) is not known. In addition, it is particularly challenging to measure the radial velocity of white dwarfs due to their wide, pressure broadened line profiles and intrinsic faintness. However, two studies have compared the  $UVW$  space motions of over 100 white dwarfs in wide binaries calculated with and without the assumption  $v_r = 0$  (Silvestri et al. 2001, 2002). Accurate radial velocities obtained from a widely separated main sequence component in each binary yielded two major conclusions: (1) the overall sample kinematics were consistent with the old, metal-poor disk population and (2) the assumption of  $v_r = 0$  did *not* significantly affect the results (Silvestri et al. 2001, 2002). This is an important result because, in the end, the sample of white dwarfs in the present work can only be tied together with kinematics.

Table 1 lists all 395 target stars observed at all facilities beginning in 1990. The first column lists the white dwarf number from McCook & Sion (1987, 1999), except where noted, followed by a name of the star in the second column. The third column lists the spectral type of the white dwarf (McCook & Sion 1987, 1999). The integer value in column three represents the effective temperature index, defined as  $10 \times q_{\text{eff}}$ , where  $q_{\text{eff}} = 5040/T_{\text{eff}}$  (McCook & Sion 1987, 1999). The fourth column lists the distance,  $d$ , in parsecs as determined photometrically, using the best available data in the literature and models, or by trigonometric parallax. The fifth and sixth columns are the proper motion,  $\mu$ , in arcseconds per year, followed by the position angle,  $\theta$ , in degrees. These quantities were taken from the most accurate and reliable source available. In decreasing order these are: the Tycho 2 catalog (Høg et al. 2000), the UCAC catalogs (Zacharias et al. 2000, 2004), the USNO B1.0 catalog (Monet et al. 2003), and the white dwarf catalog of McCook & Sion (1999) and references therein. A few proper motions were measured for this work. The seventh column lists the Galactic  $UVW$  space velocity, corrected for the solar motion  $(U, V, W) = (-9, +12, +7)$  (Wielen 1974; Mihalas & Binney 1981) relative to the local standard of rest (LSR) in  $\text{km s}^{-1}$ . These quantities were calculated from the vector  $(\alpha, \delta, d, \mu, \theta, v_r)$  where  $\alpha$  is the right ascension,  $\delta$  the declination, and  $v_r = 0$  was assumed to provide a uniform treatment of the sample.  $U$  is taken to be positive toward the Galactic anticenter,  $V$  positive in the direction of Galactic rotation, and  $W$  positive toward the North Galactic Pole. The eighth column lists

the facility or facilities at which the white dwarf was observed: S = Steward, K = Keck, I = IRTF.

The Galactic  $UVW$  space motions and statistics for the white dwarf sample was calculated in order to evaluate the most probable range of stellar ages. As stated above, smaller values of  $UVW$  and their dispersions, implying more circular Galactic orbits, correlate with younger stellar populations that have experienced fewer gravitational events since their birth in and around the spiral arms (Mihalas & Binney 1981; Binney & Merrifield 1998). Table 2 contains the kinematical properties calculated for the white dwarf sample. The quantity  $T$  is the total space velocity with respect to the LSR ( $T^2 = U^2 + V^2 + W^2$ ), and  $\sigma_T$  is the total dispersion in space velocity ( $\sigma_T^2 = \sigma_U^2 + \sigma_V^2 + \sigma_W^2$ ). The sample does not appear to consist primarily of old, metal-poor disk stars. It seems likely that the sample contains a relatively high fraction of stars with intermediate and young disk kinematics – stars with ages  $\tau \lesssim 5$  Gyr.

In Figure 2, the white dwarf sample is plotted in the  $UV$  and  $WV$  planes. Also shown in the figure are the 1 and 2  $\sigma$  velocity ellipsoids for old, metal-poor disk stars from Beers et al. (2000) – a kinematical study of the halo and thick disk utilizing a large sample of nonkinematically selected metal-poor stars. The ellipsoid parameters in Figure 2 were taken from the first row of Table 1 in Beers et al. (2000), 141 stars with  $-0.6 \leq [\text{Fe}/\text{H}] \leq -0.8$  and  $|Z| < 1$  kpc.  $Z$  is the scale height above the Galactic plane, and hence this old disk sample is unlikely to be contaminated significantly by halo stars. The ellipsoids are centered at  $(U, V, W) = (0, -35, 0)$  km s $^{-1}$  with axes  $(\sigma_U, \sigma_V, \sigma_W) = (50, 56, 34)$  km s $^{-1}$ . From Figure 2 and Table 2 it is clear that the white dwarf sample is centered much closer to  $(U, V, W) = (0, 0, 0)$ , values that represent the undisturbed circular Galactic disk orbits of younger stars (Mihalas & Binney 1981; Binney & Merrifield 1998). Older disk stars lag behind the Galactic rotation of the LSR and hence have increasingly negative  $V$  velocities with increasing age (Beers et al. 2000).

Comparison of the values in Table 2 with the values for kinematical populations of known ages from *Hipparcos* measurements of nearby stars, yields additional evidence that the white dwarf sample contains young disk stars. The average  $UVW$ , their dispersions, and the total velocity dispersion ( $\sigma_T$ ) values of the entire sample are consistent with those of disk stars of intermediate age ( $\tau = 2 - 5$  Gyr), but inconsistent with stars of age  $\tau = 5$  Gyr due to the relatively small negative value of  $\langle V \rangle$ . This comes from a direct comparison of Table 2 with Table 5 & Figures 3 – 5 of Wielen (1974), and with Table 4 of Jahreiß & Wielen (1997). In fact, the subsample in Table 2, white dwarfs with  $\mu < 0.50''$  yr $^{-1}$ , is quite consistent with stars of age  $\tau \sim 2$  Gyr (Wielen 1974; Jahreiß & Wielen 1997).

The white dwarfs surveyed in this work are not similar to the white dwarf samples of Silvestri et al. (2001) and Silvestri et al. (2002), which clearly belong to the old disk kinematical population ( $\tau \sim 5 - 10$  Gyr). Neither is the sample similar to any of the white dwarf kinematic subgroups in Sion et al. (1988) with the exception of the DH and DP stars (magnetic white dwarfs). The sample of magnetic white dwarfs in Sion et al. (1988) was expanded from only 13 stars to 26 stars in Anselowitz et al. (1999) with the same results



(both studies assumed  $v_r = 0$  as in this work) – these stars appear to have young disk kinematics. In fact, the subsample of moderate proper motion white dwarfs in Table 2 have nearly identical kinematical properties as magnetic white dwarfs, implying relatively young ages ( $\tau \sim 2$  Gyr) (Sion et al. 1988; Anselowitz et al. 1999).

### 3.3. Cooling & Overall Age

It must be kept in mind that the present sample consists of a mixture of hot and cool degenerate stars. The cooling age of a typical hot white dwarf ( $T_{\text{eff}} > 11,000$  K) is less than 500 Myr but the main sequence progenitor age is not known. Hence the total ages of hot white dwarfs in the sample are potentially consistent with relatively young disk objects. But for cool white dwarfs in the sample, it is more likely that they are intermediate age disk stars. For example, a white dwarf with  $T_{\text{eff}} < 7500$  K is at least 1.5 Gyr old according to cooling theory (Bergeron et al. 1995b).

In Figure 3 is plotted the number of white dwarfs in the sample versus effective temperature index. Exactly 90% of the sample stars have temperatures above 8000 K – implying cooling ages less than 1.1 Gyr for typical hydrogen atmosphere white dwarfs (Bergeron et al. 1995b). Moreover, 67% of the sample have temperatures above 11,500 K and typical cooling ages less than 0.4 Gyr. Hence the cooling ages of the sample stars are consistent with the total age estimate inferred from kinematics – that of a relatively young disk population.

Since one does not know the main sequence progenitor ages for the white dwarf sample, caution must be taken not to over interpret the kinematical results. In principle, any individual star of any age can have any velocity. It is possible to estimate total ages for white dwarfs if their mass is known by using the initial to final mass relation (Weidemann 1987, 1990, 2000; Bragaglia et al. 1995). However, this is only feasible for DA white dwarfs (whose masses can be determined spectroscopically), white dwarfs with dynamical mass measurements, or those with trigonometric parallaxes (Bergeron et al. 1992, 1997, 2001). The sample in Table 1 contains many degenerates with no mass estimate and therefore no way to confirm or rule out the relatively young total ages indicated by their kinematics. While their cooling ages are consistent with young disk objects, a conservative approach would be to explore a range of ages when interpreting the implications of the survey results. Realistically, a typical white dwarf in the sample is likely to be between  $\tau = 2 - 5$  Gyr old.

## 4. RESULTS

### 4.1. All Companions

Table 3 lists all companions to white dwarf sample stars detected in this work or published in the literature. Many targets were thought to be single white dwarfs when this project began in the late 1980’s but subsequently have been established to be binaries in

various studies. Although only low mass stellar and substellar companions were directly sought in this study, the overall multiplicity of white dwarfs is of astrophysical interest for many reasons. The first column lists the name of the companion. This is generally the name of the white dwarf primary plus the letter “B” for a secondary, or “C” for a tertiary. The second column lists the known or suspected spectral type of the companion, while the third column lists the primary white dwarf number. For companions discovered in this work, spectral types were estimated from optical and near-infrared colors with the longest baselines (such as  $V - K$ ). The fourth column lists the primary spectral type. The fifth and sixth columns list the separation on the sky and position angle of resolved companions. If unresolved, an upper limit to the separation is given, whereas a designation of “close” implies the system is a known radial velocity variable. The seventh and eighth columns list the best distance estimate for the white dwarf and the projected separation of the binary. The ninth column lists the absolute  $V$  magnitude for white dwarf companions or the absolute  $K$  magnitude for low mass stellar and substellar companions. The final column lists references to the initial discovery, critical data and analysis of each companion.

In all, there are 83 companion objects in 75 stellar systems containing at least one white dwarf: 76 doubles, 6 triples, and 1 quadruple system. Of all the companions, excepting GD 1400B, there are 18 white dwarfs and 64 main sequence stars, and 1 brown dwarf. There were 24 multiple systems independently discovered in this work, 20 of which are reported here for the first time and the remaining 4 previously published (Finley & Koester 1997; McCook & Sion 1999; Farihi 2004a; Scholz et al. 2004). In addition, new data and analysis of 32 binaries reported in Zuckerman & Becklin (1992) and Schultz et al. (1996) have resulted in more accurate descriptions of those systems.

#### 4.2. Near-Infrared Excess & Unresolved Companions

White dwarfs with  $T_{\text{eff}} \gtrsim 10,000$  K have blue or zero optical and near-infrared colors. Cooler white dwarfs will have colors that are just slightly red (Bergeron et al. 1997; Leggett et al. 1998; Bergeron et al. 2001). For example, a typical white dwarf with  $T_{\text{eff}} = 6750$  K will have  $V - K = 1$ ,  $J - K = 0.2$  (Bergeron et al. 1995b).

Very low mass stars and brown dwarfs have radii that are approximately 10 times larger than a typical white dwarf radius,  $R \sim 1 R_{\oplus}$  (Burrows et al. 1997). Therefore, despite very low effective temperatures and luminosities, an unresolved cool companion to a white dwarf can dominate the spectral energy distribution of the system at longer wavelengths, especially in the near-infrared (Probst 1983; Zuckerman & Becklin 1987a,b). Therefore, a white dwarf with red colors in the near-infrared or red portion of the optical spectrum can indicate the presence of an unresolved cool companion (Greenstein 1986a; Becklin & Zuckerman 1988; Zuckerman & Becklin 1992; Farihi & Christopher 2004).

There are basically two methods for obtaining parameters for unresolved low mass stellar or substellar companions to white dwarfs – optical and/or near-infrared photometry or optical

spectroscopy. Near-infrared spectroscopy is not typically performed because spectral types for low mass stars and cool dwarfs in general (M & L dwarfs) were established optically (Kirkpatrick & McCarthy 1994; Kirkpatrick et al. 1999b).

Optical spectroscopy can reveal unresolved companions to white dwarfs for a range of white dwarf to red dwarf luminosity ratios. If the white dwarf is cool enough and/or the red dwarf is bright enough, a composite spectrum can be seen even in the blue and visual portion of the optical spectrum (Greenstein 1986b; Finley et al. 1997). Red dwarf companions which are too dim, relative to their white dwarf hosts, in the blue or visual can still be seen at red optical wavelengths (7000 – 10,000 Å; Maxted et al. 1998). To extract information on the companion, one can visually examine the spectrum and compare it to known spectral types. For better accuracy, one can fit the bluest portion of the spectrum with models and effectively subtract the contribution of the white dwarf, leaving only the companion spectrum for analysis (Raymond et al. 2003).

However, the lowest luminosity companions to white dwarfs do not contribute a relatively sufficient amount of light in the optical for accurate spectral typing or study if they are unresolved (Kirkpatrick et al. 1993). Near-infrared methods must be used for these companions. Near-infrared spectroscopy can verify the presence of a companion, but has only a limited ability to provide a spectral type for the reason mentioned above. The most successful method for doing so uses near-infrared photometry. With models, one can extrapolate the flux of the white dwarf into the near-infrared and subtract its expected contribution, thereby obtaining photometry for any unresolved, very low luminosity companion (Zuckerman & Becklin 1987a; Becklin & Zuckerman 1988; Zuckerman & Becklin 1992; Green et al. 2000; Farihi & Christopher 2004). The resulting near-infrared colors (or near-infrared plus red optical colors or upper limits) can be compared with the colors of known isolated low luminosity objects such as late M dwarfs and L dwarfs for determination of spectral type (Kirkpatrick & McCarthy 1994; Kirkpatrick et al. 1999b).

In this work, both near-infrared and optical colors resulting from photometry were used to estimate spectral types for all unresolved companions, while optical spectroscopy was used to verify the presence of the companion, where possible. Most of the white dwarf primaries with unresolved cool companions are quite well studied and hence model extrapolation to longer wavelengths is likely to be reliable. The model grids of P. Bergeron (2002, private communication) for pure hydrogen and pure helium atmosphere white dwarfs were used to predict *RIJHK* fluxes for white dwarfs in such systems. These fluxes, together with the measured composite fluxes, were then used to calculate *RIJHK* magnitudes for the unresolved red dwarf component of the binary. The resulting optical and near-infrared colors were then compared to those of Kirkpatrick & McCarthy (1994) to determine spectral type. Unlike both Zuckerman & Becklin (1992) and Green et al. (2000), absolute *K* magnitudes of the companions were generally not used to estimate spectral type.

### 4.3. New Companions

Figures 4–23 are finding charts for companions reported here for the first time, including candidate companions. In the case of PG 1619+123, its newly identified common proper motion companion, HD 147528, is already known and hence no chart is provided here. The objects GD 392B, LDS 826C, & PG 0922+162B were discovered independently in the course of this survey but are previously published with finding charts (Finley & Koester 1997; Scholz et al. 2004; Farihi 2004a). GD 559B (Figure 11) is reported only in McCook & Sion (1999) with no other available journal reference.

For ease of use at the telescope, the charts are given at optical wavelengths when possible. In a few cases, the quality of a near-infrared image is superior and used instead. Generally, these are  $\sim 3'$  square field of view CCD or near-infrared array images taken at Lick Observatory or Steward Observatory. Coordinates are given for the companion if: (1) it is separated from the white dwarf primary by more than  $20''$ , (2) coordinates in the literature are inaccurate or difficult to find, (3) a finder chart is not published or difficult to find.

Table 4 lists measured proper motions for all confirmed and candidate common proper motion pairs discovered in this work. These values are the result of the mapping process discussed in §2.1. The map residuals were generally  $\sim 0.01'' \text{ yr}^{-1}$ , but never greater than  $0.02'' \text{ yr}^{-1}$ .

An important item to note is that the uncertainty in the measured proper motions is not a total measurement error. This is because there was no independent astrometric calibration apart from the point sources in each individual mapped field. In essence only *relative proper motions* were measured, not the absolute positions of the stars. The uncertainties reported by GEOMAP are the root mean square of the map residuals and do not take into account the following factors: (1) any overall nonzero motion of objects in the map, (2) the number of objects used in the map, (3) the S/N for individual point sources and their measured coordinate centroids in the map. The fields used to measure proper motions were between  $166''$  and  $300''$  in size, hence the number of field stars was limited, especially at higher galactic latitudes. Saturated stars are also unreliable because they can skew the centroiding process, as are faint field stars due to low S/N. Therefore, the Table 4 measurements should be considered of only limited accuracy. This is also the main reason that a few candidate companions have been retained for further investigation despite apparently discrepant measured proper motions (§6).

Ironically, there was only a single common proper motion companion detected solely in the near-infrared and not also in the optical. All other pairs were essentially detectable by “blinking” the first and second epoch Digitized Sky Survey scans (e.g. in the northern hemisphere, the first and second epoch Palomar Observatory Sky Survey plates). These digitized scans were also used to measure proper motions when possible because the longer time baselines provide higher accuracy and the ability to measure smaller proper motions.

There are 3 new and 11 previously known visual binaries ( $a < 10''$ ) studied here for

which no proper motion measurement was made. In a few cases, there exists insufficient time baseline between available images in which the pair is resolved to measure proper motions, or the data available in proper motion catalogs are for the composite pair (whether unresolved or extended) or absent. But for most, the companionship of the visual pair is highly probable due to one or more of the following: (1) an unchanging visual separation and position angle or elongation axis between the pair over 15–50 years (this is essentially equivalent to a common proper motion determination because most if not all of these pairs have  $\mu > 0.05'' \text{ yr}^{-1}$  and can be clearly seen moving with respect to background stars by “blinking” two DSS epochs), (2) the common photometric distance implied by the spectral energy distributions of both components together with the statistical likelihood of companionship based on proximity in the sky, (3) spectroscopic evidence presented here or elsewhere, (4) astrometric evidence presented elsewhere.

#### 4.4. Known Companions

The majority of the objects in Zuckerman & Becklin (1992) and Schultz et al. (1996) are unresolved white dwarf plus red dwarf binaries. As discussed in §4.2, the parameters of the two components must be deconvolved from one another. Most of these binaries were investigated with a thorough and updated literature search, optical photometry and spectroscopy to both confirm the identity and further constrain the properties of the low mass companion. This resulted in a higher confidence in their spectral classifications. For those partially or completely resolved pairs previously reported, all with  $1'' < a < 9''$ , §4.3 applies.

Generally speaking, the updated analysis of known low mass stellar companions has shown they have spectral types which are earlier than previous estimates. This is because early M dwarfs can contribute a significant amount of flux at optical wavelengths and cause a white dwarf to appear redder (in  $B - V$  for example) and more luminous (at  $V$  for example) than it would as a solitary star. The effective temperature inferred for the white dwarf will be too low, and the inferred distance modulus will be too close (because  $M_V$  will be too dim and  $V$  will be too bright; Farihi 2004b).

#### 4.5. Photometry

Circular aperture photometry was used to determine instrumental fluxes and magnitudes for all unresolved and resolved binary stars in this work (§2.3). Comparison with one or more standard stars yielded the true magnitudes listed in Tables 5 & 6.  $BVRI$  photometry is on the Johnson-Cousins system and  $JHK$  photometry is on the Johnson-Glass system, collectively known as the Johnson-Cousins-Glass system (Bessel & Brett 1988; Bessell 1990a).

For binary pairs that were spatially well resolved from each other ( $a > 3''$ ) and from neighboring stars, the flux measurement error was generally 5% or less for  $m < m_c$ , where

$m_c \approx (19, 18, 17)$  mag for  $(BVR I, JH, K)$ , and  $\sim 10\%$  or greater otherwise. For separations smaller than  $\sim 3''$  between target star and neighbor or companion, overlapping point spread functions (PSFs) effectively contaminate flux measurements even in small apertures of 1 – 2 pixels in radii. In these cases, the IRAF program DAOPHOT was used to simultaneously fit two or more PSFs within a given area, deconvolve and extract their individual fluxes. This method works quite well for pairs with  $\Delta m \approx 3$  mag or less and generates errors equivalent to those quoted above. Table 5 lists all photometry for resolved binary components, including those stars requiring PSF deconvolution from neighbors or companions.

Close binaries consisting of a white dwarf plus red dwarf which were indistinguishable from a single point source were treated as a single star and aperture photometry performed accordingly. This is true also for those pairs with separations ( $a < 2''$ ) too small to be accurately fit with two PSFs due to pixel scale, seeing conditions, and/or  $\Delta m > 3$  mag.

In Table 6 are the measured optical and near infrared magnitudes for all composite binaries. For each system, the table has three entries. The first line is the composite photometry itself, with all measurement errors for this work being 5% or less in this range of magnitudes. The second line gives the predicted magnitudes for the white dwarf (WD) component based on the most current hydrogen and helium atmosphere model grids of P. Bergeron (2002, private communication), which are considered more accurate than previous generations (Bergeron et al. 1995b,c). The predicted white dwarf magnitudes are calculated by adding model colors (appropriate for its  $T_{\text{eff}}$ , and  $\log g$  if known) to a photometric bandpass that is essentially uncontaminated by its cool red dwarf companion – either  $U$  or  $B$  (or  $V$  in a few rare cases). If the calculation was done from  $U$ , a reference is given for the photometry. The temperature and surface gravity used as input for the models are taken from the most reliable sources available with the reference provided. The third line gives the deconvolved magnitudes for the red dwarf (RD), generally only  $IJK$  due to large uncertainties at shorter wavelengths.

Based on comparisons with Kirkpatrick & McCarthy (1994), spectral types were estimated from  $I - K$ . Unlike  $J - K$ , which is highly degenerate across most of the M type dwarf spectral class,  $I - K$  is essentially monotonically increasing from M2 until well into the L spectral class (Kirkpatrick & McCarthy 1994; Kirkpatrick et al. 1999b).

Some binary systems lack data at one or multiple wavelengths due to unavoidable circumstances including, but not limited to: time constraints, poor weather, instrument problems, telescope pointing limits, and telescope size.

#### 4.6. Spectroscopy

The purpose of the spectroscopy was to identify the spectral class of companions. Standard stars and spectral flats were taken to ensure the target spectra were free of both detector and instrument response. None of the spectra were corrected for telluric features or extinction. In the case of white dwarfs, the purpose was to look for the presence or absence of

highly pressure broadened hydrogen or helium lines (implying spectral classes DA, DB, or DC for no lines). In the case of M dwarfs, the search was for the characteristic TiO and CaH bands.

The Kast Dual Spectrograph sits atop Mount Hamilton, which is close to the city lights of San Jose. Sodium at 5880 Å can be seen very brightly in Kast spectra and can be difficult or impossible to remove completely in low S/N observations. Hence positive and negative residuals often remain. During one observing run with the Kast, the red side of the spectrograph was used without any dichroic or blocking filter on the blue side. Hence second order blue light was present in the red spectra of all objects excepting very red objects such as single M dwarfs. This effect was mostly, but not completely, removed by calibrating with a standard star observed in the same arrangement.

The one spectroscopic observing run with the Boller & Chivens Spectrograph at Steward Observatory was over 3 nights with a very bright moon. The solar spectrum reflected from the moon can be seen quite brightly over the entire chip and was generally stable and removable. However, the regions around the Balmer lines were problematic in a few instances and some lower S/N spectra still contain residuals in the region around H $\alpha$ , H $\beta$ , and H $\gamma$ .

A few miscellaneous stars were observed with LRIS (Oke et al. 1995) at the Keck telescope because they were considered important yet too faint to obtain reliable spectra with a 3 meter class telescope. The observations were kindly performed by colleagues at other institutions. In a few cases, calibration stars were not observed and hence the flux calibration is not perfect and had to be adjusted as best possible.

In several of the binary systems reported here, the primary white dwarf is poorly documented in the literature, or missing all together. Spectra are displayed in Figures 24–31 in order of decreasing temperature for those stars which do not have published spectra or are misclassified or missing from the literature, for new white dwarf identifications, and for those systems where binarity or other issues have precluded proper analysis. Also shown are the optical spectra of all unpublished white dwarf wide binary companions discovered uniquely in this study.

Figures 32–44 present the spectra of unpublished resolved M dwarf secondaries and tertiaries, displayed in order of decreasing temperature. Figures 45–53 contain the composite spectra of white dwarf plus red dwarf pairs (at least one of which has been resolved photometrically but not spectroscopically), displayed in order of decreasing red dwarf temperature.

## 5. ANALYSIS

### 5.1. Companion Spectral Type Frequency

In Figure 54 is plotted the number of unevolved low mass companions versus spectral type for objects studied in this work. Despite excellent sensitivity to late M dwarfs and early

L dwarfs in all survey phases, very few were detected.

For comparison, Figure 55 shows similar statistics for cool field dwarfs within 20 pc of Earth taken from Reid & Hawley (2000); Cruz et al. (2003). The data plotted in Figure 55 have been corrected for volume, sky coverage, and estimated completeness. Can one reconcile Figure 55 with the common notion that there are at least as many brown dwarfs as low mass stars (Reid et al. 1999)? To resolve this possible discrepancy, most field brown dwarfs would have to be of spectral type T or later, since it is clear from the figure that, in the field, L dwarfs are much less common than stars.

However, there are several things to keep in mind regarding the relative number of field brown dwarfs versus stars. There should be a relative dearth of L dwarfs compared to T type and cooler brown dwarfs in the field because cooling brown dwarfs pass through the L dwarf stage relatively rapidly. The lower end of the substellar mass function is poorly constrained at present (Burgasser 2004) and the relative number of substellar objects versus low mass stars in the field depends on the shape of the mass function in addition to the unknown minimum mass for the formation of self-gravitating substellar objects (Low & Lynden-Bell 1976; Reid et al. 1999; Burgasser 2004). Furthermore, even for only moderately rising mass functions, such as those measured for substellar objects in open clusters (Hillenbrand & Carpenter 2000; Luhman et al. 2000; Hambly et al. 1999; Bouvier et al. 1998), there will be more brown dwarfs than stars if the minimum formed, self-gravitating substellar mass is  $< 0.010 M_{\odot}$ . Ongoing and future measurements of the local T dwarf space density will constrain the substellar field mass function.

Figures 54 & 55 are quite similar. Clearly, the peak frequency in spectral type occurs around M3.5 for both field dwarfs and companions to white dwarfs. In fact, the peak is identical; 25.6% for both populations. By itself, this could imply a common formation mechanism, a companion mass function similar to the field mass function in this mass range. But, relative to the peak, there are  $\sim 2 - 3$  times more L dwarfs and  $\sim 4 - 5$  times more M6–M9 dwarfs in the field than companions. For the T dwarf regime, uncertainty remains because only the Keck portion of the white dwarf survey was sensitive to such cool brown dwarfs (and only for certain separations) plus the current incomplete determination of the field population density.

Hence, binary systems with small mass ratios ( $q = M_2/M_1 < 0.05$ ) are rare for white dwarf progenitors (which typically have main sequence masses  $\sim 2 M_{\odot}$ ). Although there exists some speculation regarding the possibility that brown dwarfs are ejected in the early stages of multiple system or cluster formation, there is currently no evidence of this occurring. It is conceivable that low mass companions in very wide orbits may be lost to gravitational encounters in the Galactic disk over a few billion years, but given the fact that there are a dozen or so known L and T dwarfs in wide binaries, this seems like a rare mechanism, if it occurs at all.

It is possible that very low mass companions to intermediate mass stars undergo major or catastrophic alteration during the red giant or asymptotic giant branch (AGB). It has been



calculated that there is a critical mass, ( $M_c \sim 0.02 M_\odot$ ), below which low mass companions are completely evaporated or cannibalized within the AGB envelope (Livio & Soker 1984; Iben & Livio 1993). Above  $M_c$  companions may accrete a significant amount of material during inspiral, perhaps enough to transform into low mass stars (Livio & Soker 1984). It is not yet empirically known whether any of these scenarios actually occur in nature. If they do, then the possibility of secondary evaporation should be less likely for the companion mass range in question here ( $M > 0.04 M_\odot$ ), but it is not certain. In §5.4, the secondary spectral types in binaries which may have experienced a common envelope phase will be compared to those which did not.

In a way, the relative dearth of late M dwarfs alleviates a potential interpretation problem. Had it been the case that many late M dwarfs were detected but only one or two L dwarfs, it might have been argued that the L dwarfs were cooling beyond the sensitivity of the search. Since all M dwarfs (and the first few L dwarf subclasses) at  $\tau \geq 1$  Gyr are stellar according to theory, this concern does not exist. The measured dearth is real and is not caused by brown dwarf cooling and the resulting lower sensitivity.

## 5.2. The Companion Mass Function

Dynamical masses measurements do not exist for any of the companions described in this work. There are a few systems – close white dwarf plus red dwarf spectroscopic binaries – whose secondary masses have been estimated (Saffer et al. 1993; Marsh & Duck 1996; Maxted et al. 1998). This is not a mass measurement as it ultimately relies on models, and what is really measured in these systems is the mass ratio (hence the need for a white dwarf mass from models). But this method has been used successfully to estimate red dwarf masses that are consistent with both theory and existing dynamical mass measurements for low mass stars in the same range of spectral types, temperatures, and ages.

For M spectral types, the works of Kirkpatrick et al. (1991); Henry & McCarthy (1993); Kirkpatrick & McCarthy (1994); Dahn et al. (2002) contain: (1) absolute magnitudes as a function of spectral type, (2) mass versus luminosity relations, (3) spectral type as a function of mass based on all available dynamical measurements of very low mass stars. These empirical and semiempirical relationships are for disk stars of intermediate age, which is appropriate for the sample of white dwarfs in this work. These relations have been used to provide masses for spectral types M1 through M9. It is unnecessary to extrapolate these empirical relations into the L dwarf regime, because only two white dwarf plus L dwarf systems are known and both companions have published mass estimates from models, based on likely age ranges (Kirkpatrick et al. 1999a; Farihi & Christopher 2004).

Figure 56 shows the first step in the construction process – mass versus  $K$  band luminosity relations from model, empirical and semiempirical relations. The models used are from Chabrier et al. (2000) and show tracks for ages of 1 and 5 Gyr, appropriate for young to intermediate disk ages. The minimum mass for hydrogen burning (HBMM) in these models

is  $M_{\text{HBMM}} = 0.072 M_{\odot}$ . The track for 5 Gyr turns downward (relative to the track for 1 Gyr) before the stellar/substellar boundary because the lowest mass stars are still contracting onto the main sequence (Burrows et al. 1997, 2001; Chabrier et al. 2000). Below the HBMM, the downturn is the result of brown dwarf cooling.

For the ages appropriate here, dynamical masses have been measured down to spectral type M6 ( $M = 0.10 M_{\odot}$ ; Kirkpatrick & McCarthy 1994), but none later. Hence the empirical relation below this spectral type and corresponding mass is really semiempirical. Adjustments had to be made according to the progress in this field over the past decade. For example, an extrapolation of the strictly empirical relation predicts a clearly substellar mass of  $0.066 M_{\odot}$  at spectral type M9. This is not currently accepted as correct for intermediate disk ages (Burrows et al. 1997; Chabrier et al. 2000).

Figure 57 plots the absolute  $K$  magnitude versus spectral type for all the low mass stellar and substellar companions discovered in this work. Also plotted in the same figure is the combined empirical relation of Kirkpatrick & McCarthy (1994) and Dahn et al. (2002), both based on trigonometric parallax measurements. This figure demonstrates the possibility of inaccurate distance estimates for many of the white dwarf primaries and is the major reason why absolute magnitude was not used as a proximate for mass in this work. Unlike previous work (Zuckerman & Becklin 1992) and similar studies (Green et al. 2000) – both of which employed  $M_K$  as an indicator of spectral class – the present study uses spectral class itself. The reasons for this are twofold. First, in many cases photometric distances for white dwarfs are inaccurate for a variety of reasons. For example, because white dwarfs have varying radii at a given effective temperature, their distances cannot be estimated with as much confidence as main sequence stars. Binarity can also cause a white dwarf to have an erroneous distance estimate. Smart et al. (2003) found that, for a sample of six single white dwarfs, in general, the published photometric distance is an overestimate of the distance found by trigonometric parallax. Second,  $M_K$  is a proximate for luminosity, not for temperature. Color and spectral type are temperature indicators and do not require a precise distance determination. For main sequence stars, the temperature can be used with an HR diagram (i.e. an empirical radius versus temperature relation) to calculate a mass. This is, in essence, what has been done in the present work.

With perhaps one or two exceptions discussed in the Appendix, all of the Table 3 these stars have published spectra (in this work or elsewhere) which are consistent with solar metallicity. Therefore the combined correlation between absolute magnitude and spectral type of Kirkpatrick & McCarthy (1994) and Dahn et al. (2002), for low mass field stars of intermediate disk age and solar metallicity, will suffice to confidently predict secondary masses.

The final step is to combine the empirical and semiempirical relations of Figures 56 & 57 into Figure 58, which shows the resulting correlation between spectral type and mass. Figure 59 is a histogram of the number of detections versus companion mass, using the correlation data in Figure 58.

### 5.3. Sensitivities & Biases

When considering the overall survey mass sensitivity, for low mass stellar companions, age is not an issue. But for substellar objects, determination of mass sensitivity must include an age estimate. In §3.3 a likely age range for the sample was estimated to be 2 – 5 Gyr based on the overall kinematics and cooling ages, but owing to model grid availability and to avoid additional interpolation errors, calculations were performed for ages of 1 and 5 Gyr.

The average distance for the sample, calculated to be 57 pc in Table 2, along with the models of Chabrier et al. (2000), was used for determining overall mass completeness. Obviously, the sensitivity differs for objects which are closer or farther and the standard deviation of the entire sample is significant at  $\sigma_d = 47$  pc. Yet the masses, temperatures and spectral classes implied by the completeness limits for each phase of the survey (at the average distance of the sample stars) epitomize what was detectable. Table 7 summarizes these completeness limits.

Zuckerman & Becklin (1992) report a completeness down to  $K = 15$  mag. However, this completeness was limited by single detectors prior to the availability of near-infrared cameras (Zuckerman & Becklin 1987a). All of the objects in Table 1 that were observed in the IRTF survey were imaged with arrays. For spatially resolved objects, a conservative completeness limit for these observations is  $K = 16$  mag. Applying this limit at  $d = 57$  pc for the 84 white dwarfs observed in this early part of the survey (but not reobserved at Steward or Keck), these observations were complete to  $M_K = 12.2$  mag. This corresponds to a spectral type near L6,  $T_{\text{eff}} \sim 1650$  K, and  $M = 0.060 - 0.070 M_{\odot}$  for 1 – 5 Gyr (Reid et al. 1999; Kirkpatrick et al. 2000; Dahn et al. 2002; Chabrier et al. 2000; Vrba et al. 2004). GD 165B was discovered amongst the first observations in the program at  $K = 14.2$  mag and has a mass estimated at  $M = 0.072 M_{\odot}$  (Kirkpatrick et al. 1999a).

The Steward survey of 261 white dwarfs was complete to  $J = 18$  mag, implying a completeness down to  $M_J = 14.2$  mag at  $d = 57$  pc. This corresponds to a spectral type around L7,  $T_{\text{eff}} \sim 1500$  K, and  $M = 0.053 - 0.068 M_{\odot}$  for 1 – 5 Gyr (Reid et al. 1999; Kirkpatrick et al. 2000; Dahn et al. 2002; Chabrier et al. 2000). The Keck survey of 86 white dwarfs was complete to  $J = 21$  mag, implying completeness to  $M_J = 17.2$  mag at  $d = 57$  pc. This corresponds to spectral types later than T8,  $T_{\text{eff}} < 750$  K, and  $M \sim 0.020 - 0.040 M_{\odot}$  for 1 – 5 Gyr (Vrba et al. 2004; Leggett et al. 2002; Chabrier et al. 2000).

As mentioned in §2.5, all 371 sample stars were searched for near-infrared excess emission between 1 – 2  $\mu\text{m}$  using the 2MASS all sky catalog database (Cutri et al. 2003). 2MASS provides a highly accurate, uniform and consistent method for this type of search. Higher sensitivity to unresolved companions was not gained at Keck or Steward for two reasons: (1) the white dwarf was sometimes saturated in the attempt to image faint companions, especially at Keck, and (2) near-infrared excess detection requires photometric accuracy, not deep imaging.

The average temperature of a white dwarf in the sample is  $T_{\text{eff}} = 13,000$  K. This yields

$M_H = 11.8$  mag,  $M_K = 11.9$  mag for a white dwarf of typical mass ( $\log g = 8.0$ , Bergeron et al. 1995b). The 2MASS all sky catalog provides reliable photometry ( $S/N > 10$ ) down to  $H = 15.1$  mag and  $K_s = 14.3$  mag for 100% of the sky and to  $H = 15.6$  mag and  $K_s = 14.8$  mag for 50% of the sky (Cutri et al. 2003).

Taking the average of these  $H$  &  $K_s$  limiting magnitudes at 57 pc, an excess of 170% above the white flux would be detectable at  $M_K = 10.8$  mag ( $K_s = 14.5$  mag). This yields  $M_K = 11.3$  mag for a cool companion, which is around spectral type L4. However, the sensitivity to excess emission is much greater at  $H$ . At 57 pc, an excess of 21% is detectable at  $M_H = 11.6$  mag ( $H = 15.3$  mag), which yields  $M_H = 13.5$  mag for a low mass companion. This corresponds to spectral type L8,  $T_{\text{eff}} \sim 1400$  K, and  $M = 0.050 - 0.066 M_{\odot}$  for 1 – 5 Gyr (Reid et al. 1999; Kirkpatrick et al. 2000; Dahn et al. 2002; Chabrier et al. 2000).

The case of GD 1400B proves this point. Estimated at spectral type L6, it was detected using the 2MASS database in a manner identical to that performed for all 371 stars in the entire sample. Not included in the sample, GD 1400B was first identified by Wachter et al. (2003) in the initial phase of a search utilizing the 2MASS point source catalog to survey the entire sky near the positions of all white dwarfs in McCook & Sion (1999). Farihi & Christopher (2004) were the first to distinguish GD 1400 from the bulk of white dwarfs with near-infrared excess emission and identify its companion.

None of the searches were sensitive to companions beyond the field of view of the corresponding cameras. For the IRTF, only objects within  $\sim 12''$  of the white dwarf were detectable. The NIRC and Steward near-infrared camera fields of view are  $19.2''$  and  $83.2''$  from center to edge, respectively. This implies for targets at  $\langle d \rangle \pm \sigma_d$ , separations out to  $4700 \pm 3900$  AU were probed by the Steward survey, but only out to  $1100 \pm 900$  AU for the Keck survey. Although wider binaries may have been missed in the Keck and IRTF searches, they would have been picked up by the DSS blinks (§2.6), unless they were spectral type L or later, roughly speaking.

Generally speaking, M and L dwarfs were detectable at arbitrarily close physical separations (§4.2). However, T dwarfs are generally not detectable by near-infrared excess unless the white dwarf is quite cool or quite massive ( $T_{\text{eff}} < 7000$  K for  $\log g = 8.0$ , or  $T_{\text{eff}} < 9000$  K for  $\log g = 8.5$ ). There were few stars in the sample meeting this criteria and therefore T dwarfs were only detectable if resolved; at Keck this required a separation on the sky of  $\sim 1''$  (with typical Mauna Kea seeing) and at Steward  $\sim 2''$  (typical Kitt Peak seeing). However, no T dwarfs were detected.

On the brighter side, unresolved dwarf stellar companions earlier than around M1 ( $M_V = 9.3$  mag) were almost certainly selected against. Depending on the luminosity of the white dwarf, it is possible for a G–K dwarf or even an M0 dwarf to mask the presence of a nearby degenerate at optical wavelengths. These types of binaries are likely selected against in surveys which identify and catalog nearby white dwarfs. This explains in part the drop off at the higher mass end of Figures 54 & 59. However, the study was not biased against wide yellow dwarf companions and two of the white dwarfs in the sample were found to have such

secondaries.

#### 5.4. Current Mass Versus Initial Mass

In order to measure the initial mass function for companions to intermediate mass stars, a critical question remains: are the red dwarf masses observed today the same as the initial masses when the binary was formed?

When intermediate mass main sequence stars, the progenitors of white dwarfs, ascend the asymptotic giant branch, their outer regions expand by a factor of a few hundred. If such a star has a relatively close main sequence companion within this region ( $a \lesssim 1 - 2$  AU), the pair is said to share a common envelope. Generally speaking, such a close binary pair will transfer much of its orbital energy (via angular momentum) into the common envelope through friction, resulting in ejection of the envelope from the system and an inspiral to a more negative binary binding energy and smaller separation (Paczynski 1976).

It has been theorized that a low mass companion may accrete up to 70% of its final mass during a common envelope phase or may evaporate completely during the inspiral, depending on the initial masses and separations of both components (Livio & Soker 1984). Hence, there is a possibility that the masses of red dwarf secondaries in close binaries are not their initial masses. Unfortunately, there is no consensus on the topic. There appears to be evidence in support of the idea that secondaries do accrete a significant amount of mass during the common envelope phase (Drake & Sarna 2003). Yet there also appears to be evidence that low mass companions emerge unaffected (Maxted et al. 1998).

Table 8 presents the median spectral types in this survey for several different low mass companion subgroups. The “resolved” subgroup refers to all resolved binary companions. The “close” subgroup is all known radial velocity binary companions – these are the post common envelope binaries. The “unresolved / not close” subgroup is all unresolved binary companions that are not known to be radial velocity variables. Hence this subgroup contains an unknown number of post common envelope binaries. The fourth subgroup supposes that subgroup three binaries are all wide ( $a > 5$  AU), whereas the fifth subgroup supposes that subgroup three binaries are all close ( $a < 0.1$  AU). Do the Table 8 values provide any evidence that post common envelope binary secondaries have accreted a significant amount of mass (correlated here with spectral type)? If so, it is not obvious (the interested reader is referred to Farihi 2004b for further discussion).

## 6. CONCLUSIONS

Together, the various phases of this survey discovered over 40 previously unrecognized white dwarf binary and multiple systems. The wide field, common proper motion survey alone discovered at least 20 new white dwarf multiple systems. Based on the analysis of §5.4,

there is no reason why all unevolved companion stars should not be included in the initial mass function.

It is worthwhile to mention that none of the 371 survey stars were found to have near-infrared excess similar to G29-38 and GD 362 – the only two single white dwarfs known to be orbited by circumstellar dust (Zuckerman & Becklin 1987a; Becklin et al. 2005; Kilic et al. 2005).

Before making an estimate of the substellar companion fraction, GD 1400B must be discussed. Although not included in the sample, it is an important datum in the overall statistics of low mass companions to white dwarfs – a long, hard, and much sought after datum (16 years passed between the discoveries of the first and second L dwarf companions to white dwarfs). GD 1400 is a white dwarf not unlike the sample white dwarfs, with  $T_{\text{eff}} = 11,600$  K and a moderate proper motion of  $\mu \approx 0.05'' \text{ yr}^{-1}$  (Koester et al. 2001; Fontaine et al. 2003; Zacharias et al. 2004). Hence its inclusion here is perfectly consistent with the sample stars, the search methods and resultant sensitivities (§5.3). Due to these consistencies and the fact that GD 1400B is a vital statistic, it has been included in the analyses and conclusions.

The calculated fraction of white dwarfs with substellar companions, within the range of masses and separations to which this work was sensitive, is  $f_{bd} = 0.4 \pm 0.1\%$ . This represents the first measurement of the low mass tail of the companion mass function for intermediate mass stars, main sequence A and F stars (plus relatively few B stars) with masses in the range  $1.2 M_{\odot} < M < 8 M_{\odot}$ . This value is consistent with similar searches around solar type main sequence stars for comparable sensitivities in mass and separation (Oppenheimer et al. 2001; McCarthy & Zuckerman 2004). Therefore that the process of star formation eschews the production of binaries with  $M_2/M_1 < 0.05$  is clear from the relative dearth of both L and late M dwarfs discovered in this work.

The authors wish especially to thank Steward Observatory for the use of their facilities over the years – this research would not have been possible without their munificent support. J. Farihi thanks C. McCarthy for numerous useful discussions and very generous computing support over the years. P. Bergeron kindly provided his models for use throughout this paper. Part of the data presented herein were obtained at Keck Observatory, which is operated as a scientific partnership among the California Institute of Technology (CIT), the University of California and the National Aeronautics and Space Administration (NASA). This publication makes use of data acquired at the NASA Infrared Telescope Facility, which is operated by the University of Hawaii under Cooperative Agreement no. NCC 5-538 with NASA, Office of Space Science, Planetary Astronomy Program. Some data used in this paper are part of the Two Micron All Sky Survey, a joint project of the University of Massachusetts and the Infrared Processing and Analysis Center (IPAC)/CIT, funded by NASA and the National Science Foundation (NSF). 2MASS data were retrieved from the NASA/IPAC Infrared Science Archive, which is operated by the Jet Propulsion Laboratory, CIT, under contract with NASA. The authors acknowledge the Space Telescope Science

Institute for use of the Digitized Sky Survey. This research has been supported in part by grants from NSF and NASA to UCLA.

## A. INDIVIDUAL OBJECTS & SYSTEMS

In this section are discussions of: misclassified stars, unrelated proper motion stars, candidate companions, and noteworthy confirmed multiple systems. Complete details may be found in Farihi & Christopher (2004). The following references are used throughout this section. For white dwarf model colors, absolute magnitudes, masses, surface gravity, effective temperatures, and ages: Bergeron et al. (1995b,c); P. Bergeron (2002, private communication). For empirical M dwarf colors and absolute magnitudes: Kirkpatrick & McCarthy (1994); Dahn et al. (2002).

### A.1. Nondegenerates

Some stars in Table 1 are noted which are not white dwarfs and for which no literature reference can be found explicitly correcting the misclassification. The correct classification is presented here. These are listed as white dwarfs in the catalog of McCook & Sion (1999) and also in the same current online catalog.

#### A.1.1. *G187-9*

*G187-9* is classified as type DC in McCook & Sion (1999), but it was classified more or less correctly as early as 1967 (Wagman 1967). It has spectral type M2 and  $M_V = 11.27$  mag (Reid et al. 1995). A main sequence M2 star has  $M_V = 10.2$  mag and hence *G187-9* is subluminescent, and by definition a subdwarf. It has a high proper motion of  $\mu = 0.7'' \text{ yr}^{-1}$ .

#### A.1.2. *GD 617* & *PG 0009+191*

*GD 617* is classified as type DAB5 (Greenstein 1984; McCook & Sion 1999) but has been reclassified as a very hot subdwarf showing Balmer lines, neutral helium, and continuum flux from an unresolved F/G star (Lamontagne et al. 2000). Photometry verifies the probability of an unresolved main sequence companion. It has  $V - K = +0.8$ , which is too red for a single hot helium burning star. Hence *GD 617* is very likely type sdB+F/G.

*PG 0009+191* is classified as type DA (Green et al. 1986; McCook & Sion 1987) but does not appear in McCook & Sion (1999). The absence hints at probable nondegeneracy. The spectrum of *PG 0009+191* appears to be that of a hot subdwarf, type sdB (Farihi 2004b)

### A.1.3. *PG 1126+185 & PG 0210+168*

PG 1126+185 is classified as type DC8 (Green et al. 1986; McCook & Sion 1999). It was reclassified as DC+G/K by Putney (1997). It is not possible to detect a DC star (cool helium atmosphere or very cool hydrogen atmosphere white dwarf) around a main sequence G or K star, since the difference in brightness at  $V$  would be at least 6 magnitudes. Were it not for the blue continuum, the spectrum in Figure 2 of Putney (1997) makes a great case for a metal-poor nondegenerate star; weak lines of Mg, Fe, Na can be seen in addition to Balmer lines and Ca H & K. Photometry done here gives  $V - K = 1.88$ , which is consistent with a G/K type star. But PG 1126+185 also has  $U - B = -1.12$ , implying a very hot object and confirming the steep blue continuum seen in its spectrum. Smart et al. (2003) have measured a zero parallax for PG 1126+185 – clearly inconsistent with a white dwarf, given its relative brightness at  $V = 14.0$  mag.

To explain both the blue continuum and the observed absorption features of PG 1126+185, a composite system consisting of one hot star and one cool star is needed. The luminosities should be comparable given the spectrum. A typical G star has  $M_V \approx 5$  mag, but is there a hot star that has a comparable absolute  $V$  magnitude? Subdwarf B stars have  $M_V \approx 4.5$  mag (Maxted et al. 2000c). Therefore, the most likely explanation for the spectrum of PG 1126+185 is a composite binary consisting of an sdB+G/K. This is also consistent with the zero parallax measurement.

PG 0210+168 shares a story similar to PG 1126+185. It was typed DC originally (Green et al. 1986; McCook & Sion 1999) and then reclassified as DC+F/G by Putney (1997). Again, it is simply not possible to detect a DC white dwarf in the optical against the flux of an F or G star. In this case the brightness difference would be at least 8 magnitudes. Figure 2 of Putney (1997) clearly shows weak metal lines, a Balmer series, plus Ca H & K. Its spectrum is very similar to that of PG 1126+185 and shows a strong blue continuum as well. PG 0210+168 was not observed for optical photometry in the course of this work, so its  $UBV$  colors are not known, but with  $V - K \approx 1.5$ , it is quite certain that PG 0210+168 contains a cool star together with a hot star. Following the same reasoning as for PG 1126+185, the conclusion is that it is very likely an sdB+F/G composite binary.

## A.2. Uncommon Proper Motion

Common proper motion is a necessary but insufficient condition to establish physical companionship for wide binaries. In this section, evidence is presented which illustrates this.

Measuring proper motion accurately is a nontrivial task requiring good S/N on dozens if not hundreds of background, near zero motion sources. And still, what is almost always measured is relative proper motion – that is, the motion of an object relative to nearby stationary sources (Monet et al. 2003; Lépine et al. 2003). In identification of common proper motion companions, this issue is not really important. A wide binary pair should



have the same absolute and relative proper motion, assuming zero orbital motion. However, the issues raised in §4.3 are valid and do contribute to measurement uncertainties. Given the limited accuracy of the proper motions measured for this work, many candidates were flagged which turned out to be background stars. This is desirable – the error was on the side of caution and real candidates were not thrown out.

In the end, only reliable trigonometric parallaxes and/or orbital motion can determine binarity in widely separated pairs with absolute certainty. This is illustrated by three white dwarf target primaries in the sample: G47-18, G66-36, & G116-16. All three of these stars are reported to be members of a wide binary containing a white dwarf in McCook & Sion (1999). However, further investigation proves these cases to be false positives. None of the following pairs are physically associated.

#### *A.2.1. G47-18 & G116-16*

G47-18 was reported as a common proper motion binary with the F6 dwarf HD 77408 (Eggen & Greenstein 1967). The white dwarf has  $\mu = 0.324'' \text{ yr}^{-1}$  at  $\theta = 270.2^\circ$  and  $\pi = 0.049''$  (three measurements; McCook & Sion 1999). However, HD 77408 has  $\mu = 0.420'' \text{ yr}^{-1}$  at  $\theta = 269.5^\circ$  and  $\pi = 0.0199''$  (Perryman et al. 1997).

G116-16 was reported as a common proper motion binary with the G0 dwarf G116-14 (Eggen & Greenstein 1965). The white dwarf has  $\mu = 0.252'' \text{ yr}^{-1}$  at  $\theta = 180.1^\circ$  and  $\pi = 0.035''$  (Dahn et al. 1982), while G116-14 has  $\mu = 0.281'' \text{ yr}^{-1}$  at  $\theta = 173.1^\circ$  and  $\pi = 0.0194''$  (Perryman et al. 1997).

#### *A.2.2. G66-36*

G66-36 was reported as a common proper motion binary with the G5 dwarf G66-35 (Oswalt 1981). However, G66-36 is not a white dwarf but a metal-poor M2 star at  $d = 25 \text{ pc}$  (Reid et al. 1995). Its proper motion is  $\mu = 0.32'' \text{ yr}^{-1}$  at  $\theta = 173^\circ$  (McCook & Sion 1999), while G66-35 has  $\mu = 0.297'' \text{ yr}^{-1}$  at  $\theta = 187.1^\circ$  and  $\pi = 0.0152''$  (Perryman et al. 1997). It is noteworthy that this is a case of a subdwarf being mistaken for a white dwarf and two stars with different proper motion being identified as companions.

### **A.3. Proper Motion Confusion**

Motions in the Galactic disk are primarily responsible for the proper motion of nearby stars (Binney & Tremaine 1987; Binney & Merrifield 1998). Therefore, in principle, two unrelated stars can have nearly identical proper motions, both in magnitude and direction. In addition, some proper motion confusion is due to limited measurement accuracy, as exemplified in §A.2. Unlike the objects in the previous section, the following potential candidate

wide binaries have never appeared in the literature.

### A.3.1. GD 248

In early 2002, a candidate common proper motion companion to the DC5 white dwarf GD 248 was identified. A measurement utilizing digitized POSS plates separated by nearly 40 years seemed to indicate common proper motion. Another measurement using near-infrared images separated by almost 5 years gave similar results but with uncertainty three times as large.

A Keck LRIS spectrum (Farihi 2004b) covering 4900 – 10,000 Å revealed Na at 5880 Å, a strong MgH band at 5100 Å, and a variety of other fairly weak features – all indicative of a metal-poor late K or very early M star (Reid & Hawley 2000).

Thus, the candidate companion to GD 248 is an ultrahigh velocity background star. At an estimated distance of  $\sim 800$  pc (assuming  $M_V = 10.1$  mag, 2 magnitudes below the main sequence for spectral type K7), its tangential velocity of  $v_{\text{tan}} \approx 530$  km s $^{-1}$  is just under the escape velocity of the Galaxy (Binney & Tremaine 1987). A precise proper motion measurement has been performed on the nonphysical pair and their error ellipses differ by exactly  $1\sigma = 0.008''$  yr $^{-1}$  (S. Lépine 2002, private communication).

### A.3.2. GD 304, PG 1026+002, & PG 1038+633

Candidate common proper motion companions to the white dwarfs GD 304, PG 1026+002, & PG 1038+633 were identified during the course of the survey. Table 9 lists the data.

Ultimately, spectra revealed (Farihi 2004b) that the candidate companions to PG 1026+002, & PG 1038+633 were high velocity background stars of similar temperature to the candidate companion to GD 248. The candidate companion to GD 304 has a much redder  $V - K$  color than the other three objects in Table 9.

Assuming  $M_V = 9.8$  mag (1 magnitude below the main sequence for spectral type M0) for the candidate companion to PG 1026+002, its tangential velocity is  $v_{\text{tan}} \approx 390$  km s $^{-1}$ . Using  $M_V = 9.1$  mag for the candidate companion to PG 1038+633 (1 magnitude below the main sequence for a K7 star), its tangential velocity is  $v_{\text{tan}} \approx 400$  km s $^{-1}$ . These values are less than that of the candidate companion to GD 248, but still quite high. For the candidate companion to GD 304 however, a slightly more modest tangential velocity of  $v_{\text{tan}} \approx 210$  km s $^{-1}$  is calculated assuming a main sequence absolute magnitude of  $M_V = 10.8$  mag for spectral type M3. For all four high velocity background stars, a spectrum was a critical discriminant.

#### A.4. Candidate Companions

These objects show common proper motion of varying degree of agreement along with colors and/or spectra consistent with companionship. Data for candidate companions are listed in Tables 3, 4, 5, & 10.

##### A.4.1. GD 84

GD 84B is an especially tentative companion due to the relative lack of agreement in the measured proper motions. A more precise measurement could not be made for the candidate companion because it is passing in front of another star in the digitized POSS I scans.

This candidate is retained because it and GD 84 have similar photometric distances. Weidemann & Koester (1995) give spectral type DQ5.6 for GD 84 ( $T_{\text{eff}} = 9000$  K), which yields  $M_V = 12.59$  mag and a photometric distance of  $d = 33$  pc for  $\log g = 8.0$ . The M dwarf, verified by its optical spectrum in Figures 38 & 39, appears to be a normal solar metallicity star. Using  $K = 10.55$  mag from Table 5 and  $M_K = 7.80$  mag for spectral type M4, its photometric distance is  $d = 35$  pc.

##### A.4.2. GD 683

The UCAC1 catalog (Table 4; Zacharias et al. 2000) lists nearly identical proper motion measurements for GD 683 and GD 683B. But for some unknown reason in the UCAC2 catalog, the proper motion of GD 683B changes to approximately half of its former value and GD 683 is completely absent (Zacharias et al. 2004). Because of this discrepancy, a (less accurate) measurement was made for this work (Table 10).

Furthermore, with  $K = 11.28$  mag from Table 4 and  $M_K = 6.00$  mag for spectral type M2 (solar metallicity), the photometric distance to GD 683B is  $d = 114$  pc. There exist two temperature and surface gravity determinations for the DA white dwarf GD 683; their average gives  $T_{\text{eff}} = 30,000$  K and  $\log g = 7.79$ , which imply  $M_V = 9.31$  mag and a photometric distance of  $d = 121$  pc, consistent with companionship between the pair.

##### A.4.3. PG 0933+729

PG 0933+729B is retained as a candidate because there currently exists no optical photometric nor spectroscopic data. The photographic magnitudes,  $B_{pg} = 16.6$  mag,  $R_{pg} = 14.4$  mag in the USNO catalog, together with the near-infrared magnitudes in Table 5, imply a  $V - K$  color of an early M dwarf (type M2 or earlier) and a photometric distance  $\sim 120$  pc. The white dwarf is type DA3,  $T_{\text{eff}} = 17,400$  K at  $d \approx 90$  pc (Liebert et al. 2005).

## A.5. Outstanding Doubles & Triples

New information gleaned in this work – specifically, data on previously unknown companions – provides more accurate descriptions and parameterizations of many single and a few double degenerates. In several cases of confirmed white dwarf plus red dwarf binaries, the photometric distance to the white dwarf does not agree with the photometric distance to the red dwarf. In cases where the red dwarf appears overluminous, this may be explained by binarity. However, there are several cases where the red dwarf appears significantly underluminous. Although a metal-poor M companion would be subluminous with respect to the main sequence, it is more likely that the distance to the white dwarf is inaccurate as none of the M dwarf companions appear to have metal-poor spectra.

### A.5.1. G21-15

G21-15 is a triple degenerate, only the second known. Its hierarchy is similar to the only other known triple degenerate (WD 1704+481; Maxted et al. 2000a), with one close double degenerate (Saffer et al. 1998) plus the widely separated cool white dwarf reported here. Maxted & Marsh (1999) report a 6.27 d period in the single lined DA spectroscopic binary.

This system has a trigonometric parallax  $\pi = 0.0182 \pm 0.0023''$  and hence distance  $d = 54.9 \pm 7.1$  pc (Bergeron et al. 2001). Treating the primary DA as a single star, the photometric analysis of Bergeron et al. (2001) yields  $T_{\text{eff}} = 12,240$  K,  $\log g = 7.00$ ,  $M = 0.23 M_{\odot}$ , and  $M_V = 10.19 \pm 0.28$  mag. The spectroscopic analysis of the primary gives  $T_{\text{eff}} = 14,800$  K,  $\log g = 7.61$ , and  $M = 0.39 M_{\odot}$  (Bragaglia et al. 1995; Maxted & Marsh 1999; Bergeron et al. 2001). The spectroscopic method produces the wrong absolute magnitude but more accurately determines mass, which is an intermediate value of the masses of the individual double degenerate components (Bergeron et al. 1991).

If one assumes that the two white dwarfs are equally luminous, the mass of each component ( $M \approx 0.4 M_{\odot}$ ; Bergeron et al. 2001), is still less than the cutoff for CO core white dwarfs. Hence it is possible that the close binary consists of two low mass, He core white dwarfs (Bergeron et al. 1992; Marsh et al. 1995). This scenario is consistent with the spectroscopy, photometry, and parallax. But this fails to correctly predict the single lined DA nature of the system, unless one of the stars is a yet undetected DB, which is unlikely (Bergeron et al. 1992; Bergeron & Liebert 2002).

The other possibility is two white dwarfs with different luminosities – some combination of different masses and temperatures. Is there a scenario which is consistent with all the observations? The answer is yes. In order to display a single lined DA spectrum with a 6.27 d period, whose Balmer line profiles yield  $\log g \approx 7.6$ ,  $M \approx 0.4 M_{\odot}$ , one needs a relatively low mass hot component and a relatively high mass cool component. The observational data can be reproduced by assuming two DA stars at 55 pc, one with  $M = 0.60 M_{\odot}$  (log

$g = 8.0$ ),  $T_{\text{eff}} = 10,000$  K,  $M_V = 12.15$  mag, and the other with  $M = 0.35 M_{\odot}$  ( $\log g = 7.4$ ),  $T_{\text{eff}} = 15,000$  K,  $M_V = 10.38$  mag. Therefore the most likely nature of the double degenerate is a He core and a CO core white dwarf.

The optical and near-infrared colors of G21-15C (Table 5) are consistent with a helium atmosphere (it is too red for a hydrogen atmosphere) degenerate with  $T_{\text{eff}} = 4750$  K. The trigonometric parallax gives  $M_V = 15.30 \pm 0.28$  mag and indicates a radius corresponding to  $\log g \approx 8.0$ , or  $M = 0.57 M_{\odot}$ . The cooling age of a helium atmosphere white dwarf with such parameters is 6.6 Gyr. Its kinematics are consistent with a disk star of age  $\tau = 5 - 10$  Gyr (Table 1).

It is somewhat surprising that such an old disk white dwarf is not more massive than  $M = 0.57 M_{\odot}$ . If correct, this implies the total age of G21-15C, and hence the entire system, is likely to be closer to 8 Gyr. The initial to final mass relation for white dwarfs indicates that degenerate stars less massive than  $0.6 M_{\odot}$  have descended from main sequence progenitors less massive than  $2 M_{\odot}$  (Weidemann 1987, 1990, 2000; Bragaglia et al. 1995). Such a progenitor should have had a main sequence lifetime of more than 1.5 Gyr (Girardi et al. 2000), yielding a total age for G21-15C of  $\tau > 8.1$  Gyr.

Designating the brighter, He core white dwarf G21-15A and the fainter, putative CO core white dwarf G21-15B, the cooling age of G21-15C can be used as a constraint on the overall age of the system and place upper limits to the masses of both main sequence progenitor components of the double degenerate. Using  $T_{\text{eff}} = 15,000$  K for G21-15A and  $T_{\text{eff}} = 10,000$  K for G21-15B, they have been cooling for 0.1 and 0.6 Gyr respectively. If the above analysis is correct, the entire system is at least 8.1 Gyr old and hence the progenitors of G21-15A & B were very nearly solar mass stars (Girardi et al. 2000).

A He core white dwarf is born as it ascends the red giant branch for the first time, its outer layers stripped before helium burning can begin (Bergeron et al. 1992; Marsh et al. 1995). G21-15A began this ascent after at least 8 Gyr on the main sequence, corresponding to a star with  $M \leq 1.10 M_{\odot}$  (Girardi et al. 2000). G21-15B completed its main sequence evolution 0.5 Gyr before component A became a red giant, and hence came from a slightly more massive progenitor with  $M \sim 1.15 M_{\odot}$  (Girardi et al. 2000).

Now a complete picture, albeit speculative, of the entire evolution of the double degenerate can emerge. The progenitors of G21-15A & B were probably two nearly solar mass stars with separation  $\lesssim 1$  AU. The more massive component B left the main sequence first, without any mass transfer in the relatively wide binary during its first red giant phase. Upon ascending the asymptotic giant branch, component B forms a common envelope around the binary and the orbit shrinks significantly due to loss of angular momentum. The resulting close separation is enough to cause component A to overfill its Roche lobe as a first ascent giant and become a He core white dwarf (Nelemans et al. 2001).

### A.5.2. GD 319

GD 319 is a triple system consisting of an sdB with a close unseen companion (Saffer et al. 1998) plus the widely separated M3.5 dwarf reported here. The lower limit for the mass of the unseen companion is  $M \sin i = 0.9 M_{\odot}$ , which is in a 0.6 d orbit around the sdB (Maxted et al. 2000c).

Although not a white dwarf, GD 319 was included in the survey due to its presence in McCook & Sion (1987). It was later reclassified as type sdB by Saffer et al. (1998), who also first detected its radial velocity variations. sdB stars such as GD 319 are thought to be helium burning stars with very thin hydrogen envelopes which eventually cool to become white dwarfs with  $M \approx 0.5 M_{\odot}$  (Saffer et al. 1994). These hot subdwarfs may form analogously to low mass white dwarfs, their surface hydrogen layers mostly removed by a close companion (Iben & Livio 1993). Hence, GD 319 is representative of a white dwarf system.

There is a K star located  $\approx 3''$  away from GD 319, but it was shown to be physically unrelated (McAlister et al. 1996). Most photometry reported in the literature for GD 319 is contaminated by the K star. The values for GD 319AB in Table 5 are measurements from images in which both stars were well resolved from one another and there should be no such contamination (McAlister et al. 1996; Farihi 2004b). The near-infrared photometry was performed on images taken at Keck Observatory and the results indicate the K star is a foreground object.

Although the mass of the close companion GD 319B is unknown, the lower limit indicates that it is a likely M dwarf, unless  $i < 9^{\circ}$ . It is difficult to say whether the near-infrared photometry of the sdB+dM reveals a near-infrared excess. The measured  $V - K = -0.80$  is slightly less blue than one would expect for a 30,000 K star but an effective temperature for GD 319 has not been established. In any case, were the unseen companion a dK and not a dM star, one would expect a definite excess at  $K$  band. To illustrate, an M0V star has  $M_K \approx 5.0$  mag, while an sdB has  $M_V \approx 4.5$  mag (Maxted et al. 2000c) plus  $V - K \approx -1$  for a 30,000 K object. Their combined contribution at  $2.2 \mu\text{m}$  would be  $M_K \approx 4.5$  mag – an excess of  $\sim 1$  mag, but this excess is not seen, so the unseen companion cannot be a K dwarf.

The wide tertiary component, GD 319C, can be used to constrain the distance to the system. This is helpful because at  $d \sim 400$  pc, GD 319 is too far away for a trigonometric parallax measurement. Using empirical optical and near-infrared absolute magnitudes for an M3.5 dwarf, the distance modulus for GD 319C is  $m - M = 7.39 \pm 0.10$  or  $d = 300 \pm 14$  pc. This yields  $M_V = 5.3$  mag for GD 319A. This further constrains the spectral type of GD 319B to later than  $\sim$  M3.5 (because such a companion would imply  $V - K \approx -0.5$  for GD 319AB), implying a mass in the range  $0.3 M_{\odot} > M \geq 0.09 M_{\odot}$ . This in turn limits the inclination of the orbit by  $\sin i > 0.09/0.3 = 0.3$ , which yields  $i > 17.5^{\circ}$ .

### A.5.3. *LDS 826*

LDS 826 is a triple system consisting of a white dwarf plus red dwarf visual pair together with the widely separated M8 dwarf reported here and in Scholz et al. (2004). The data analyzed for this work indicate the system is a DA5.5+M3.5+dM8 which differs slightly from that given in Scholz et al. (2004). There is a significant amount of published data on this system and its components which may be inaccurate according to the uncontaminated (§4.5) photometric data presented here (see Farihi (2004b) for details).

### A.5.4. *PG 0824+288*

PG 0824+288 is a triple system consisting of a DA1 plus dwarf carbon star double lined spectroscopic binary (Heber et al. 1993) in a visual pair with the M3.5 dwarf reported here. The spectroscopic binary has been searched unsuccessfully for radial velocity variability (Maxted et al. 2000). An astrometric measurement of the blended ( $a \sim 3''$ ) visual double between POSS I & II epochs reveals the pair moving together with the proper motion listed in Table 4. The visual binary was first suspected by Green & Margon (1994), but remained unconfirmed until now.

One can estimate the distance by noting that the visual magnitude of the composite spectroscopic binary,  $V = 14.22$  mag, is estimated to have a 25% contribution from the dwarf carbon star, PG 0824+288B (Heber et al. 1993), yielding  $V = 14.53$  mag for the white dwarf. Two spectroscopic analyses of PG 0824+288A give significantly different mass estimates but similar effective temperatures; Marsh et al. (1997) give  $T_{\text{eff}} = 51,900$  K and  $\log g = 8.00$ , while Finley et al. (1997) give  $T_{\text{eff}} = 50,500$  K and  $\log g = 7.43$  (Marsh et al. 1997). The absolute magnitudes predicted by models for these two spectroscopic parameter fits are quite different –  $M_V = 9.09$  mag ( $d = 122$  pc) versus  $M_V = 8.12$  mag ( $d = 191$  pc).

The nearby visual M dwarf companion, PG 0824+288C, has an estimated spectral type of M3.5 (Green & Margon 1994). This is consistent with its estimated color,  $V - K \approx 4.8$ , calculated from the  $\Delta g = 3.0$  mag difference between the components of the visual pair (Green & Margon 1994), plus the measured  $K$  magnitude. Comparing the  $J$  &  $K$  values in Table 5 with the absolute magnitudes of an M3.5 dwarf, the distance modulus is  $m - M = 5.31$ , or  $d = 115$  pc, which is inconsistent with the mass and radius determined by Finley et al. (1997). Therefore, it appears likely that PG 0824+288A is a  $\log g = 8.0$  white dwarf with a mass of  $M = 0.70 M_{\odot}$  at  $d \approx 120$  pc.

### A.5.5. *PG 1204+450*

PG 1204+450 is a triple system consisting of a double lined DA spectroscopic binary plus the widely separated M4 dwarf companion reported here (Saffer et al. 1998; Maxted et al. 2002b). The spectroscopic binary consists of an approximate DA2+DA3 with a 1.6 d

period and a mass ratio of  $M_A/M_B = 0.87$  (Maxted et al. 2002b). They resolved the H $\alpha$  line core into two components and give  $T_{\text{eff}} = 31,000$  K,  $M = 0.46 M_{\odot}$  for PG 1204+450A and  $T_{\text{eff}} = 16,000$  K,  $M = 0.52 M_{\odot}$  for PG 1204+450B. One should keep in mind that these are estimates and that it is not possible to perform a spectroscopic fit of the Balmer lines for the individual components.

Liebert et al. (2005) give  $T_{\text{eff}} = 22,600$  K,  $M = 0.52 M_{\odot}$  in a recent update of previous work (Bergeron et al. 1992), which treats the double degenerate as a single star. If these newer parameters are accurate, then the individual component masses inferred by Maxted et al. (2002b) should change similarly to 0.50 and 0.57  $M_{\odot}$  for components A & B respectively.

The wide M4 companion, PG 1241+450C, should be able to constrain the effective temperatures and absolute magnitudes of PG 1241+450 A & B by constraining the distance to the system. Using empirical optical and near-infrared absolute magnitudes for an M4 dwarf, the distance modulus for PG 1241+450C is  $m - M = 5.30 \pm 0.11$  or  $d = 115 \pm 6$  pc. This implies an absolute magnitude for PG 1241+450AB of  $M_V = 9.74$  mag. If the flux ratio at  $V$  is similar to the estimated luminosity ratio from Maxted et al. (2002b), this implies  $M_V = 10.17$  mag and  $M_V = 10.95$  mag for components A & B respectively. Using these absolute magnitudes and estimated masses from the previous paragraph, models predict  $T_{\text{eff}} = 22,000$  K for PG 1204+450A and  $T_{\text{eff}} = 16,500$  K for PG 1204+450B.

#### A.5.6. PG 1241–010

PG 1241–010 is a triple system consisting of a close double degenerate plus the visual M9 companion reported here. The close binary is a single lined DA in a 3.3 d orbit (Marsh et al. 1995).

Liebert et al. (2005) give  $T_{\text{eff}} = 23,800$  K,  $M = 0.40 M_{\odot}$  in a recent update of previous work (Bergeron et al. 1992), treating the double degenerate as a single star. As in the case of G21-15 above, this close binary is likely to be composed of one relatively hot He core white dwarf plus another relatively cool CO core white dwarf. The spectroscopically determined absolute magnitude for PG 1241–010,  $M_V = 9.3$  mag (Bergeron et al. 1992; Liebert et al. 2005), is almost certainly an underestimate due to the presence of not one but two white dwarfs. Unfortunately, parameter estimates for the individual components do not exist in the literature

PG 1241–010C was first recognized by Zuckerman & Becklin (1992) and is one of the latest known confirmed companions to a white dwarf. The photometric distance to the tertiary may be used as a constraint on the distance to the system. Its  $I$  band magnitude was very difficult to measure due to the  $\Delta I > 4$  mag difference between components C & AB, just 3'' apart. In any case, its colors (Table 5) are consistent with spectral types M8–M9. Comparing its apparent  $K$  magnitude with absolute magnitudes of M8 and M9 spectral standards, the resulting distance modulus is bounded by  $4.14 < m - M < 4.44$  or  $d = 72 \pm 5$  pc.



This distance yields  $M_V = 9.71 \pm 0.15$  mag for PG 1241–010AB, but a single 24,000 K DA white dwarf with  $\log g = 7.5$  ( $M = 0.41 M_\odot$ ) should have  $M_V = 9.65$  mag according to models, implying that PG1241–010B contributes almost nothing to the overall  $V$  band flux. A distance around  $d = 72$  pc is also inconsistent with the previous spectroscopic mass determination of  $M = 0.31 M_\odot$  ( $M_V = 9.2$  mag) for PG 1241–010AB. Assuming the above distance bounds and the spectroscopic temperature of PG 1241–010A are correct (with  $\log g = 7.5$ ), the maximum contribution from PG 1241–010B is  $M_V = 12.3$  mag, implying  $T_{\text{eff}} < 10,000$  K for a  $\log g = 8.0$  white dwarf. However, it is possible that PG 1241–010C is itself binary, indicating a distance up to  $d = 109$  pc (two identical M8 dwarfs) and more consistent with the spectroscopically determined parameters of PG 1241–010AB.

#### A.5.7. G261-43

G261-43A is a DA3 white dwarf with a trigonometric parallax of  $\pi = 0.471''$  (McCook & Sion 1999). McMahan (1989) reports and compares three independent determinations of effective temperature and surface gravity, all of which agree very well at  $T_{\text{eff}} = 15,400$  K and  $\log g = 7.9$ . Models predict  $M = 0.57 M_\odot$  and  $M_V = 11.04$  mag, compared with  $M = 0.61 M_\odot$  and  $M_V = 11.19$  mag from its parallax. Hence, G261-43 is a DA white dwarf with a typical mass (Bergeron et al. 1992).

The binary nature of G261-43 was first reported by Zuckerman et al. (1997). An almost certain white dwarf itself, G261-43B is located only  $1.4''$  away and quite faint relative to its primary ( $\Delta V \approx 3.5$  mag).

The roughly estimated effective temperature of G261-43B ( $\sim 5000$  K; Zuckerman et al. 1997) is probably a bit too low given the photometry. Although the near-infrared photometry had good S/N, the optical measurements were difficult due to the brightness ratio of primary to secondary (B. Zuckerman 2004, private communication). Using the three most reliable magnitudes available ( $I = 15.7$  mag,  $J = 15.34$  mag,  $K = 15.05$  mag) and the resulting colors, hydrogen atmosphere models predict  $T_{\text{eff}} = 6000$  K almost exactly, regardless of surface gravity. Combining this effective temperature with the trigonometric parallax gives  $\log g = 8.39$  and  $M = 0.84 M_\odot$  for G261-43B. Therefore, the difference in radii between components A & B is likely to be significant (Zuckerman et al. 1997).

If this analysis is correct, the main sequence progenitor of G261-43A spent about 4.4 Gyr on the main sequence and as a giant. This is the difference between the 4.6 Gyr cooling age of component B and the 0.2 Gyr cooling age of component A. The mass of a main sequence star with such a lifetime, including post main sequence evolution, should be just greater than  $1.3 M_\odot$  (Girardi et al. 2000).

#### A.5.8. PG 0901+140

PG 0901+140 is a visual double degenerate with a separation on the sky of  $3.6''$ . Despite several studies and comparable luminosities between its two components ( $\Delta V \approx 0.5$  mag), the binarity has never been mentioned in the literature (Green et al. 1986; Bergeron et al. 1990; Liebert et al. 2005).

Liebert et al. (2005) give  $T_{\text{eff}} = 9200$  K,  $\log g = 8.29$ , and  $M_V = 12.91$  mag for PG 0901+140 by spectroscopic analysis, assuming it is a single star. Comparison of hydrogen atmosphere model colors to the optical and near-infrared photometry in Table 5 yields  $T_{\text{eff}} = 9500$  K for the brighter component PG 0901+140A, and  $T_{\text{eff}} = 8250$  K for the fainter component PG 0901+140B. These effective temperatures are quite consistent with the combined effective temperature determination, whereas the spectroscopically determined mass ( $M = 0.79 M_{\odot}$ ; Liebert et al. 2005) is an intermediate value of the masses of the individual double degenerate components (Bergeron et al. 1991). Assuming a luminosity ratio of 1.6:1 between components A & B (from the 0.5 mag average of  $\Delta V$  and  $\Delta R$ ), a reasonable guess at the individual masses is  $M = 0.78 M_{\odot}$  for PG 0901+140A and  $M = 0.81 M_{\odot}$  for PG 0901+140B. If correct, this would place the system at a little more than  $d = 40$  pc.

Further speculation is not worthwhile, since the component parameters of the resolved double degenerate can be determined from individual spectra. Such a determination would be very useful for the white dwarf initial to final mass relation – analogous to the analysis of PG 0922+162A & B by Finley & Koester (1997).

#### A.5.9. LP 618-14

LP 618-14 was identified by S. Salim (2002, private communication) during a survey intended to find previously unidentified white dwarfs in the new Luyten two tenths catalog (Salim & Gould 2002). Its reduced proper motion placed it within the white dwarf sequence while its Sloan colors were a little too red for a single degenerate star.

Its spectrum in Figure 49 reveals the blue continuum of a cool DA or DC star plus the TiO bands of a red dwarf. Unfortunately, the spectrum has sufficiently low S/N as to preclude a more precise estimate of the white dwarf effective temperature. Also the *UBV* photometry was performed on images acquired under less than ideal weather conditions. The  $U - B = -0.45 \pm 0.15$  color of LP 618-14 is consistent with a large range of effective temperatures: 6000 – 13,000 K for a hydrogen atmosphere white dwarf with  $\log g = 8.0$ , up to 15,000 K for  $\log g \leq 7.5$ , but only 6000 – 8000 K for  $\log g \geq 8.5$  or for a helium atmosphere at any value of  $\log g$ . Additionally, it is not known whether the red dwarf contributes significantly at *B* band. A good blue spectrum and photometric *UBV* data would end this ambiguity.

The luminosity contribution of the two components is further confused by the scenario described in §4.4 because the distance to the system is not known. The reduced proper

motion indicates LP 618-14 should be within 50 pc of the sun ( $\mu = .32'' \text{ yr}^{-1}$ ), but this interpretation is thwarted by predicting a spectral type later than M7 for the red dwarf companion ( $M_K \geq 10.0 \text{ mag}$ ). This appears to be inconsistent with the spectrum in Figure 49. Alternatively, if one constrains the spectral type of the secondary to be no later than M5, then the system is located at  $d > 100 \text{ pc}$  and has a very high tangential velocity ( $v_{tan} > 150 \text{ km s}^{-1}$ ). This results in a white dwarf with a relatively large radius at  $\sim 9000 \text{ K}$  – a He core degenerate with  $M < 0.4 M_\odot$ . This is a real possibility for any white dwarf in a close binary (Marsh et al. 1995) but further investigation is required before firm conclusions may be drawn.

#### A.5.10. LP 761-114

LP 761-114 is first mentioned in Oswalt et al. (1996) as a white dwarf in a wide binary system, where it is reported as the lowest luminosity star in a sample used to place a lower limit to the age of the Galactic disk. Silvestri et al. (2002) and Holberg et al. (2002) corroborate this interpretation, reporting  $V = 17.45 \text{ mag}$ ,  $V - I = 1.75$ ,  $T_{\text{eff}} = 4020 \text{ K}$ , and a photometric distance of  $d = 15.3 \text{ pc}$ .

However, the M2 dwarf common proper motion companion absolutely rules out a distance  $d < 30 \text{ pc}$  (see below). Also, this bright neighbor can easily contaminate photometric measurements of the cool white dwarf. The M2 companion  $7.7''$  distant positively dominates the binary flux ratio at all wavelengths, including  $U$  band where it is over 2 magnitudes brighter(!) than the white dwarf. It gets much worse toward longer wavelengths with  $\Delta V = 4.3 \text{ mag}$ ,  $\Delta I = 5.8 \text{ mag}$ .

The photometry presented for LP 761-114 in Table 5 was measured with near zero contamination as described in §4.5, and tells a slightly different story than existing analyses (Oswalt et al. 1996; Silvestri et al. 2002; Holberg et al. 2002). The  $V$  magnitude measured here is 0.4 mag fainter and the measured color of  $V - I = 0.73$  is much bluer – a clear sign that prior measurements were contaminated by the relatively bright M companion.

The resulting optical and near-infrared colors of LP 761-114 are not consistent with a 4000 K helium atmosphere white dwarf (Holberg et al. 2002). Comparing its colors (e.g.  $U - B = -0.31$ ,  $V - J = 1.17$ ) with models of cool helium and hydrogen atmosphere white dwarfs, one finds very good agreement with a hydrogen atmosphere degenerate at  $T_{\text{eff}} = 6000 \text{ K}$ . The near-infrared measurements were extremely difficult due to the  $\Delta m = 6.5 - 7 \text{ mag}$  brightness difference between components and these data possess the lowest (but still reliable) S/N of all the photometry performed on this system.

Is this interpretation consistent with the photometric distance to the M2 dwarf companion? Comparing the optical and near-infrared magnitudes of LP 761-113 from Table 5 with spectral standard absolute magnitudes, the distance modulus is  $m - M = 3.38 \pm 0.04$  or  $d = 47.4 \pm 0.9 \text{ pc}$ . This yields  $M_V = 14.45 \text{ mag}$  for the white dwarf, indicating  $\log g = 8.17$  or  $M = 0.70 M_\odot$  – a reasonable mass for a white dwarf that has been cooling for more than

3.2 Gyr.

*A.5.11. PG 1539+530*

PG 1539+530 is listed as a DA2 in McCook & Sion (1987) but is mysteriously absent from McCook & Sion (1999). The PG catalog lists type DA2 for this star and in the comments column of Table 5 is the note “DBL” (Green et al. 1986). The removal of an object from the white dwarf catalog is usually a sign of misclassification, but in this case the original classification is the correct one.

The composite spectrum of PG 1539+530AB is shown in Figure 46. It clearly displays the spectral features of an early M dwarf plus a few pressure broadened Balmer lines typical of hot white dwarfs. The  $H\alpha$  line has been completely masked by the brighter M companion, but at least 3 more hydrogen lines are visible out to a partial  $H\epsilon$ .

The pair has been resolved at a separation of  $2.7''$  on the sky. The M dwarf component, PG 1539+530B, has colors and a spectrum consistent with spectral type M2. The white dwarf component, PG1539+530A, has optical and near-infrared colors consistent with a  $T_{\text{eff}} = 25,000$  K DA star and is actually fainter than its companion at  $V$  band and longward. Comparison of the photometry in Table 5 with the optical and near-infrared absolute magnitudes for M2 dwarfs yields a photometric distance of  $d = 162 \pm 4$  pc for PG 1539+530B. At this distance, a 25,000 K DA white dwarf has  $M_V = 10.47$  mag,  $\log g = 8.09$  and a mass of  $M = 0.69 M_{\odot}$  according to models.

*A.5.12. PG 2244+031*

PG 2244+031 is noted as a DA1 with a composite spectrum in the PG catalog (Green et al. 1986). The present work designates the system as a visual binary consisting of the DA1 white dwarf PG 2244+031A plus an M3.5 dwarf companion at  $2.4''$ , PG 2244+031B. The composite optical spectrum of the binary is shown in Figure 48.

However, there is significant confusion in the literature regarding the coordinates, identity, finding chart, and designated WD number for PG 2244+031. In fact, there are no less than four objects associated with PG 2244+031; the following paragraphs should clarify the situation.

Object 1, PG 2244+031 (WD 2244+031) was first reported as type DC by Green (1980) and this paper contains the only published finding chart for any of the four objects. The coordinates given in Table 3 of Green (1980) for object 1 more or less correctly identify the position of PG 2244+031AB. The correct coordinates are  $22^{\text{h}}44^{\text{m}}49.7^{\text{s}}$ ,  $+03^{\circ}05'54''$  B1950 or  $22^{\text{h}}47^{\text{m}}22.3^{\text{s}}$ ,  $+03^{\circ}21'45''$  J2000.

Object 2, HS 2244+0305 (WD 2244+030) is designated as a DA1 (Homeier et al. 1998)

with coordinates identical to those of object 1 listed above, but is listed separately from PG 2244+031 in the current version of the online white dwarf catalog. This is an error; WD 2244+031 and WD 2244+030 are the same object.

Object 3 is the star which is identified in the finding chart of Green (1980) for PG 2244+031. This chart points to coordinates  $22^{\text{h}}44^{\text{m}}16^{\text{s}}$ ,  $+03^{\circ}06'20''$  B1950 or  $22^{\text{h}}46^{\text{m}}48^{\text{s}}$ ,  $+03^{\circ}22'10''$  J2000 and a completely different object from PG 2244+031. Photometry was performed on object 3 and it has  $B - V = 0.44$  and  $V - K = 1.37$ . These values are consistent with the colors of a G0 star.

Object 4 is the star corresponding to the coordinates in the PG catalog for PG 2244+031. These coordinates neither match the finding chart of Green (1980) nor the coordinates in Table 3 of Green (1980). The PG coordinates are  $22^{\text{h}}44^{\text{m}}25^{\text{s}}$ ,  $+03^{\circ}08'52''$  B1950 or  $22^{\text{h}}46^{\text{m}}57^{\text{s}}$ ,  $+03^{\circ}24'41''$  J2000 (Green et al. 1986). No finding chart is provided as the identity and coordinates of object 3 in Green (1980) and object 4 in Green et al. (1986) are assumed to be one and the same. However, photometry was performed on object 4 and it has  $B - V = 0.50$  and  $V - K = 1.51$ . These values are consistent with the colors of a G5 star.

In summary, the objects PG 2244+031, WD 2244+031, HS 2244+0305, & WD 2244+030 are identical to the DA1+M3.5 visual binary described here as PG 2244+031AB. All published coordinates for these objects are in error with the exception of those in Green (1980), and more accurately in Homeier et al. (1998). The only correct finding chart in the literature is the one shown here in Figure 22.

#### A.5.13. GD 74

GD 74A is well cited in the literature but only one study has produced a distance estimate. Bergeron et al. (1992) give  $T_{\text{eff}} = 16,900$  K,  $\log g = 7.99$ ,  $M = 0.59 M_{\odot}$ , and  $M_V = 11.11$  mag for GD 74A. If correct, this would place the DA white dwarf at just under  $d = 60$  pc.

However, the optical and near-infrared colors inferred from the photometry in Table 5 indicate an effective temperature higher than 17,000 K for GD 74. With colors such as  $V - K = -0.79$ , hydrogen atmosphere white dwarf models predict a temperature much closer to 25,000 K. Such a DA2 star with  $\log g = 8.0$  would have a photometric distance closer to 85 pc. Comparison of the photometry in Table 5 with the optical and near-infrared absolute magnitudes for M4 dwarfs yields a photometric distance of  $d = 97 \pm 6$  pc for GD 74B.

#### A.5.14. GD 123

GD 123A is a DA white dwarf that has been repeatedly studied in the literature, with a well corroborated  $T_{\text{eff}}$  near 30,000 K. The average of five independent spectroscopic analyses gives  $T_{\text{eff}} = 29,500$  K,  $\log g = 7.92$ , and  $M_V = 9.86$  mag (Finley et al. 1997; Marsh et al.

1997; Vennes et al. 1997; Napiwotzki et al. 1999; Liebert et al. 2005). This would place the GD 123 system near  $d = 81$  pc.

The binarity of GD 123 was first found by Green et al. (1986) who noted a composite spectrum of a DA4+K. Optical and near-infrared analysis done here indicates that GD 123B is an M4.5 dwarf with photometric distance  $d = 67 \pm 2$  pc.

#### A.5.15. GD 337

GD 337A is reported as a DA2 white dwarf in McCook & Sion (1999), recently corroborated by Liebert et al. (2005) who give  $T_{\text{eff}} = 22,400$  K,  $\log g = 7.80$ , and  $M_V = 10.23$  mag. A photometric distance of  $d = 151$  pc is inferred from these data. GD 337 also has three parallax measurements in McCook & Sion (1999), all of which give  $\pi \leq 0.004''$

Probst (1983) first detected the still unresolved companion by its near-infrared excess emission. The presence of a late type companion has been confirmed by its observed composite spectrum (Green et al. 1986; Greenstein 1986b). The analysis here places GD 337B at spectral type M4.5. Comparing its inferred optical and near-infrared magnitudes with the absolute magnitudes of M4.5 dwarfs, its photometric distance is  $d = 180 \pm 5$  pc.

#### A.5.16. GD 984

GD 984A is a well studied hot DA white dwarf. At least five independent spectroscopic studies have been carried out, yielding average parameters of  $T_{\text{eff}} = 49,000$  K,  $\log g = 7.85$ , and  $M_V = 8.95$  mag (Finley et al. 1997; Marsh et al. 1997; Vennes et al. 1997; Napiwotzki et al. 1999; Koester et al. 2001). If correct, this would place the system near  $d = 108$  pc.

There is some spread in the derived effective temperatures and surface gravities for GD 984A, perhaps due to its unresolved companion, GD 984B. The M2 dwarf contaminates the Balmer lines of the white dwarf as blue as  $H\gamma$ , making spectroscopic parameter fits less certain (Finley et al. 1997). The spread in temperature estimates ranges from 43,000–57,000 K and surface gravity from  $\log g = 7.7 - 8.2$  (Marsh et al. 1997; Koester et al. 2001).

What does the photometric distance to GD 984B say? Comparing its optical and near-infrared photometry in Table 6 with the absolute magnitudes for an M2 dwarf, the distance is  $d = 185 \pm 2$  pc. There is a significant difference between this distance for GD 984B and  $d = 108$  pc derived for GD 984A. Since there is a fair amount of room for uncertainty in parameters of the white dwarf, it is quite possible the farther distance is the correct one. At  $d = 185$  pc, GD 984A would have  $M_V = 7.77$  mag. Even with  $T_{\text{eff}} = 60,000$  K, this would imply a radius too large for a single white dwarf with  $M \geq 0.5 M_{\odot}$ . At  $T_{\text{eff}} = 50,000$  K, this implies  $\log g = 7.23$  or  $M = 0.43 M_{\odot}$ . Therefore, if GD 984A is 185 pc away, then it is almost certainly a double degenerate or low mass, He core white dwarf.

#### A.5.17. LTT 8747

LTT 8747A is a nearby cool DA star ripe for a trigonometric parallax measurement. The ARICNS database (Gliese & Jahreiß 2000) gives a *photometric* parallax of  $0.051 \pm 0.006''$  but it is not included in a recent list of white dwarfs within 20 pc (Holberg et al. 2002). The reason stated in Holberg et al. (2002) for exclusion is that it belongs to a group of white dwarfs which “all have trigonometric parallaxes smaller than  $0.05''$ ” while citing McCook & Sion (1999). This may be an error because the ARICNS value of  $0.051''$  is cited in McCook & Sion (1999) by mistake as a *trigonometric* parallax and no other value or measurement exists in the literature.

The photometric distance of 19.6 pc may be reliable as it is based only on *UBV* photometry (ARICNS). Zuckerman et al. (2003) report  $T_{\text{eff}} = 7660$  K and  $\log g = 7.80$  from *UBVRI* photometry and parallax (which must be the same *photometric* parallax mentioned above). This effective temperature is likely a bit too low as LTT 8747B contributes to the *I* band flux, causing the white dwarf to appear slightly cooler.

The analysis here finds  $T_{\text{eff}} = 8500$  K is quite consistent with both the *UBV* and Stromgren colors of LTT 8747A (both published and those measured in this work; Eggen & Greenstein 1965; McCook & Sion 1999). This results in a photometric distance of  $d = 22.6$  pc for  $\log g = 8.0$ .

The possible radial velocity companion (Schultz et al. 1996; Maxted et al. 2000), LTT 8747B is certainly a late M dwarf by both its contribution to the composite spectrum in Figure 53 (at least one band of VO can be seen) and by the  $J - K = 1.10$  composite color of the binary (Kirkpatrick et al. 1991; Kirkpatrick & McCarthy 1994; Kirkpatrick et al. 1999b). The deconvolved colors of LTT 8747B indicate an M8 dwarf with an uncertainty of 1 spectral type. If it has an absolute *K* magnitude typical of an M8 dwarf, then  $d = 19.4$  pc is inferred. At this distance LTT 8747A would have  $M_V = 13.10$  mag,  $\log g = 8.20$ , and  $M = 0.73 M_{\odot}$  for  $T_{\text{eff}} = 8500$  K.

#### A.5.18. PG 0308+096

PG 0308+096 is a post common envelope binary consisting of a DA2 white dwarf and the M4.5 dwarf reported here in a 0.3 d orbit (Saffer et al. 1993). A recent spectroscopic analysis gives  $T_{\text{eff}} = 25,900$  K,  $\log g = 8.08$ , and  $M_V = 10.37$  mag for PG 0308+096A (Liebert et al. 2005). The distance inferred from these white dwarf parameters is  $d = 101$  pc. Comparison of the optical and near-infrared magnitudes of PG 0308+096B with the absolute magnitudes for M4.5 dwarfs, yields a photometric distance  $d = 114$  pc.

*A.5.19. PG 0950+185*

PG 0950+185 is a visual double containing a hot DA white dwarf plus the M2 dwarf reported here 1.1" distant (Green et al. 1986; Greenstein 1986b). The only spectroscopic analysis in the literature gives  $T_{\text{eff}} = 31,800$  K,  $\log g = 7.68$ ,  $M = 0.50 M_{\odot}$ , and  $M_V = 9.29$  mag for PG 0950+185A (Liebert et al. 2005). The distance inferred from these parameters is  $d = 201$  pc.

If this is correct, the implied absolute magnitude of  $M_K = 5.28$  mag for PG 0950+185B is significantly brighter than the expected value of  $M_K = 6.00$  mag for a single M2 dwarf. The difference between the standard optical and near-infrared magnitudes of an M2 dwarf at  $d = 201$  pc and the apparent magnitudes of PG 0950+185B are 0.59 mag at  $I$ , 0.60 mag at  $J$ , 0.70 mag at  $H$ , and 0.72 mag at  $K$ . Hence, if the  $d = 201$  pc distance is accurate, it is likely that PG 0950+185B is a binary M2 dwarf consisting of two nearly equal luminosity stars.

*A.5.20. PG 0956+045*

PG 0956+045 is a visual double containing a DA3 white dwarf plus the M4.5 dwarf reported here 2.0" distant (McCook & Sion 1999). The only spectroscopic analysis in the literature gives  $T_{\text{eff}} = 18,200$  K,  $\log g = 7.81$ ,  $M = 0.52 M_{\odot}$ , and  $M_V = 10.62$  mag for PG 0956+045A (Liebert et al. 2005). The distance inferred from these parameters is  $d = 113$  pc. With empirical optical and near-infrared absolute magnitudes for an M4.5 dwarf, the distance modulus for PG 0956+045B is  $m - M = 6.25 \pm 0.17$  or  $d = 178 \pm 15$  pc.

The  $V$  &  $R$  magnitudes for PG 0956+045B are unusual and do not seem to match what might be expected from a mid M dwarf. Specifically, they are significantly fainter than an extrapolation from the  $IJK$  magnitudes would predict and color indices involving  $V$  &  $R$  appear to be inconsistent with color indices involving only the other photometric bands. It is possible that the  $V$  band magnitude for PG 0956+045B is unreliable due to both low S/N plus additional uncertainty from deconvolving its PSF from the much brighter PG 0956+045A. However, the  $R$  band measurement has  $S/N > 200$ , and is both reliable and robust – the measurement was repeated in numerous ways, always with near zero residuals after PSF subtraction and predicting the correct relative instrumental magnitude for PG 0956+045A (certainly within the typical 0.05 mag standard error). As an example of the resulting discrepancy, the  $I - K = 2.34$  color is consistent with a spectral type of M4 and one might expect something near  $R - I \approx 1.6$  for this spectral type. But PG 0956+045B has  $R - I = 2.24$  and, by itself, predicts a spectral type between M6–M6.5. A spatially resolved optical spectrum of PG 0956+045B might shed light on this issue.

Concerning the mismatch of photometric distances, there are three distinct possibilities. One is that the flux of the red secondary may have contaminated the spectroscopic analysis of Liebert et al. (2005), causing PG 0956+045A to appear cooler than it actually is. A



hotter, more luminous white dwarf would be more consistent with a distance near  $d = 180$  pc. But its measured colors, such as  $V - K = -0.58$ , are consistent with a white dwarf of  $T_{\text{eff}} \approx 17,000$  K. The second possibility is that PG 0956+045B is an M dwarf at  $d = 113$  pc with  $M_K = 8.66$  mag, corresponding to a spectral type near M5.5 for the main sequence. This seems unlikely since such an M dwarf should have  $I - K \approx 3.0$ . A variation of this second prospect could be made by invoking a subdwarf M star to explain the discrepancy between the colors of the secondary and the absolute magnitude implied by  $d = 113$  pc. While this is certainly possible, it is unlikely based on the disk like kinematics of the PG 0956+045 system (Table 1). The third possible explanation is simply that the white dwarf distance has been underestimated due to binarity. A combination of the above factors could explain the discrepancy between the inferred distances of PG 0956+045A & B. In any case, the difference between their photometric distance moduli is greater than 0.9 and is worthy of further exploration.

#### A.5.21. PG 1015+076

PG 1015+076A is a DA2 star that has been repeatedly misclassified as a much cooler white dwarf due to the presence of a background main sequence star  $2.0''$  distant (Green et al. 1986; Zuckerman et al. 2003). The background star has  $V - K = 1.61$  and is probably a G type star. The spectrum of PG 1015+076A in Figure 24 is almost certainly contaminated at some level by the continuum light of the nearby G star. This is why  $H\beta$  &  $H\gamma$  are diluted while  $H\alpha$  is nearly absent. The optical photometry for PG 1015+076A and background G star was performed without mutual contamination. Its optical colors from Table 5 (plus  $U - B = -0.98$ ) indicate  $T_{\text{eff}} \approx 25,000$  K for the white dwarf.

PG 1015+076B is the M3 dwarf common proper motion companion to PG 1015+076A. Comparing its optical and near-infrared magnitudes in Table 5 with the expected absolute magnitudes of a typical M3, the distance modulus is  $m - M = 6.44 \pm 0.06$ , implying  $d = 194 \pm 6$  pc. At this distance PG 1015+076A should have  $M_V = 10.16$  mag, which corresponds to  $\log g = 7.89$ , or  $M = 0.59 M_{\odot}$  for  $T_{\text{eff}} = 25,000$  K.

#### A.5.22. PG 1210+464

PG 1210+464 is an unresolved binary DA+dM, evidenced by its composite spectrum and near infrared excess (Green et al. 1986; Zuckerman & Becklin 1992; Schultz et al. 1996). The white dwarf, PG 1210+464A, has spectroscopic parameters  $T_{\text{eff}} = 27,700$  K,  $\log g = 7.85$ , and  $M_V = 9.87$  mag (Liebert et al. 2005). Hence, its photometric distance is around  $d = 139$  pc. The companion, PG 1210+464B, is estimated to be spectral type M2 based on its deconvolved  $R - I$  and  $I - K$  colors. Comparing its optical and near near-infrared magnitudes in Table 6 with the expected absolute magnitudes of a typical M2 dwarf, the distance is  $d = 111 \pm 4$  pc.

*A.5.23. PG 1654+160*

PG 1654+160 is a relatively rare DB+dM system – the only such system out of 61 white dwarf plus M dwarf pairs discovered or described in this work. PG 1654+160A itself is an uncommon object, a DBV (Winget et al. 1984; Beauchamp et al. 1999).

Spectroscopic investigation indicates the pulsating helium atmosphere white dwarf has parameters in the range  $T_{\text{eff}} = 24,300 - 27,800$  K,  $\log g = 7.95 - 8.00$ , depending on whether there is a trace amount of hydrogen in its atmosphere or none. Helium atmosphere models predict that a white dwarf with  $T_{\text{eff}} = 26,000$  K and  $\log g = 8.0$  would have  $M_V = 10.38$  mag and  $M = 0.61 M_{\odot}$ . If correct, this would place the PG 1654+160 system at a distance near  $d = 171$  pc.

Recent astroseismological analysis of data acquired using the Whole Earth Telescope may corroborate the spectroscopically determined parameters of PG 1654+160A. Detection of nearly equal spacing between pulsation periods was found to be consistent with the expected mean period spacing of a normal mass ( $M \approx 0.6 M_{\odot}$ ) DB white dwarf pulsating in nonradial  $\ell = 1$  modes (Handler et al. 2003).

However, the photometric distance to the M4.5 dwarf companion is positively inconsistent with this interpretation. Comparing the optical and near-infrared magnitudes of PG 1654+160B with absolute magnitudes expected of an M4.5 dwarf yields a distance modulus of  $m - M = 4.49 \pm 0.11$  or  $d = 79 \pm 4$  pc.

This serious discrepancy calls into question the binary nature of the apparent common proper motion pair. It is quite easy to see the elongated pair moving together while blinking the digitized POSS I & II red sensitive plates. Both the relative proper motion and the elongation are readily visible using the blue and near-infrared sensitive scans, but the contrast is best for the red plates where the components have nearly equal brightness. However, the pair is not well resolved in either of the two POSS epochs, and therefore accurate photocenters (centroids) are not possible for any of these digitized scans. The position angle corresponding to the elongation axis appears constant over the 46 year baseline between POSS epochs, consistent with the  $131.0^{\circ}$  value (epoch 2003.3) in Table 3. Using a single centroid for the elongated pair in the POSS I & II red sensitive plate scans, a proper motion of  $\mu = 0.085''$   $\text{yr}^{-1}$  at  $\theta = 137^{\circ}$  is obtained over a 39 year baseline. This value is somewhat greater than the USNO B1.0 catalog value in Table 1 but consistent with an object whose photocenter is biased depending on whether blue (white dwarf dominated centroid), red (maximum elongation) or near-infrared sensitive (red dwarf dominated centroid) POSS plates are used for astrometry. If the two stars are unrelated, and one is a stationary background star, the pair would have separated by as much as  $4.5''$  since the epoch 1950.4 POSS I red plate was observed. The conclusion based on this analysis is that the visual pair is likely a physical binary based on its common proper motion.

Still there remains the  $\Delta m = 1.75$  mag discrepancy between the expected magnitude of an M4.5 dwarf at  $d = 79$  pc versus  $d = 171$  pc. Clearly, the PG 1654+160 system requires

follow up observations and analysis in order to constrain both its distance and the parameters of its components.

#### A.5.24. *PG 1659+303*

PG 1659+303A is a DA white dwarf with spectroscopically determined parameters  $T_{\text{eff}} = 13,600$  K,  $\log g = 7.95$ , and  $M_V = 11.35$  mag (Liebert et al. 2005), corresponding to  $d = 53$  pc. The  $V - K = 4.28$  color of PG 1659+303B places it between spectral types M2–M2.5. Its measured spectrum in Figure 33 is consistent with this interpretation and gives no indication of subsolar metallicity (i.e. it is not a subdwarf). Comparing the expected optical and near-infrared absolute magnitudes with the apparent magnitudes in Table 5, the distance falls in the range  $d = 67 - 82$  pc.

#### A.5.25. *Rubin 80*

Rubin 80A is listed as a DA6 in McCook & Sion (1999) while referencing an unpublished spectrum taken around 1979. Caution is warranted because an unresolved low mass stellar companion can contaminate both spectra and colors, thus causing a white dwarf to appear cooler than it is (Farihi 2004b). Greenstein (1986a) first noted the companion to Rubin 80A in its composite spectrum as well as commenting that the companion affected his measured colors of the white dwarf. Zuckerman et al. (2003) give  $T_{\text{eff}} = 7765$  K based on *UBVRI* colors, but this might be too cool due to the inclusion of the *RI* bands in the determination. Examining only the  $U - B = -0.57$  and  $B - V = +0.28$  colors (this work finds  $U - B = -0.55$ ,  $B - V = +0.29$ ), an effective temperature near 8000 K ( $\log g = 8$ ) is implied by both color indices independently. Hence it appears the DA6 type is likely to be accurate, assuming the flux of Rubin 80B does not contribute at *B* (a safe assumption).

However, the blue continuum slope of Rubin 80 (Figure 52) is slightly steeper than that of LTT 8747 ( $T_{\text{eff}} = 8500$  K, Figure 53), which is consistent with Rubin 80A having a higher effective temperature than LTT 8747. Both stars were observed on the same night with the same instrument, setup and calibration. Possible errors in flux calibration were searched for unsuccessfully and a variety of standard star sensitivity functions were used, all producing similar results. In order to deconvolve the *IJK* magnitudes of the companion, an effective temperature of 9000 K was used for the values in Table 6. While this may be too high, it turns out to be more consistent with the resulting parameters for the red dwarf companion, Rubin 80B. Some representative, plausible white dwarf parameters are given in Table 11. Details can be found in Farihi (2004b).

*A.5.26. Ton S 392*

TS 392A is a very hot DA white dwarf that is not well studied. The only published paper containing data on TS 392A is Greenstein (1979), who notes the white dwarf is a “very hot” narrow lined DA. The coordinates in McCook & Sion (1999) are inaccurate by almost 3'. Accurate coordinates are given in Figure 23 and have been checked against a photographic finding chart provided by J. Greenstein (B. Zuckerman 2002, private communication).

The near-infrared excess of TS 392 was noticed in January 1992 at the IRTF, but remained unpublished until now. Wachter et al. (2003) were the first to publish near-infrared magnitudes for TS 392 which indicate the presence of a cool stellar companion.

The spectrum in Figure 47 has a turnover near its blue end that is almost certainly not real. Possible errors in flux calibration were searched for unsuccessfully. Attempting to correct the turnover to the expected continuum resulted in a sensitivity function that produced grossly incorrect shapes for all other stars taken on the same night with the same instrument and setup. In fact, all the other stars similarly observed appear to have accurately flux calibrated spectra. TS 392 was observed at a high airmass of 2.40 and this may be the source of the error. In any case, the spectrum verifies a fairly steep blue continuum from a hot DA white dwarf with weak  $H\alpha$  &  $H\beta$  absorption, plus TiO bands from its  $\sim 1''$  distant M dwarf companion.

Virtually nothing was known or published about this system until now, so distance estimates and parameter determinations should be considered somewhat preliminary. Treating TS 392A as a  $T_{\text{eff}} = 50,000$  K white dwarf, the deconvolved magnitudes of TS 392B result in colors consistent with an M3 dwarf,  $\pm 1$  spectral type, at a distance of 409 pc.

## REFERENCES

- Alexander, J., & Lourens J. 1969, MNSSA, 28, 95
- Anselowitz, T., Wasatonic, R., Matthews, K., Sion, E., & McCook, G. 1999, PASP, 111, 702
- Beauchamp, A., Wesemael, F., Bergeron, P., Fontaine, G., Saffer, R., Liebert, J., & Brassard, P. 1999, ApJ, 516, 887
- Becklin, E., Farihi, J., Jura, M., Song, I., Weinberger, A., & Zuckerman, B. 2005, ApJ, 632, L119
- Becklin, E., & Zuckerman, B. 1988, Nature, 336, 656
- Beers, T., Chiba, M., Yoshii, Y., Platais, I., Hanson, R., Fuchs, B., & Rossi, S. 2000, AJ, 119, 2866
- Bergeron, P., Kidder, K., Holberg, J., Liebert, J., Wesemael, F., & Saffer, R. 1991, ApJ, 443, 764

- Bergeron, P., Leggett, S., & Ruiz, M. 2001, *ApJS*, 133, 413
- Bergeron, P., & Liebert, J. 2002, *ApJ*, 566, 1091
- Bergeron, P., Ruiz, M., & Leggett, S. 1997, *ApJS*, 108, 339
- Bergeron, P., Saffer, R., & Liebert, J. 1992, *ApJ*, 394, 228
- Bergeron, P., Saumon, D., & Wesemael, F. 1995b, *ApJ*, 443, 764
- Bergeron, P., Wesemael, F., & Beauchamp, A. 1995c, *PASP*, 107, 1047
- Bergeron, P., Wesemael, F., Fontaine, G., & Liebert, J. 1990, *ApJ*, 351, L21
- Bessell, M. 1990, *PASP*, 102, 1181
- Bessell, M., & Brett, J. 1988, *PASP*, 100, 1134
- Binney, J., & Merrifield, M. 1998, in *Galactic Astronomy*, (New Jersey: Princeton)
- Binney, J., & Tremaine, S. 1987, in *Galactic Dynamics*, (New Jersey: Princeton)
- Bond, H., Grauer, A., Green, R., & Liebert, J. 1984, *ApJ*, 279, 751
- Bouvier, J., Stauffer, J., Martín, E., Barrado y Navascués, D., Wallace, B., & Béjar, V. 1998, *A&A*, 336, 490
- Bragaglia, A., Renzini, A., & Bergeron, P. 1995, *ApJ*, 443, 735
- Burgasser, A. 2004, *ApJS*, 155, 191
- Burgasser, A., Kirkpatrick, J., Reid, I., Brown, M., Miskay, C., & Gizis, J. 2003, *ApJ*, 586, 512
- Burrows, A., et al. 1997, *ApJ*, 491, 856
- Burrows, A., Hubbard, W., Lunine, J., & Liebert, J. 2001, *RvMP*, 73, 719
- Butler, P., Marcy, G., Vogt, S., & Fischer, D. 2000, *IAU Symposium* 202
- Chabrier, G., Baraffe, I., Allard, F., & Hauschildt, P. 2000, *ApJ*, 542, 464
- Close, L., Siegler, N., Potter, D., Brandner, W., & Liebert, J. 2002, *ApJ*, 567, L53
- Cooke, B., et al. 1992, *Nature*, 355, 61
- Cruz, K., Reid, I., Liebert, J., Kirkpatrick, J., & Lowrance, P. 2003, *AJ*, 126, 2421
- Cutri, R., et al. 2003, *2MASS All Sky Catalog of Point Sources (Infrared Processing and Analysis Center)*
- Dahn, C., & Harrington, R. 1976, *ApJ*, 204, L91

- Dahn, C., et al. 1982, *AJ*, 87, 419
- Dahn, C., et al. 2002, *AJ*, 124, 1170
- Downes, R. 1986, *ApJS*, 61, 569
- Drake, J., & Sarna, M. 2003, *A&A*, 594, 55
- Duquennoy, A., & Mayor, M. 1991, *A&A*, 248, 485
- Eggen, O., & Greenstein, J. 1965, *ApJ*, 141, 83
- Eggen, O., & Greenstein, J. 1967, *ApJ*, 150, 927
- Farihi, J. 2004a, *ApJ*, 610, 1013
- Farihi, J. 2004b, Ph.D. Thesis, UCLA<sup>1</sup>
- Farihi, J., & Christopher, M. 2004, *AJ*, 128, 1868
- Finley, D., & Koester, D. 1997, *ApJ*, 489, L79
- Finley, D., Koester, D., & Basri, G. 1997, *ApJ*, 488, 375
- Fischer, D., & Marcy, G. 1992, *ApJ*, 396, 178
- Fontaine, G., Bergeron, P., Billères, M., & Charpinet, S. 2003, *ApJ*, 591, 1184
- Girardi, L., Bressan, A., Bertelli, G., & Chiosi, C. 2000, *A&AS*, 141, 371
- Gliese, W. & Jahreiß, H. 1991, *Third Catalogue of Nearby Stars* (Heidelberg: Astronomisches Rechen-Institut)
- Green, R. 1980, *ApJ*, 238, 685
- Green, P., Ali, B., & Napiwotzki, R. 2000, *ApJ*, 540, 992
- Green, P., & Margon, B. 1994, *ApJ*, 423, 723
- Green, R., Schmidt, M., & Liebert, J. 1986, *ApJS*, 61, 305
- Greenstein, J. 1974, *ApJ*, 189, L131
- Greenstein, J. 1979, *ApJ*, 227, 244
- Greenstein, J. 1984, *ApJ*, 276, 602
- Greenstein, J. 1986, *ApJ*, 304, 334
- Greenstein, J. 1986, *AJ*, 92, 867

---

<sup>1</sup>Available at <http://www.whitedwarf.org>

- Hambly, N., Hodgkin, S., Cossburn, M., & Jameson, R. 1999, MNRAS, 303, 835
- Handler, G., et al. 2003, MNRAS, 340, 1031
- Hawarden, T., Leggett, S., Letawsky, M., Ballantyne, D., & Casali, M. 2001, MNRAS, 325, 563
- Heber, U., Bade, N., Jordan, S., & Voges, W. 1993, A&A, 267, L31
- Henry, T., & McCarthy, D. 1990, ApJ, 350, 334
- Henry, T., & McCarthy, D. 1993, AJ, 106, 773
- Hillenbrand, L., & Carpenter, J. M. 2000, ApJ, 540, 236
- Hintzen, P., & Jensen, E. 1979, PASP, 91, 492
- Hinz, J., McCarthy, D., Simons, D., Henry, T., Kirkpatrick, J., & McGuire, P. 2002, AJ, 123, 2027
- Høg, E., et al. 2000, A&A, 355, 27
- Holberg, J., Oswalt, T., & Sion, E. 2002, ApJ, 571, 512
- Homeier, D., Koester, D., Hagen, H., Jordan, S., Heber, U., Engels, D., Reimers, D., & Dreizler, S. 1998, A&A, 338, 563
- Hunt, L., Mannucci, F., Testi, L., Migliorini, S., Stanga, R., Baffa, C., Lisi, F., & Vanzi, L. 1998, AJ, 115, 2594
- Iben, I., & Livio, M. 1993, PASP, 105, 1373
- Jahreiß, H., & Wielen, R. 1997, Hipparcos '97, ed. B. Battrock (Noordwijk: ESA), 675
- Kalirai, J. S., Richer, H. B., Reitzel, D., Hansen, B. M. S., Rich, R. M., Fahlman, G. G., Gibson, B. K., & von Hippel, T. 2005, ApJ, 618, L123
- Kawaler, S., et al. 1995, ApJ, 450, 350
- Kawka, A., Vennes, S., Dupuis, J., & Koch, R. 2000, AJ, 120, 3250
- Kilic, M., von Hippel, T., Leggett, S. K., & Winget, D. E. 2005, ApJ, 632, L115
- Kirkpatrick, J., Allard, F., Bida, T., Zuckerman, B., Becklin, E., Chabrier, G., & Baraffe, I. 1999a, ApJ, 519, 834
- Kirkpatrick, J., Henry, T., & Liebert, J. 1993, ApJ, 406, 701
- Kirkpatrick, J., Henry, T., & McCarthy, D. 1991, ApJS, 77, 417
- Kirkpatrick, J., & McCarthy, D. 1994, AJ, 107, 333

- Kirkpatrick, J., et al. 1999b, *ApJ*, 519, 802
- Kirkpatrick, J., et al. 2000, *AJ*, 120, 447
- Koester, D., et al. 2001, *A&A*, 378, 556
- Lamontagne, R., Demers, S., Wesemael, F., Fontaine, G., & Irwin, M. 2000, *AJ*, 119, 241
- Landolt, A. 1983, *AJ*, 88, 439
- Leggett, S. 1992, *ApJS*, 82, 351
- Leggett, S., et al. 2002, *ApJ*, 564, 452
- Leggett, S., Ruiz, M., & Bergeron, P. 1998, *ApJ*, 497, 294
- Lépine, S., Shara, M., & Rich, M. 2003, *AJ*, 126, 921
- Liebert, J., Bergeron, P., & Holberg, J. 2004, *ApJS*, 156, 47
- Liebert, J., Bergeron, P., Schmidt, G., & Saffer, R. 1993, *ApJ*, 418, 426
- Livio, M., & Soker, N. 1984, *MNRAS*, 208, 783
- Low, C., & Lynden-Bell, D. 1976, *MNRAS*, 176, 376
- Lowrance, P. 2001, Ph.D. Thesis, UCLA
- Luhman, K., Rieke, G., Young, E., Cotera, A., Chen, H., Rieke, M., Schneider, G., & Thompson, R. 2000, *ApJ*, 540, 1016
- Marley, M., Saumon, D., Guillot, T., Freedman, R., Hubbard, W., Burrows, A., & Lunine, J. 1996, *Science*, 272, 1919
- Marsh, T. 2000, *NewAR*, 44, 119
- Marsh, M., et al. 1997, *MNRAS*, 286, 369
- Marsh, T., Dhillon, V., & Duck, S. 1995, *MNRAS*, 275, 828
- Marsh, T., & Duck, S. 1996, *MNRAS*, 278, 565
- Matthews, K., & Soifer, B. 1994, *Near-infrared Astronomy with Arrays: the Next Generation*, ed. I. McLean (Dordrecht: Kluwer), 239
- Maxted, P., Burleigh, M., Marsh, T., & Bannister, N. 2002, *MNRAS*, 334, 833
- Maxted, P., & Marsh, T. 1999, *MNRAS*, 307, 122
- Maxted, P., Marsh, T., & Moran, C. 2000, *MNRAS*, 319, 305
- Maxted, P., Marsh, T., & Moran, C. 2002, *MNRAS*, 332, 745



- Maxted, P., Marsh, T., Moran, C., Dhillon, V., & Hilditch, R. 1998, *MNRAS*, 300, 1225
- Maxted, P., Marsh, T., Moran, C., & Han, Z. 2000, *MNRAS*, 314, 334
- Maxted, P., Moran, C., Marsh, T., & Gatti, A. 2000, *MNRAS*, 311, 877
- McAlister, H., Mason, B., Hartkopf, W., Roberts, L., & Shara, M. 1996, *AJ*, 112, 1169
- McCarthy, C., & Zuckerman, B. 2004, *AJ*, 127, 2871
- McCook, G., & Sion, E. 1987, *ApJS*, 65, 603
- McCook, G., & Sion, E. 1999, *ApJS*, 121, 1
- McLean, I., et al. 1993, *SPIE*, 1946, 513
- McMahan, R. 1989, *ApJ*, 336, 409
- Mihalas, D., & Binney, J. 1981, in *Galactic Astronomy*, (San Francisco: W. H. Freeman & Co.)
- Monet, D., et al. 2003, *AJ*, 125, 984
- Nakajima, T., Durrance, S., Golimowski, D., & Kulkarni, S. 1994, *ApJ*, 428, 797
- Nakajima, T., Oppenheimer, B., Kulkarni, S., Golimowski, D., Matthews, K., & Durrance, S. 1995, *Nature*, 378, 463
- Napiwotzki, R., Green, P., & Saffer, R. 1999, *ApJ*, 517, 399
- Nelemans, G., Yungelson, L., Portegies Zwart, S., & Verbunt, F. 2001, *A&A*, 365, 491.
- Oke, J. B., et al. 1995, *PASP*, 107, 375
- Oppenheimer, B., Golimowski, D., Kulkarni, S., Matthews, K., Nakajima, T., Creech-Eakman, M., & Durrance, S. 2001, *AJ*, 121, 2189
- Oswalt, T. 1981, Ph.D. Thesis, Ohio State University
- Oswalt, T., Hintzen, P., & Luyten, W. 1988, *ApJS*, 66, 391
- Oswalt, T., Smith, J., Wood, M., & Hintzen, P. 1996, *Nature*, 382, 692
- Paczynski, B. 1976, *Proceedings of IAU Symposium 73*, eds. P. Eggleton, S. Mitton, & J. Whelan (Dordrecht: D. Reidel), 75
- Perryman, M., et al. 1997, *A&A*, 323, L49
- Probst, R. 1983, *ApJS*, 53, 335
- Putney, A. 1997, *ApJS*, 112, 527

- Raymond, S., et al. 2003, *AJ*, 125, 2621
- Reed, M., Kawaler, S., & O'Brien, M. 2000, *ApJ*, 545, 429
- Reid, I., Gizis, J., Kirkpatrick, J., & Koerner, D. 2001, *AJ*, 121, 489
- Reid, I., & Hawley, S. 2000, in *New Light on Dark Stars*, (New York: Springer)
- Reid, I., Hawley, S., & Gizis, J. 1995, *AJ*, 110, 1838
- Reid, I., et al. 1999, *ApJ*, 521, 613
- Reylé, C., Robin, A., Scholz, R., & Irwin, M. 2002, *A&A*, 390, 491
- Rieke, M., Rieke, G., Green, E., Montgomery, E., & Thompson, C. 1993, *SPIE*, 1946, 179
- Saffer, R., Bergeron, P., Koester, D., & Liebert, J. 1994, *ApJ*, 432, 351
- Saffer, R., Livio, M., & Yungelson, L. 1998, *ApJ*, 502, 394
- Saffer, R., Wade, R., Liebert, J., Green, R., Sion, E., Bechtold, J., Foss, D., & Kidder, K. 1993, *AJ*, 105, 1945
- Salim, S., & Gould, A. 2002, *ApJ*, 575, 83
- Schmidt, G., Liebert, J., & Smith, P. 1998, *AJ*, 116, 451
- Schmidt, G., & Smith, P. 1995, *ApJ*, 448, 305
- Schmidt, G., Smith, P., & Harvey, D. 1995, *AJ*, 110, 398
- Scholz, R., Lodieu, N., Ibata, R., Bienaymé, O., Irwin, M., McCaughrean, M., & Schwöpe, A. 2004, *MNRAS*, 347, 685
- Schroeder, D., et al. 2000, *AJ*, 119, 906
- Schultz, G., Zuckerman, B., & Becklin E. 1996, *ApJ*, 460, 402
- Schwartz, R. 1972, *PASP*, 84, 28
- Schwartz, R., Dawkins, D., Findley, D., & Chen, D. 1995, *PASP*, 107, 667
- Siegler, N., Close, L., Mamajek, E., & Freed, M. 2003, *ApJ*, 598, 1265
- Silvestri, N., Oswald, T., & Hawley, S. 2002, *AJ*, 124, 1118
- Silvestri, N., Oswald, T., Wood, M., Smith, J., Reid, I., & Sion, E. 2001, *AJ*, 121, 503
- Sion, E., Fritz, M., McMullin, J., & Lallo, M. 1988, *AJ*, 96, 251
- Smart, R., et al. 2003, *A&A*, 404, 317

- Tweedy, R., Holberg, J., Barstow, M., Bergeron, P., Grauer, A., Liebert, J., & Fleming, T. 1993, *AJ*, 105, 1938
- Vennes, S., Thejll, P., Galvan, R., & Dupuis, J. 1997, *ApJ*, 480, 714
- Vennes, S., Thorstensen, J., & Polomski, E. 1999, *ApJ*, 523, 386
- Vrba, F., et al. 2004, *AJ*, 127, 2948
- Wachter, S., Hoard, D., Hansen, K., Wilcox, R., Taylor, H., & Finkelstein, S. 2003, *ApJ*, 586, 1356
- Wagman, N. 1967, *AJ*, 72, 957
- Weidemann, V. 1987, *A&A*, 188, 74
- Weidemann, V. 1990, *ARA&A*, 28, 103
- Weidemann, V. 2000, *A&A*, 363, 647
- Weidemann, V., & Koester, D. 1995, *A&A*, 297, 216
- Wielen, R. 1974, *Highlights of Astronomy*, Volume 3, (Dordrecht: D. Reidel), 395
- Winget, D., Robinson, E., Nather, R., & Balachandran, S. 1984, *ApJ*, 279, L15
- Zacharias, N., et al. 2000, *AJ*, 120, 2131
- Zacharias, N., et al. 2004 *AJ*, 127, 3043
- Zuckerman, B., & Becklin, E. 1987a, *ApJ*, 319, 99
- Zuckerman, B., & Becklin, E. 1987b, *Nature*, 330, 138
- Zuckerman, B., & Becklin, E. 1992, *ApJ*, 386, 260
- Zuckerman, B., Becklin, E., Macintosh, B., & Bida, T. 1997, *AJ*, 113, 764
- Zuckerman, B., Koester, D., Reid, I., & Hünsch, M. 2003, *ApJ*, 596, 477

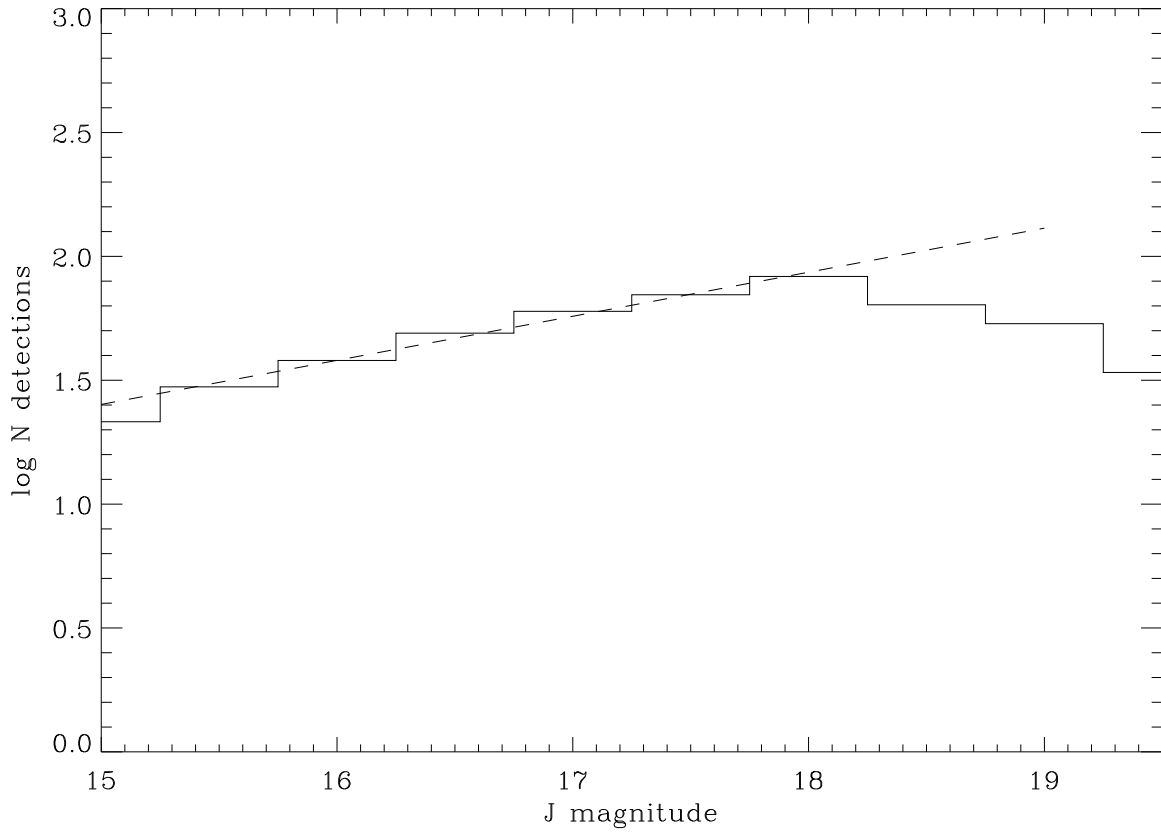


Fig. 1.— Number of objects detected as a function of  $J$  magnitude for an ensemble of representative images from all observing runs at Steward Observatory, indicating the completeness limit is  $J = 18$  mag.

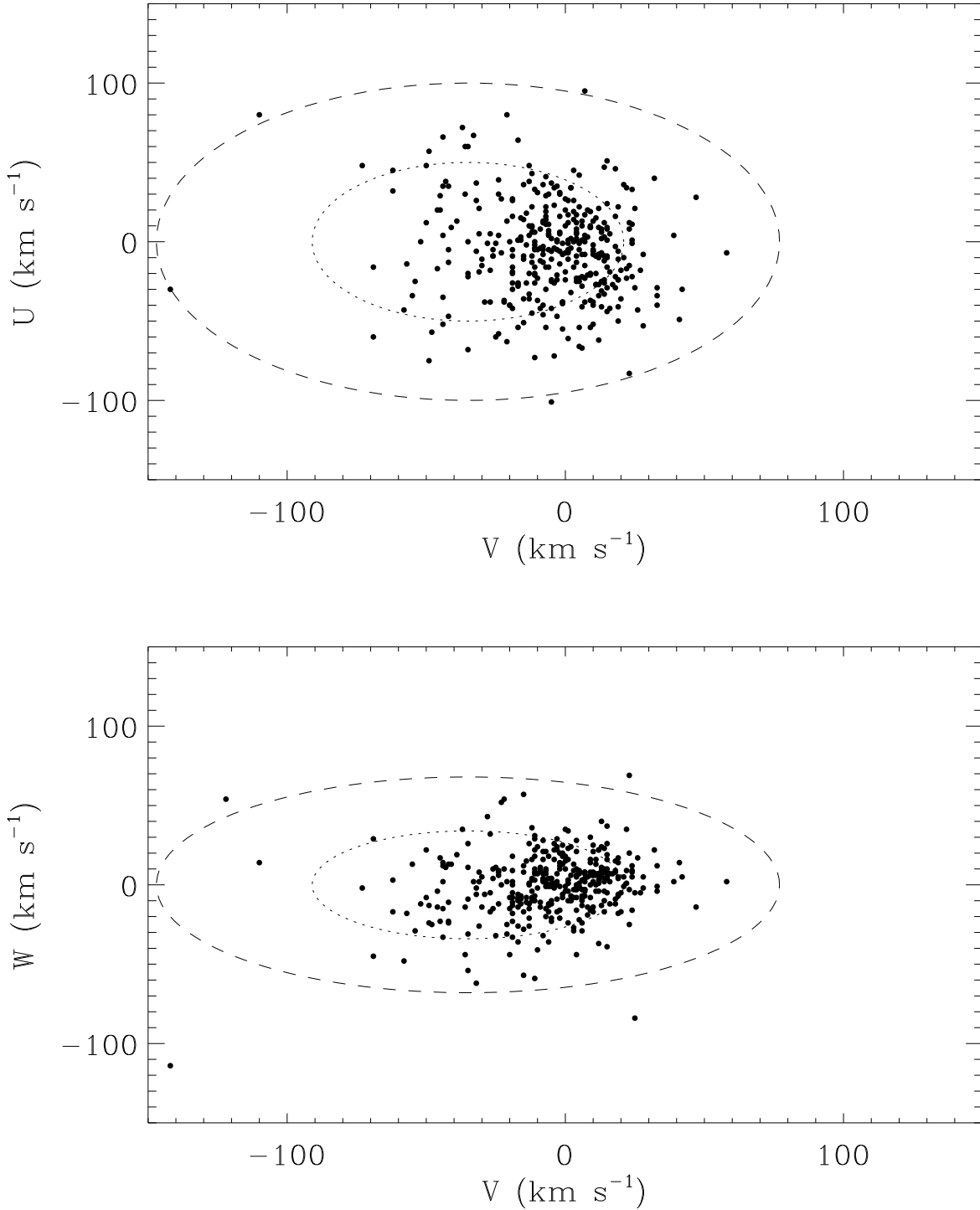


Fig. 2.— Galactic space velocity distribution in the  $UV$  and  $WV$  planes for all 371 white dwarfs in the sample, assuming  $v_r = 0$ . The ellipses represent the 1 and  $2\sigma$  contours for old, metal-poor disk stars from (Beers et al. 2000).

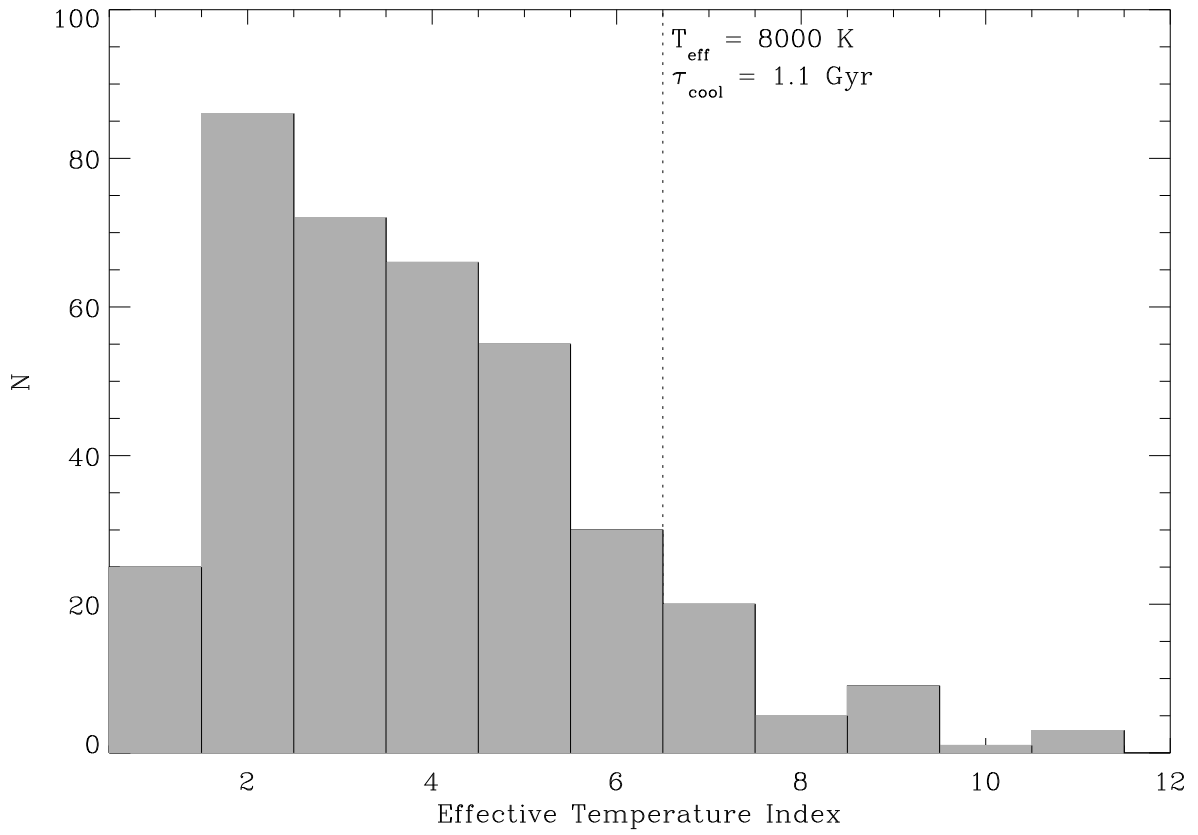


Fig. 3.— Number of sample white dwarfs versus effective temperature index (as discussed in text §3.3). The dotted line represents a cooling age of 1.08 Gyr for a typical DA white dwarf (Bergeron et al. 1995b).

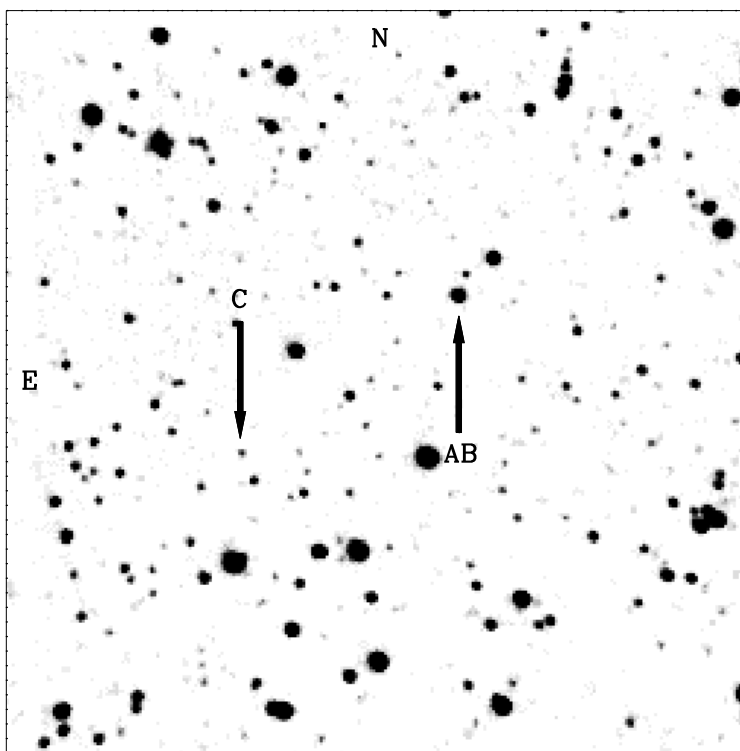


Fig. 4.— Near near-infrared finding chart for G21-15C, taken at *J* band with the Bok 2.3 meter telescope in July 2001. The image is  $166''$  square with  $0.65''$  pixels. The coordinates for the companion are  $18^{\text{h}}27^{\text{m}}16.4^{\text{s}}$ ,  $+04^{\circ}04'09''$  J2000.

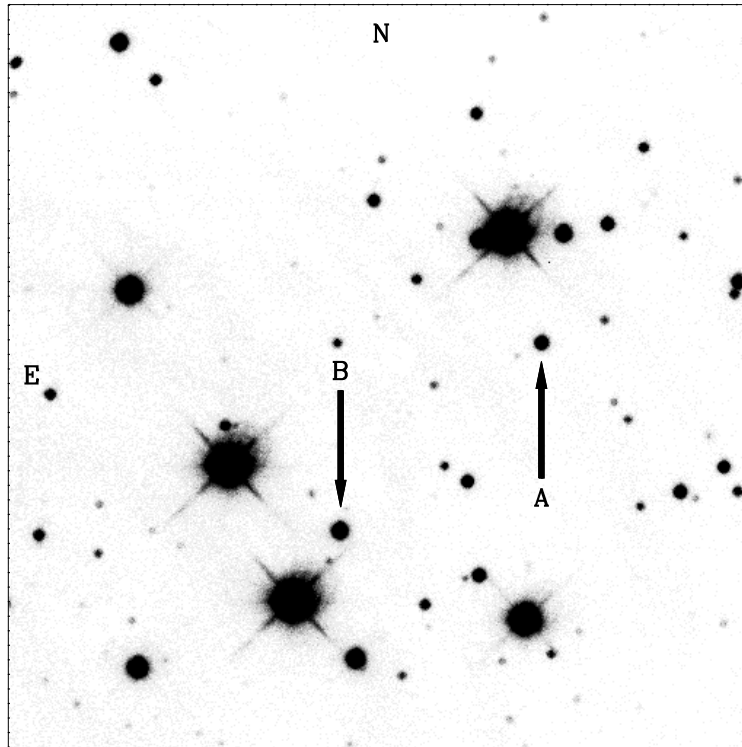


Fig. 5.— Optical finding chart for GD 60B, taken at *I* band with the Nickel 1 meter telescope in January 2003. The image is  $184''$  square with  $0.36''$  pixels. The coordinates for the companion are  $04^{\text{h}}20^{\text{m}}15.2^{\text{s}}$ ,  $+33^{\circ}34'48''$  J2000.



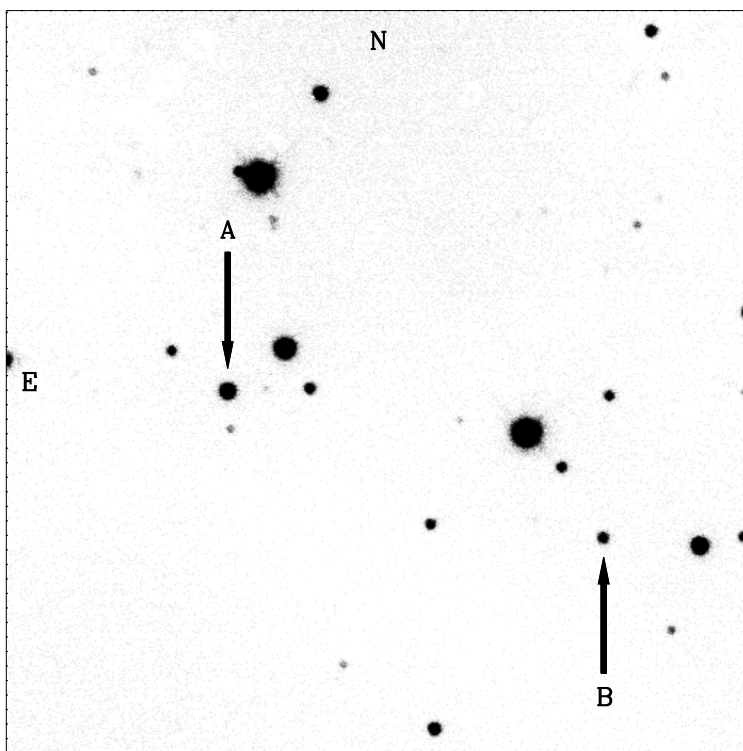


Fig. 6.— Optical finding chart for GD 74B, taken at  $R$  band with the Nickel 1 meter telescope in January 2003. The image is  $184''$  square with  $0.36''$  pixels. The coordinates for the companion are  $06^{\text{h}}28^{\text{m}}55.8^{\text{s}}$ ,  $+41^{\circ}30'11''$  J2000.

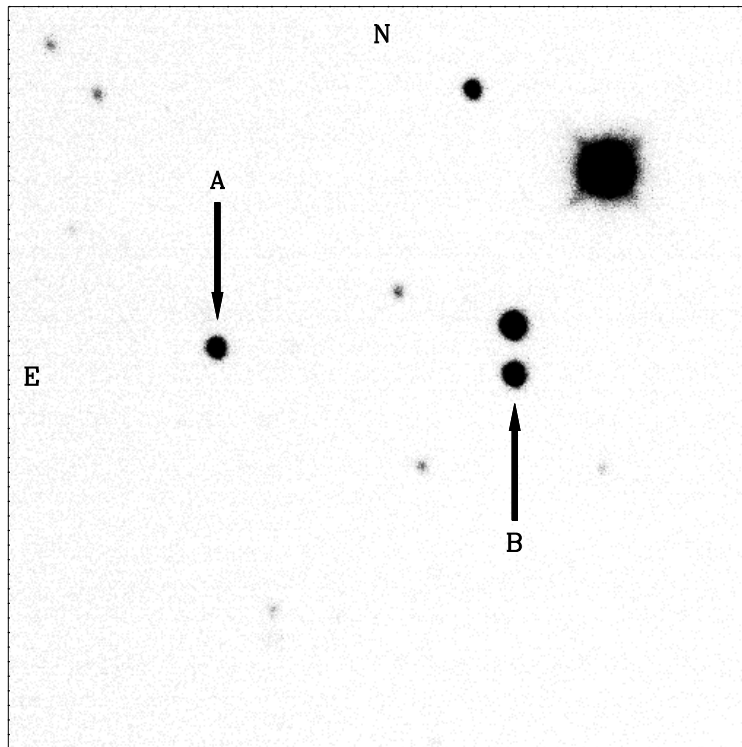


Fig. 7.— Optical finding chart for GD 84B, taken at  $R$  band with the Nickel 1 meter telescope in October 2001. The image is  $184''$  square with  $0.36''$  pixels. The coordinates for the companion are  $07^{\text{h}}17^{\text{m}}54.6^{\text{s}}$ ,  $+45^{\circ}47'48''$  J2000.

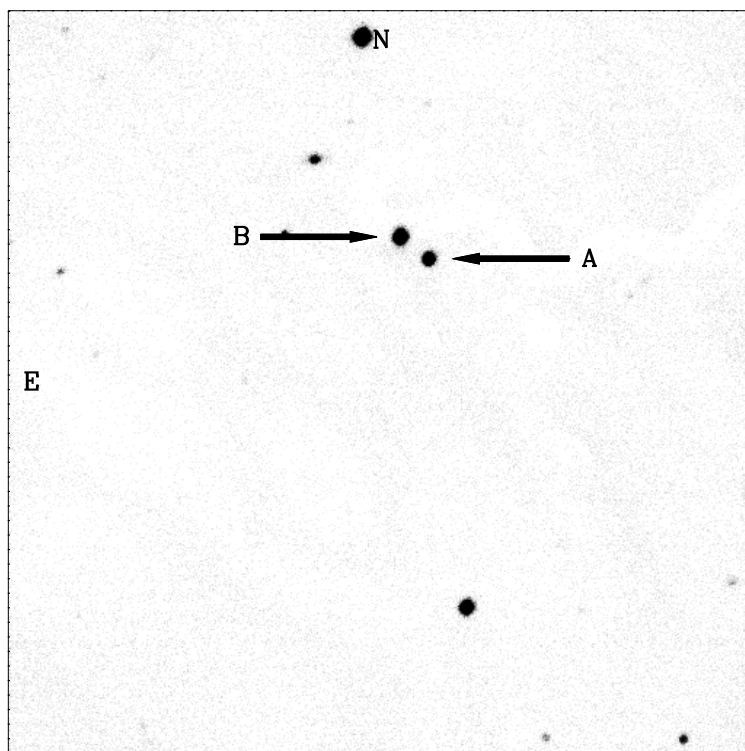


Fig. 8.— Optical finding chart for GD 267B, taken at *I* band with the Nickel 1 meter telescope in March 2003. The image is  $184''$  square with  $0.36''$  pixels.

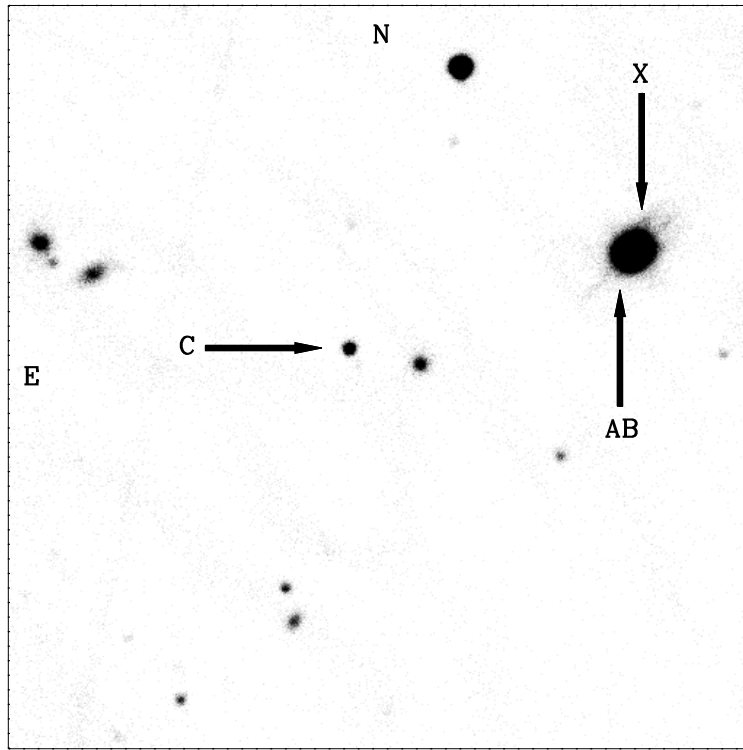


Fig. 9.— Optical finding chart for GD 319C, taken at *I* band with the Nickel 1 meter telescope in March 2002. The image is  $184''$  square with  $0.36''$  pixels. The coordinates for the companion are  $12^{\text{h}}50^{\text{m}}12.7^{\text{s}}$ ,  $+55^{\circ}05'36''$  J2000. The object labelled ‘X’ is a foreground K dwarf located  $\sim 2.5''$  away from GD 319AB.

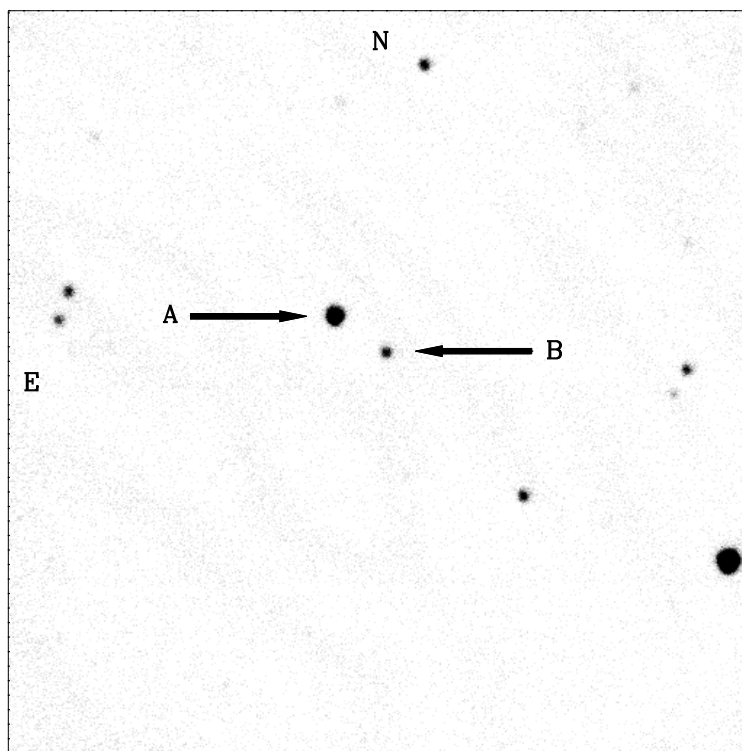


Fig. 10.— Optical finding chart for GD 322B, taken at *I* band with the Nickel 1 meter telescope in March 2002. The image is  $184''$  square with  $0.36''$  pixels.

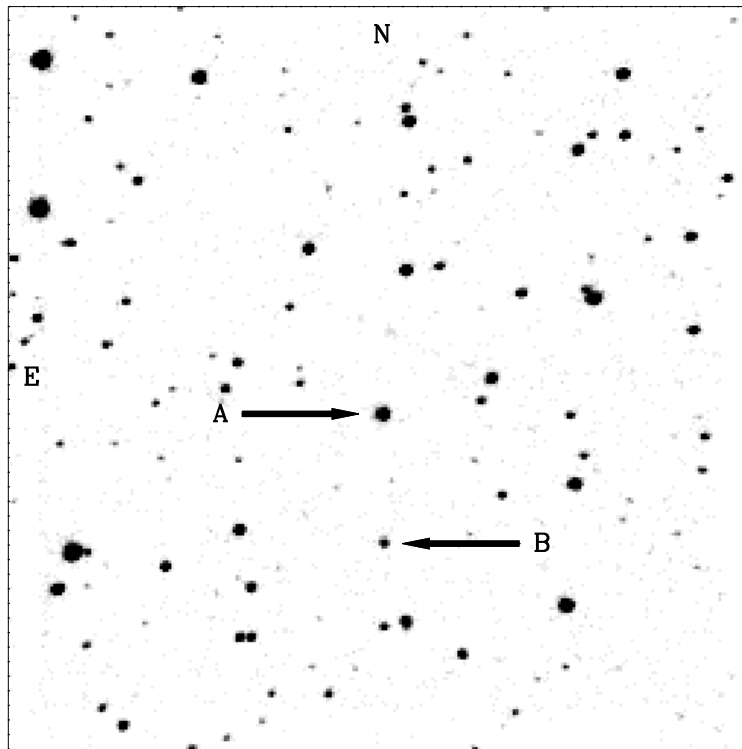


Fig. 11.— Near near-infrared finding chart for GD 559B, taken at  $J$  band with the Bok 2.3 meter telescope in October 1996. The image is  $166''$  square with  $0.65''$  pixels. The coordinates for the companion are  $23^{\text{h}}21^{\text{m}}17.2^{\text{s}}$ ,  $+69^{\circ}25'54''$  J2000.

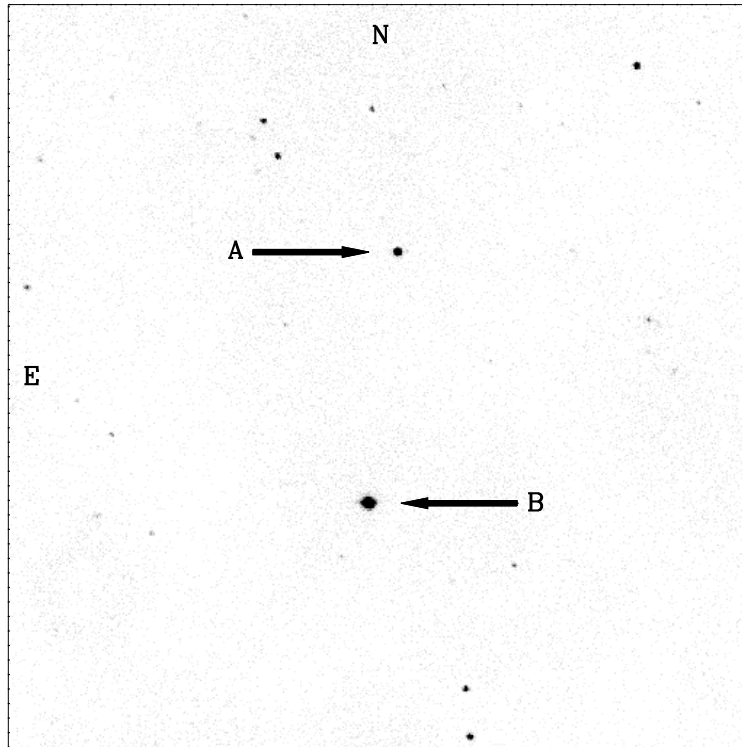


Fig. 12.— Optical finding chart for GD 683B, taken at *I* band with the Swope 1 meter telescope in November 2003. The image is  $328''$  square with  $0.44''$  pixels. The coordinates for the companion are  $01^{\text{h}}08^{\text{m}}21.6^{\text{s}}$ ,  $-35^{\circ}36'33''$  J2000.

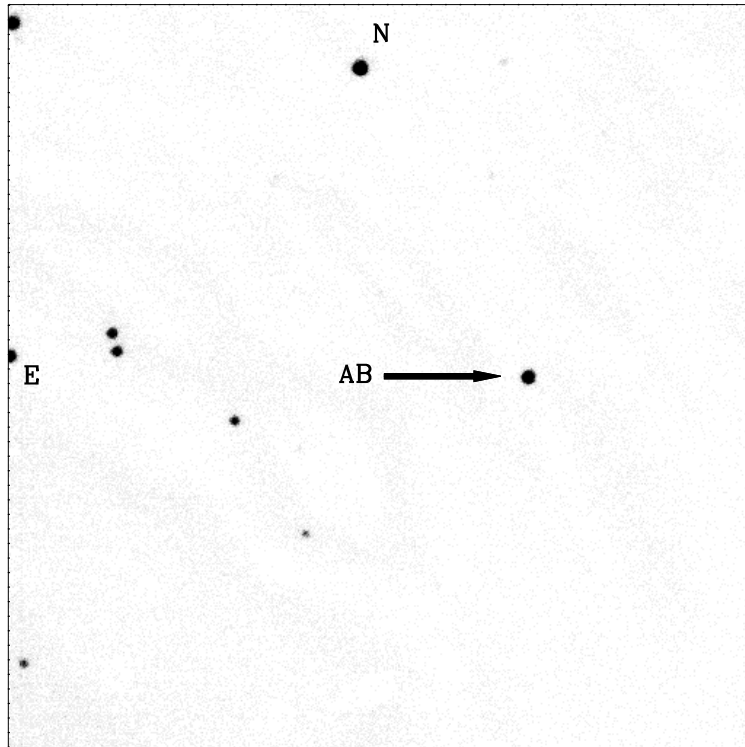


Fig. 13.— Optical finding chart for LP 618-14, taken at *I* band with the Nickel 1 meter telescope in June 2002. The image is  $184''$  square with  $0.36''$  pixels. The coordinates for the composite binary are  $13^{\text{h}}36^{\text{m}}16.1^{\text{s}}$ ,  $+00^{\circ}17'33''$  J2000.



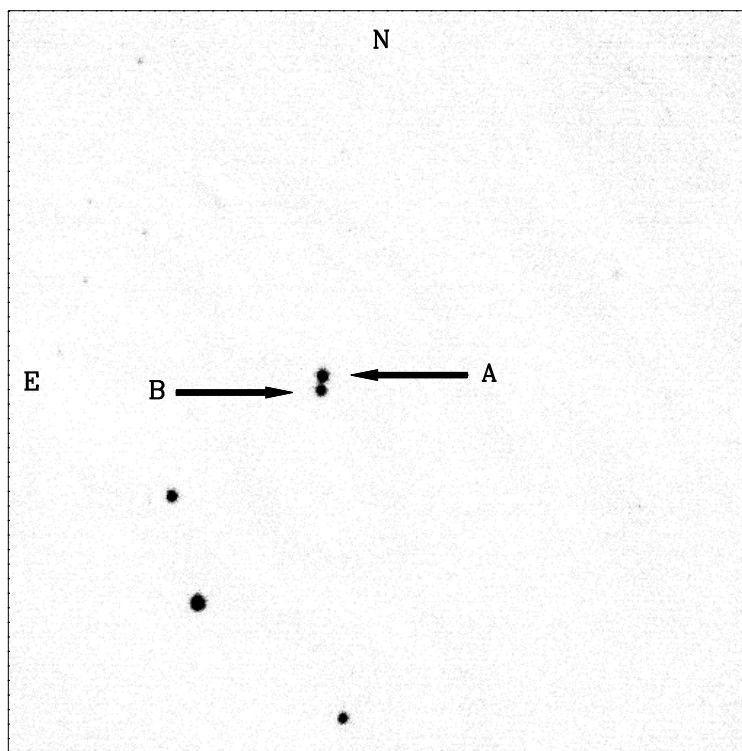


Fig. 14.— Optical finding chart for PG 0901+140B, taken at  $I$  band with the Nickel 1 meter telescope in April 2003. The image is  $184''$  square with  $0.36''$  pixels.

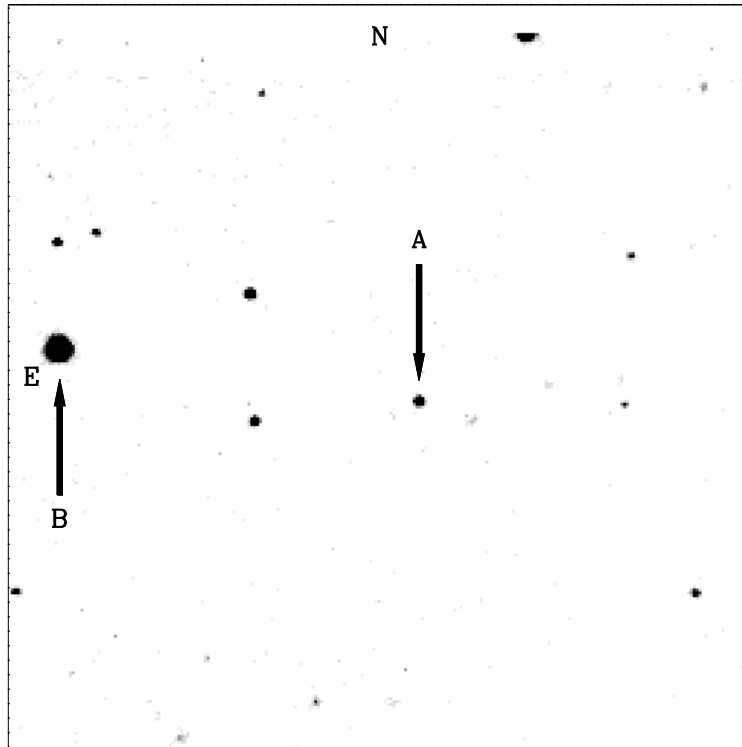


Fig. 15.— Near near-infrared finding chart for PG 0933+729B, taken at  $J$  band with the Bok 2.3 meter telescope in December 2002. The image is  $166''$  square with  $0.65''$  pixels. The coordinates for the companion are  $09^{\text{h}}38^{\text{m}}39.8^{\text{s}}$ ,  $+72^{\circ}42'31''$  J2000.

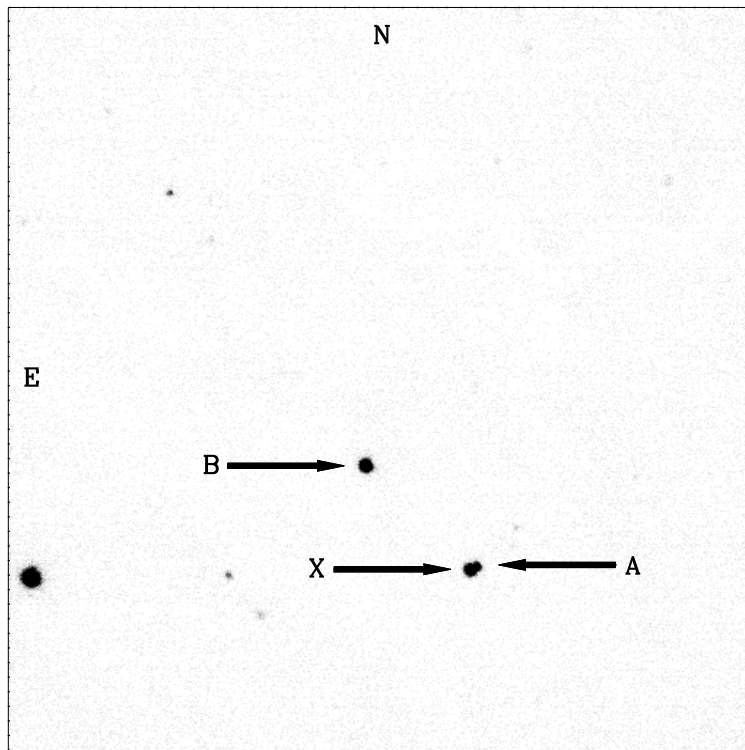


Fig. 16.— Optical finding chart for PG 1015+076B, taken at *I* band with the Nickel 1 meter telescope in March 2003. The image is  $184''$  square with  $0.36''$  pixels. The coordinates for the companion are  $10^{\text{h}}18^{\text{m}}03.5^{\text{s}}$ ,  $+07^{\circ}21'50''$  J2000. The object labelled ‘X’ is a background G dwarf located  $2.0''$  away from PG 1015+076A.

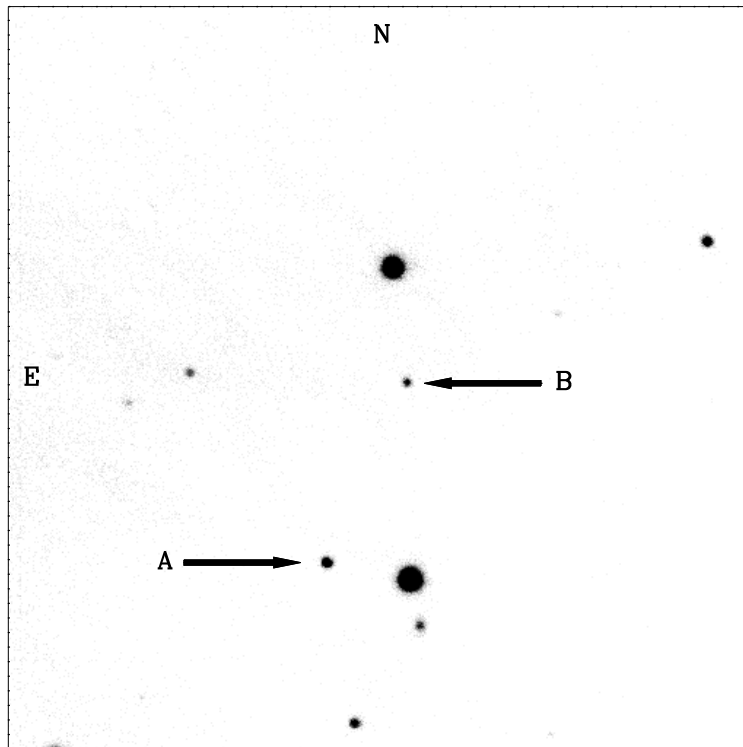


Fig. 17.— Optical finding chart for PG 1017+125B, taken at *I* band with the Nickel 1 meter telescope in January 2003. The image is 184'' square with 0.36'' pixels. The coordinates for the companion are  $10^{\text{h}}19^{\text{m}}54.6^{\text{s}}$ ,  $+12^{\circ}17'18''$  J2000.

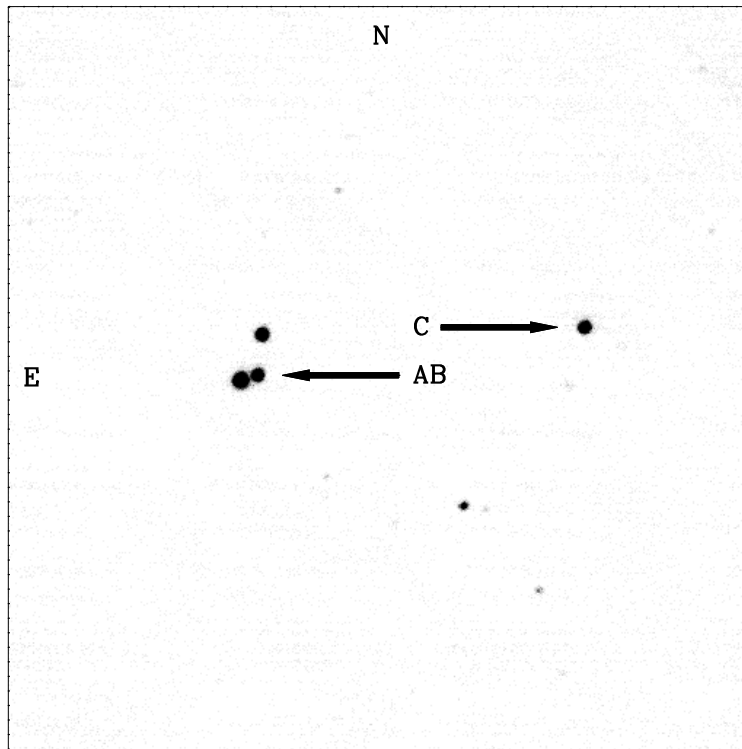


Fig. 18.— Optical finding chart for PG 1204+450C, taken at *I* band with the Nickel 1 meter telescope in April 2003. The image is 184'' square with 0.36'' pixels. The coordinates for the companion are  $12^{\text{h}}06^{\text{m}}39.8^{\text{s}}$ ,  $+44^{\circ}50'09''$  J2000.

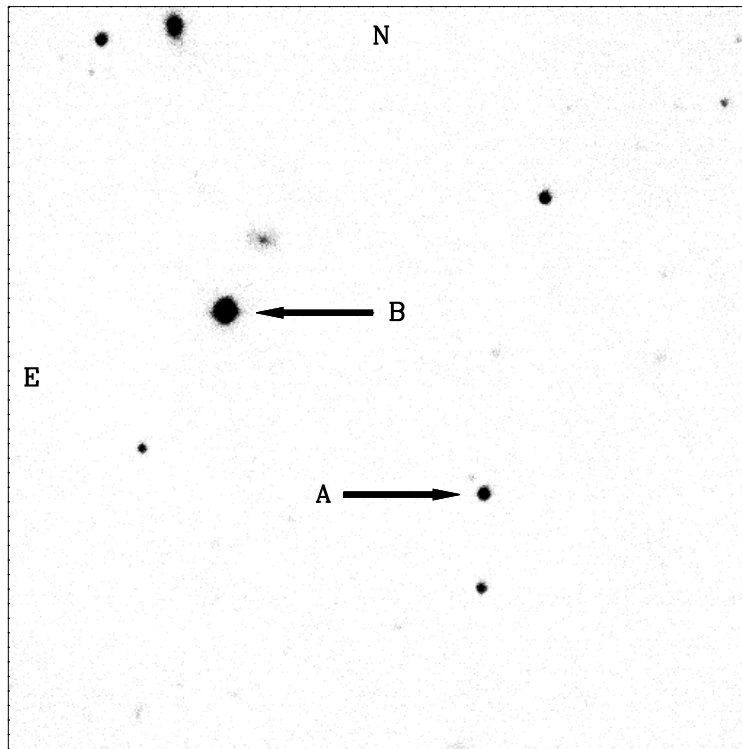


Fig. 19.— Optical finding chart for PG 1449+168B, taken at *I* band with the Nickel 1 meter telescope in April 2003. The image is  $184''$  square with  $0.36''$  pixels. The coordinates for the companion are  $14^{\text{h}}52^{\text{m}}16.1^{\text{s}}$ ,  $+16^{\circ}38'48''$  J2000.

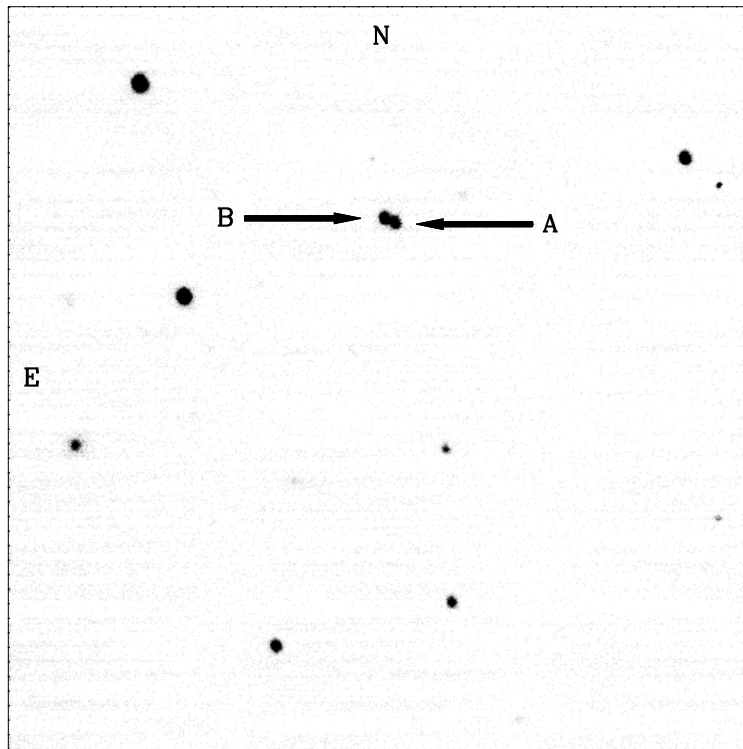


Fig. 20.— Optical finding chart for PG 1539+530B, taken at *V* band with the Nickel 1 meter telescope in April 2003. The image is 184'' square with 0.36'' pixels.

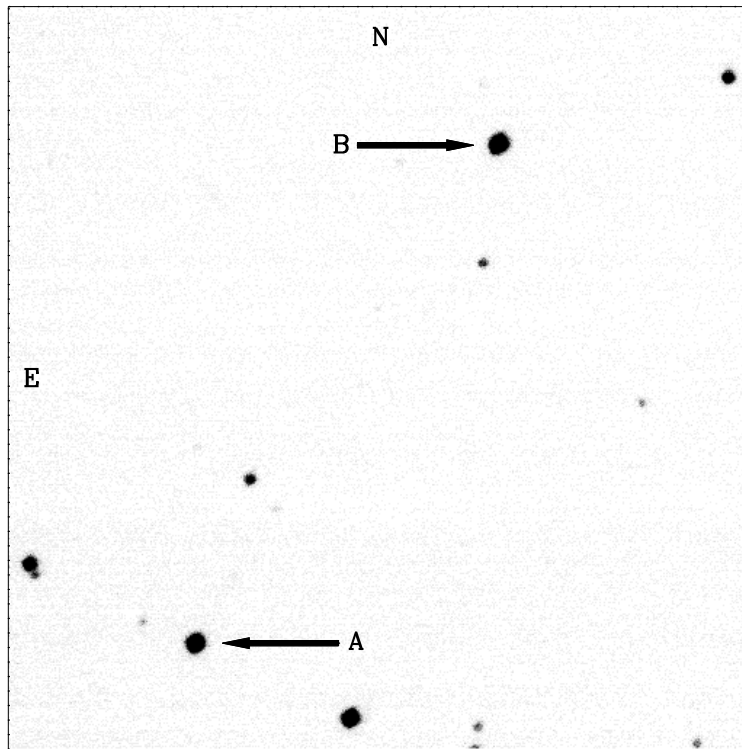


Fig. 21.— Optical finding chart for PG 1659+303B, taken at  $V$  band with the Nickel 1 meter telescope in April 2003. The image is  $184''$  square with  $0.36''$  pixels. The coordinates for the companion are  $17^{\text{h}}01^{\text{m}}02.3^{\text{s}}$ ,  $+30^{\circ}17'45''$  J2000.



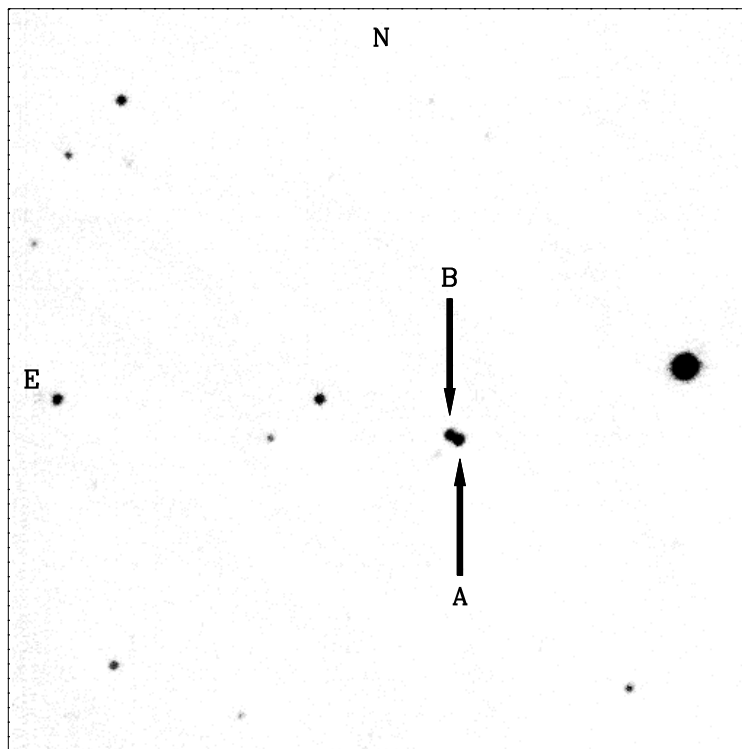


Fig. 22.— Optical finding chart for PG 2244+031B, taken at *I* band with the Nickel 1 meter telescope in July 2003. The image is 184'' square with 0.36'' pixels.

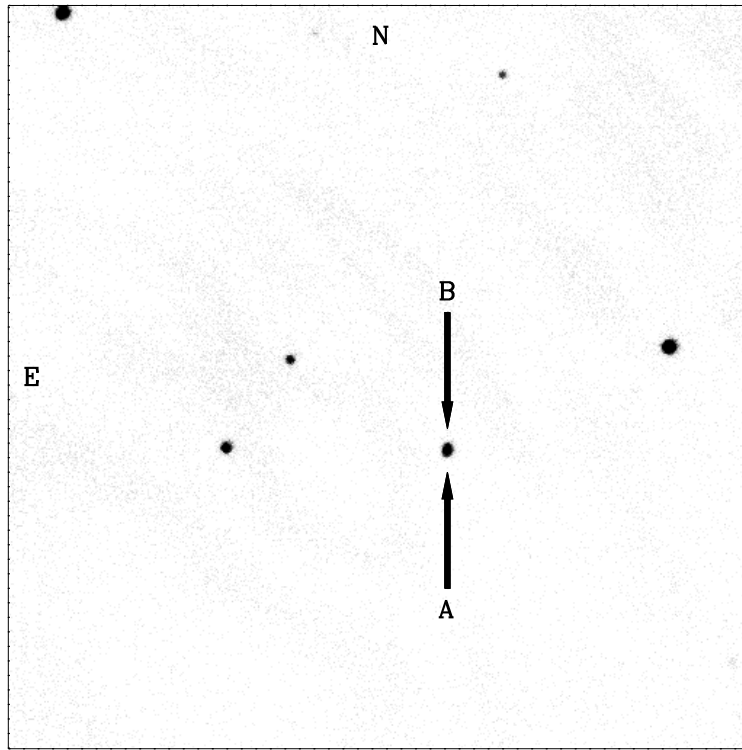


Fig. 23.— Optical finding chart for Ton S 392B, taken at  $I$  band with the Nickel 1 meter telescope in October 2003. The image is  $184''$  square with  $0.36''$  pixels. The coordinates for the binary are  $03^{\text{h}}59^{\text{m}}04.9^{\text{s}}$ ,  $-23^{\circ}12'25''$  J2000. At a separation of  $\sim 1.2''$ , the companion is just barely resolved in this image.

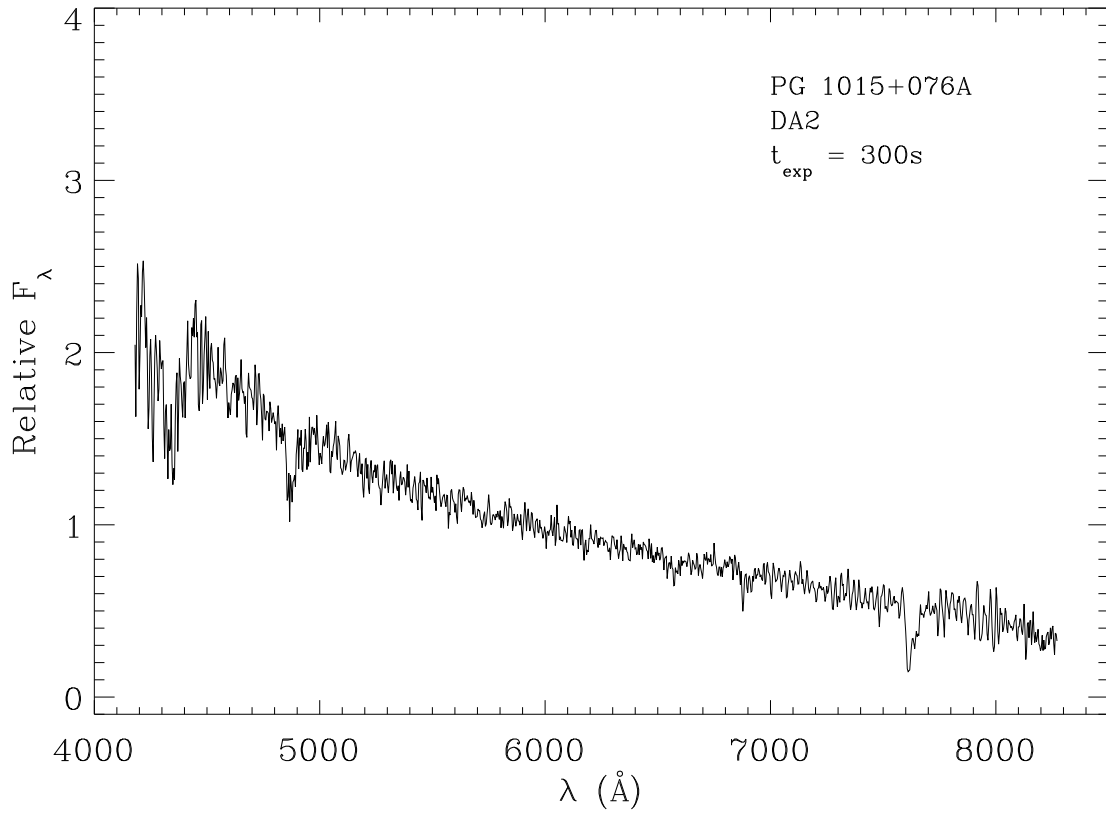


Fig. 24.— Optical spectrum of PG 1015+076A taken with the Boller & Chivens Spectrograph on the Bok 2.3 meter in April 2003.

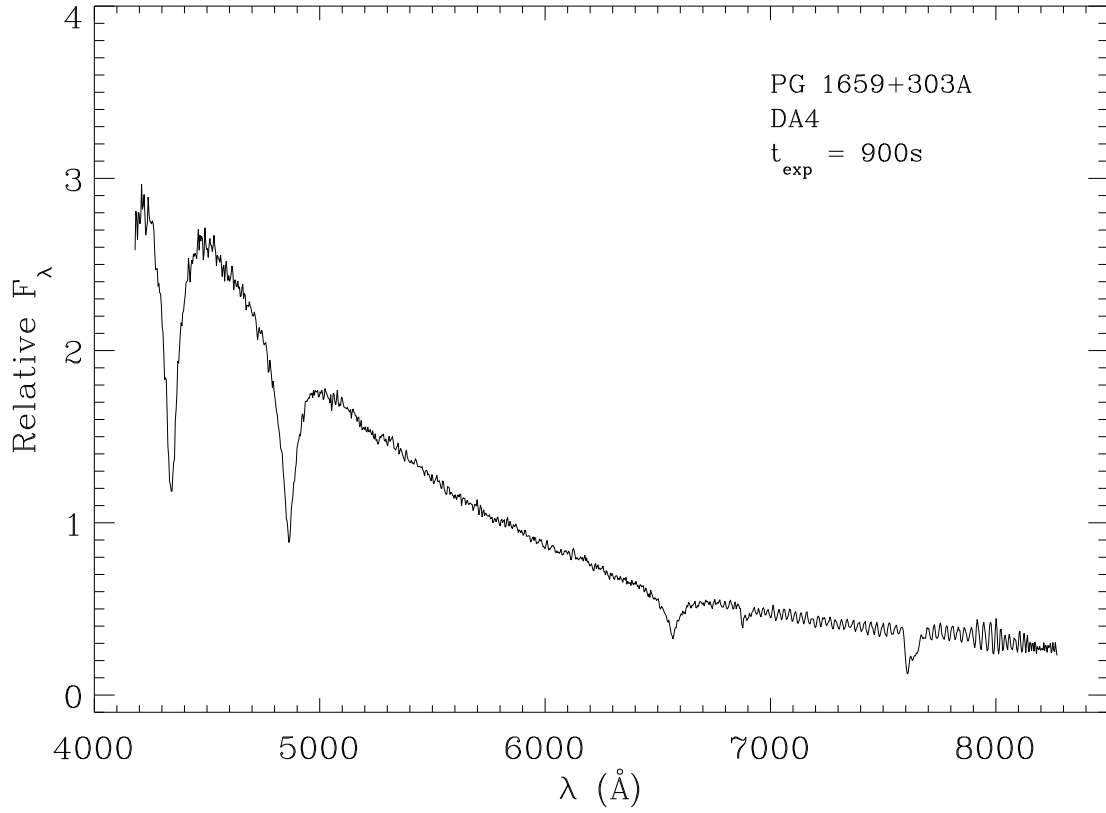


Fig. 25.— Optical spectrum of PG 1659+303A taken with the Boller & Chivens Spectrograph on the Bok 2.3 meter in April 2003.

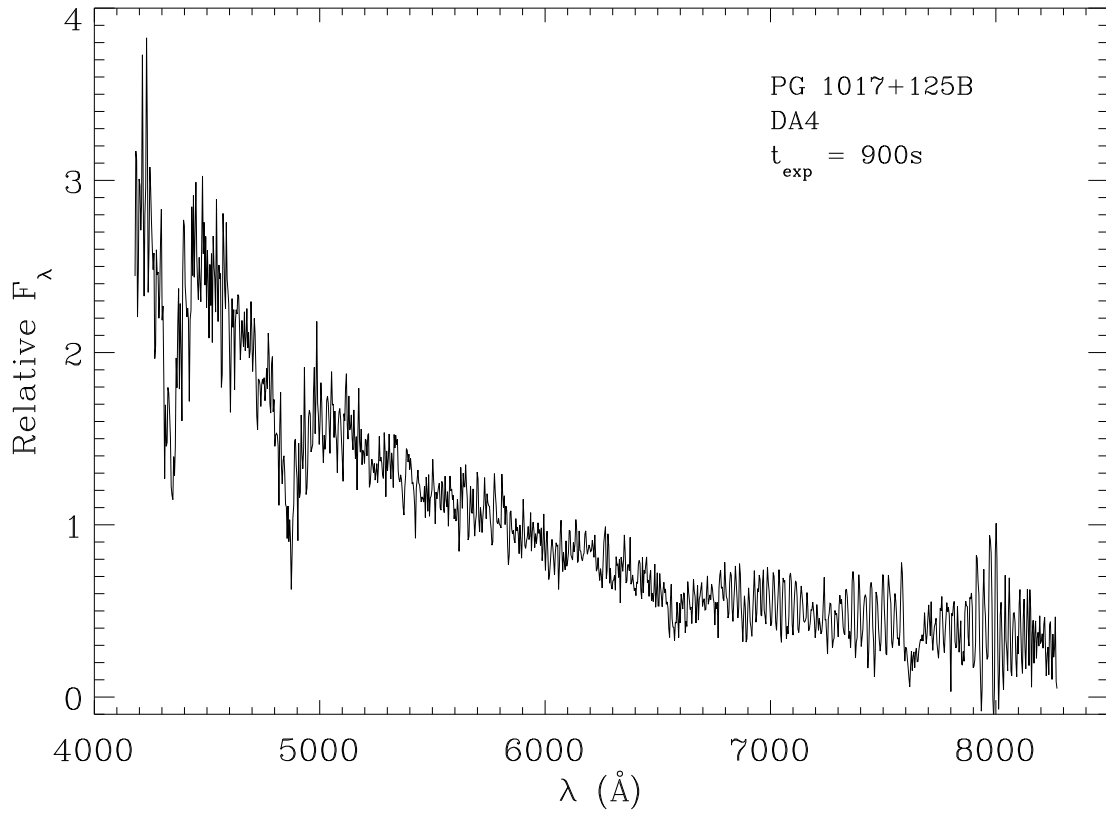


Fig. 26.— Optical spectrum of PG 1017+125B taken with the Boller & Chivens Spectrograph on the Bok 2.3 meter in April 2003.

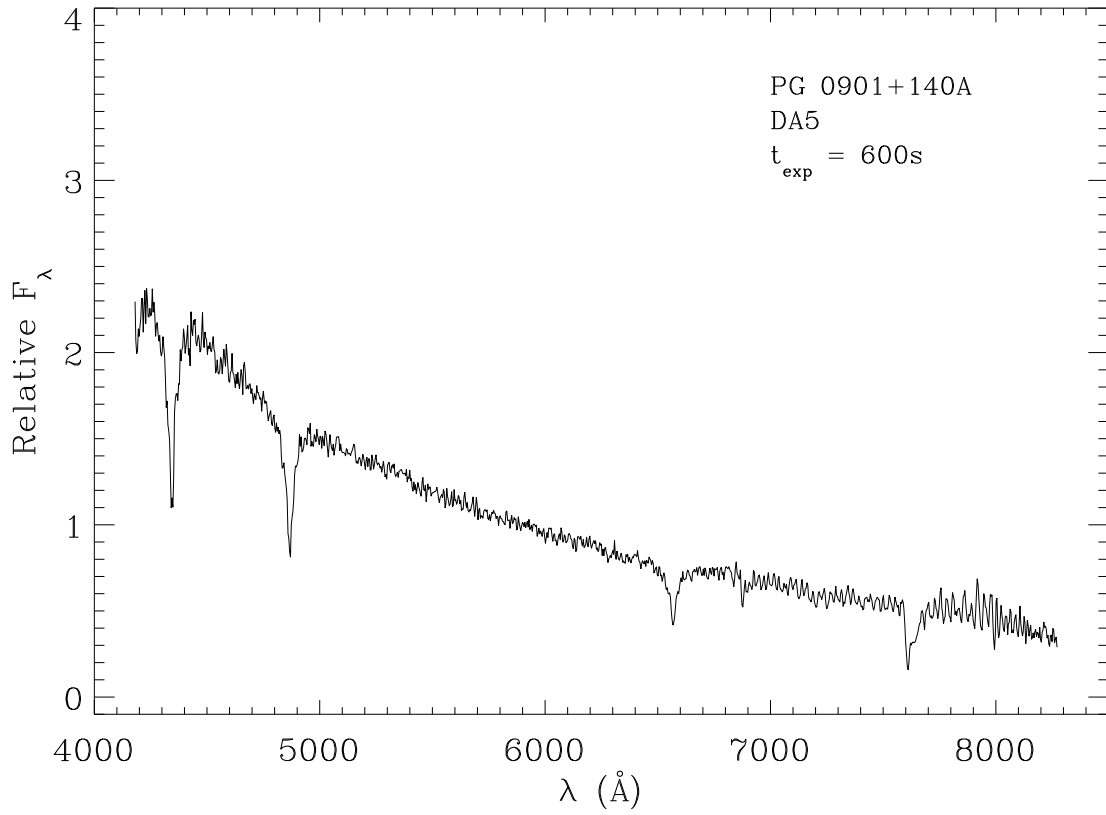


Fig. 27.— Optical spectrum of PG 0901+140A taken with the Boller & Chivens Spectrograph on the Bok 2.3 meter in April 2003.

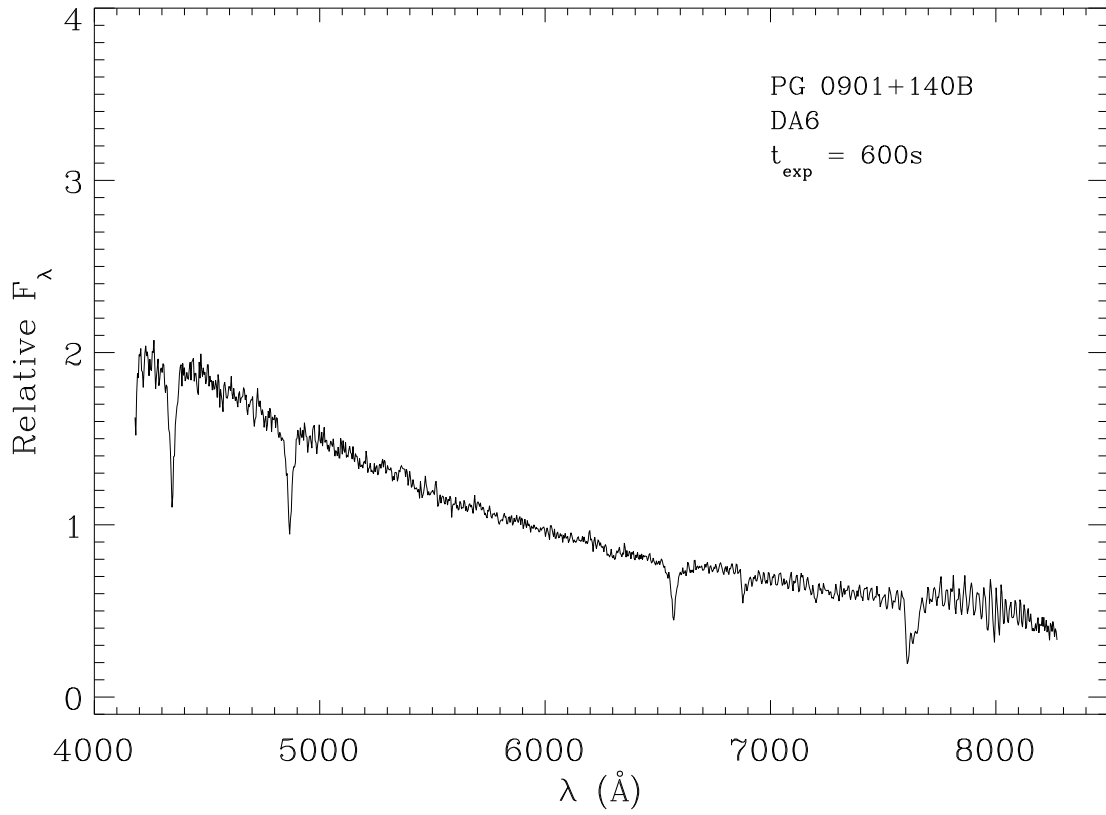


Fig. 28.— Optical spectrum of PG 0901+140B taken with the Boller & Chivens Spectrograph on the Bok 2.3 meter in April 2003.

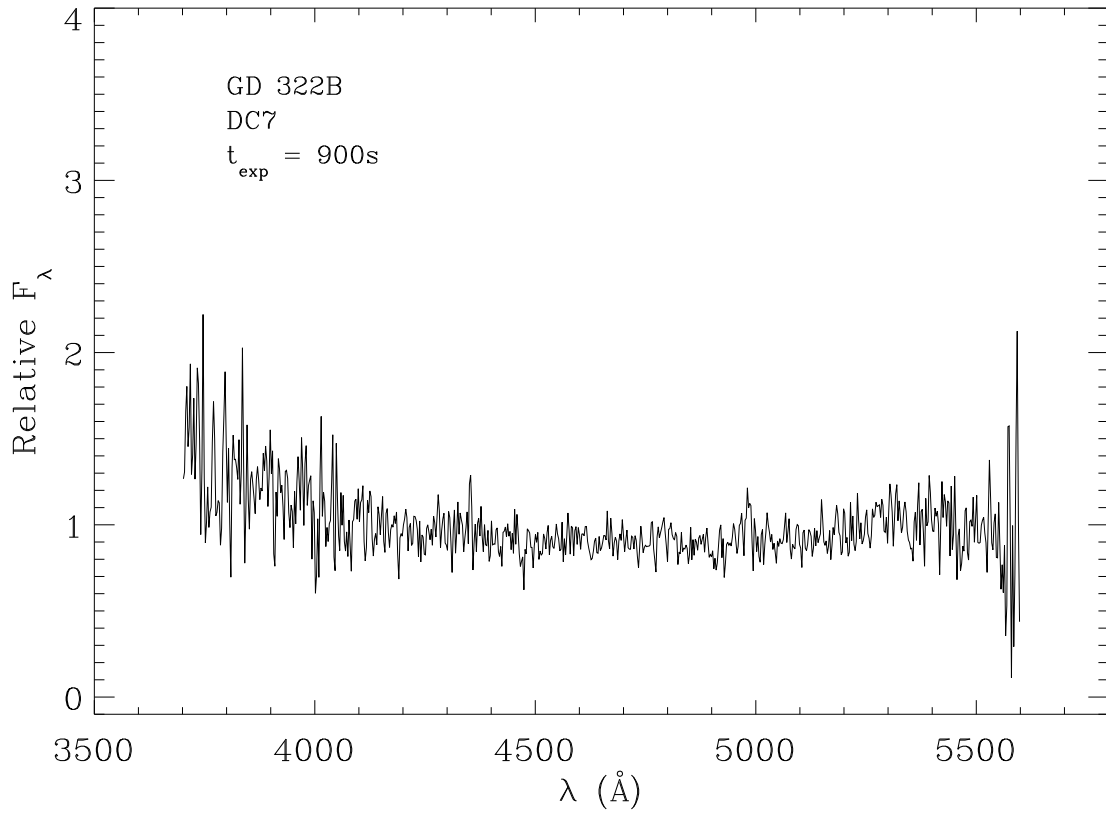


Fig. 29.— Blue optical spectrum of GD 322B taken with the Kast Spectrograph on the Shane 3 meter telescope in August 2002.



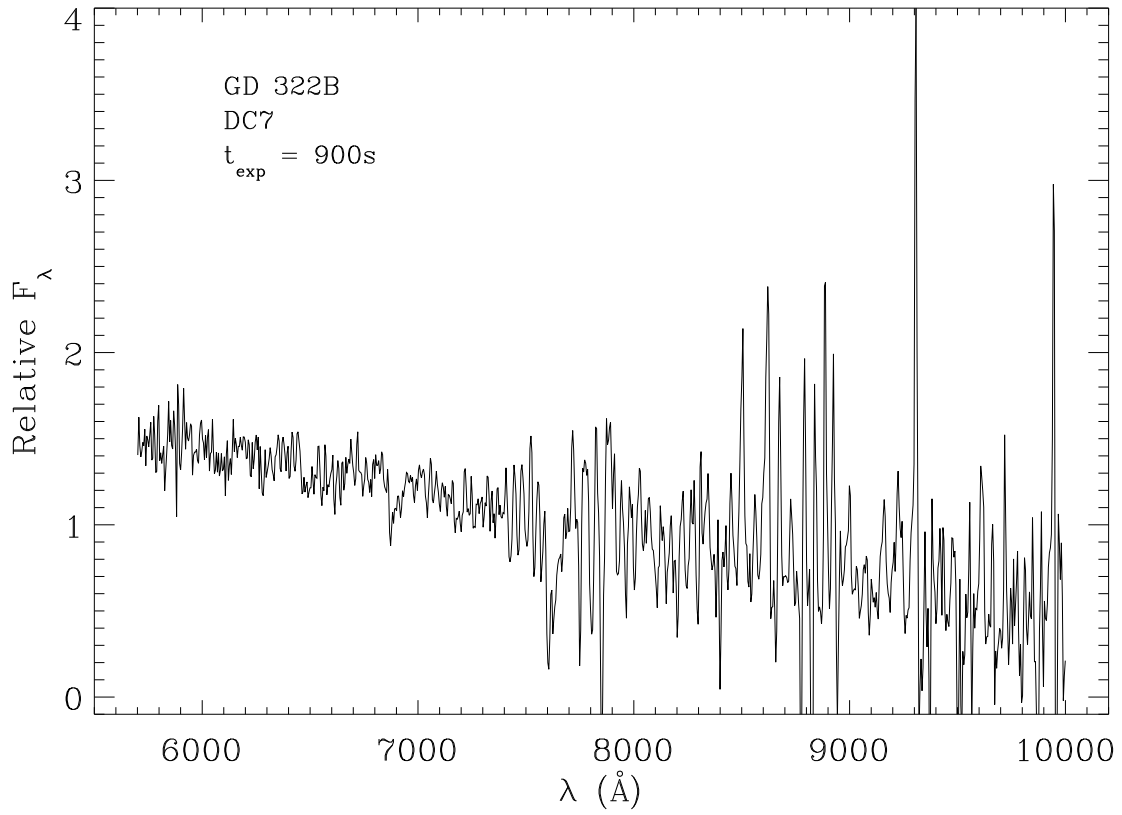


Fig. 30.— Red optical spectrum of GD 322B taken with the Kast Spectrograph on the Shane 3 meter telescope in August 2002.

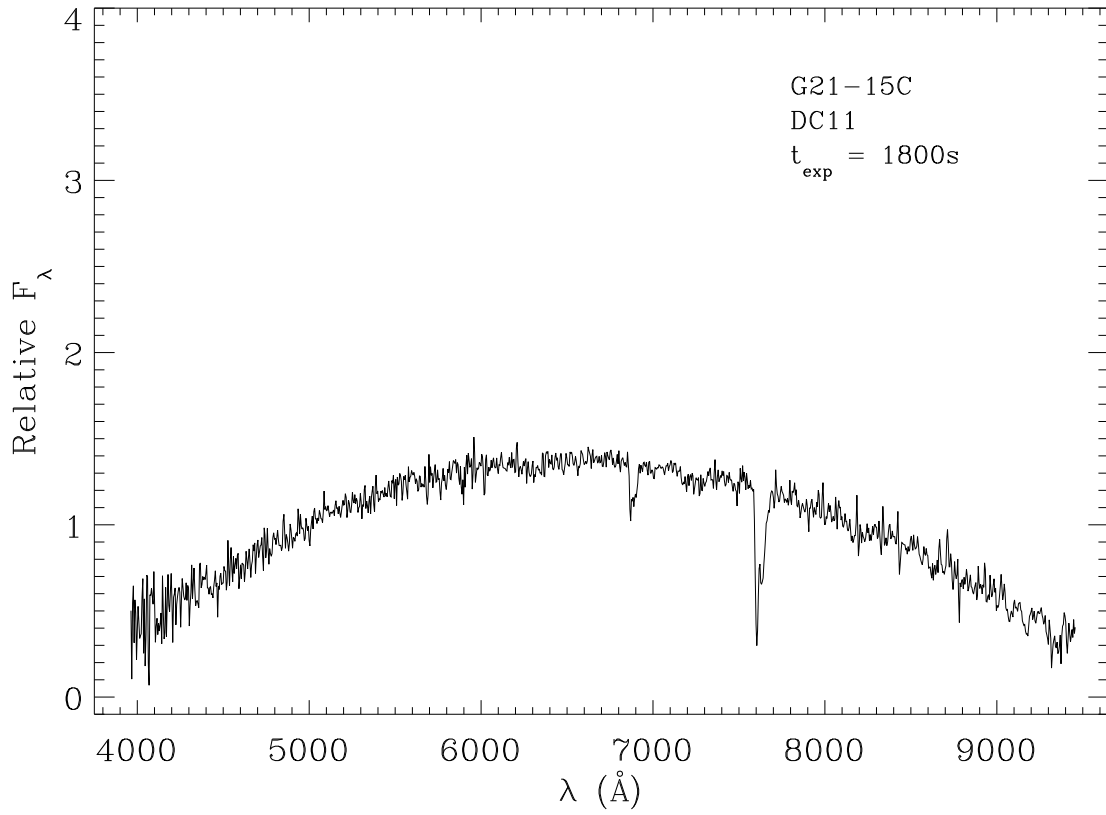


Fig. 31.— Optical spectrum of G21-15C taken with the Kast Spectrograph on the Shane 3 meter telescope in August 2003.

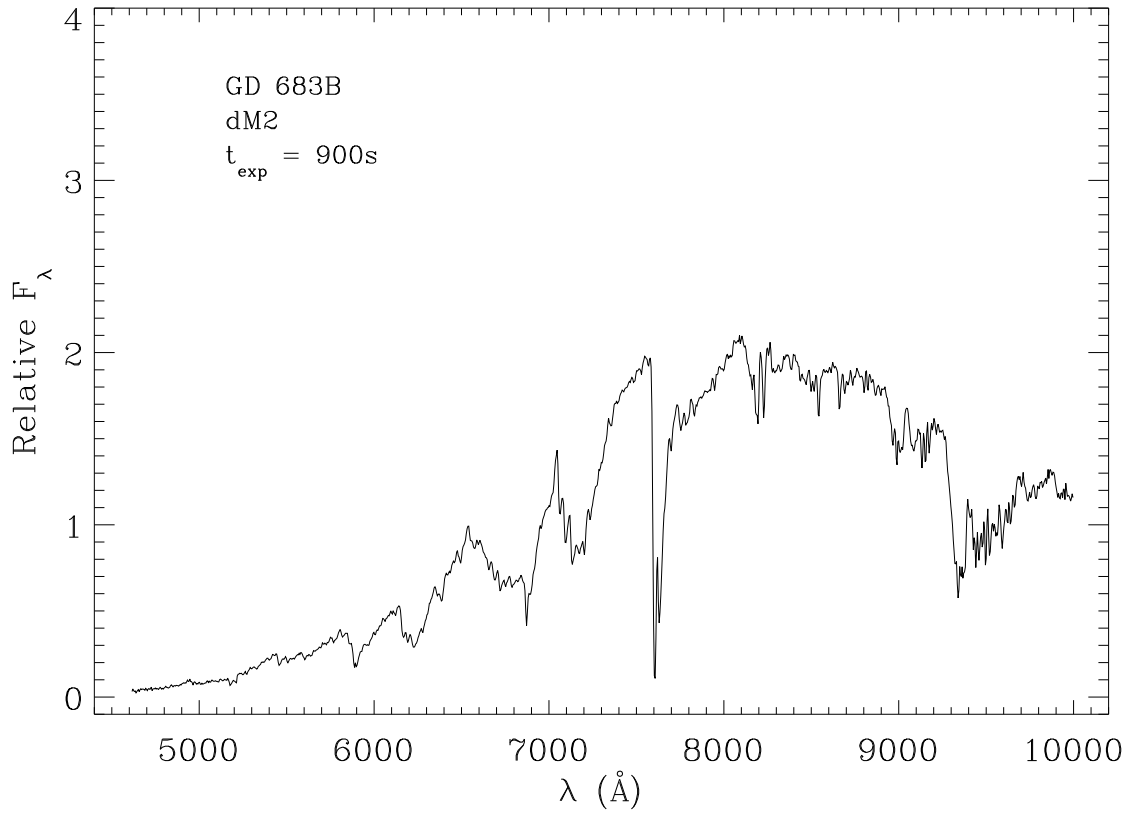


Fig. 32.— Optical spectrum of GD 683B taken with the Kast Spectrograph on the Shane 3 meter telescope in August 2003.

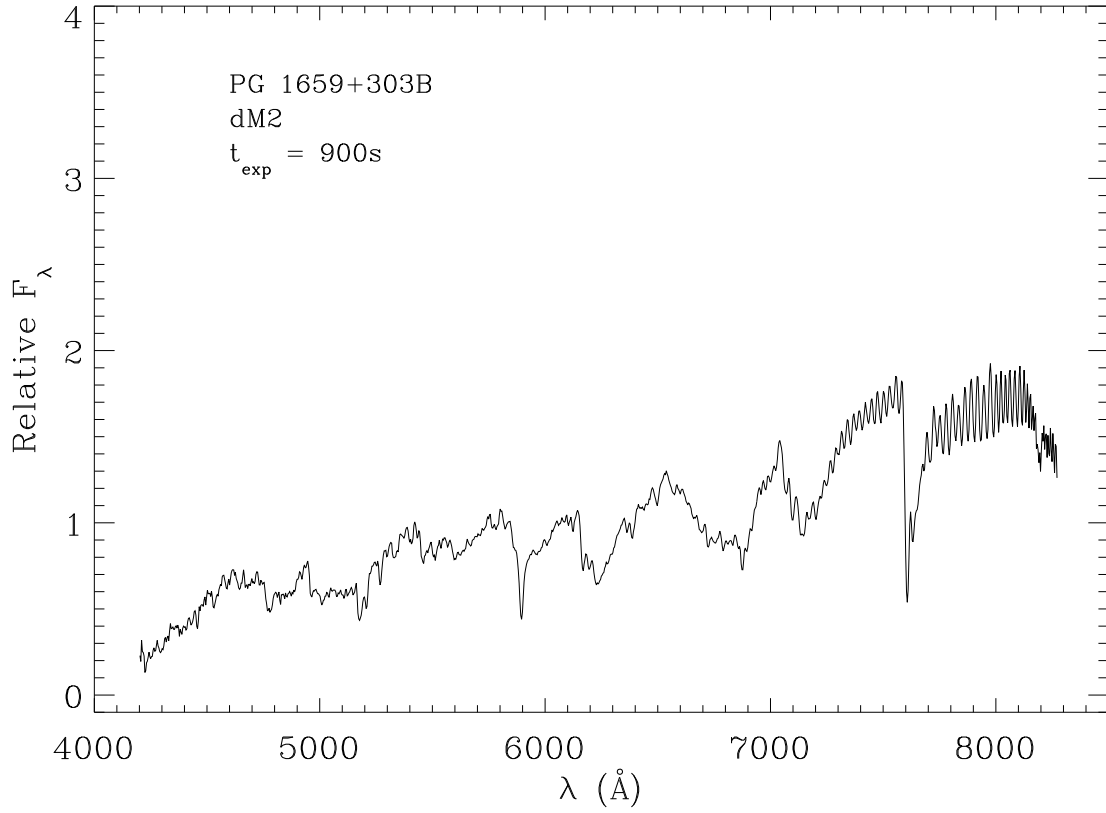


Fig. 33.— Optical spectrum of PG 1659+303B taken with the Boller & Chivens Spectrograph on the Bok 2.3 meter in April 2003.

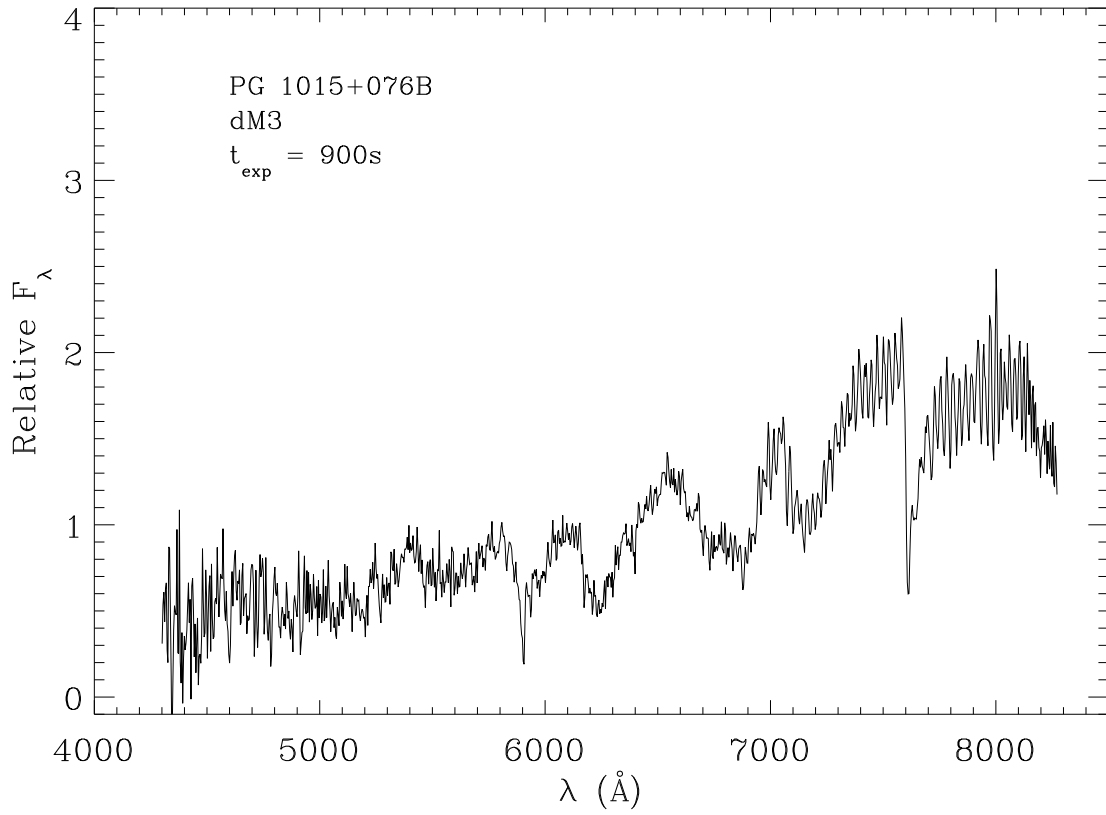


Fig. 34.— Optical spectrum of PG 1015+076B taken with the Boller & Chivens Spectrograph on the Bok 2.3 meter in April 2003.

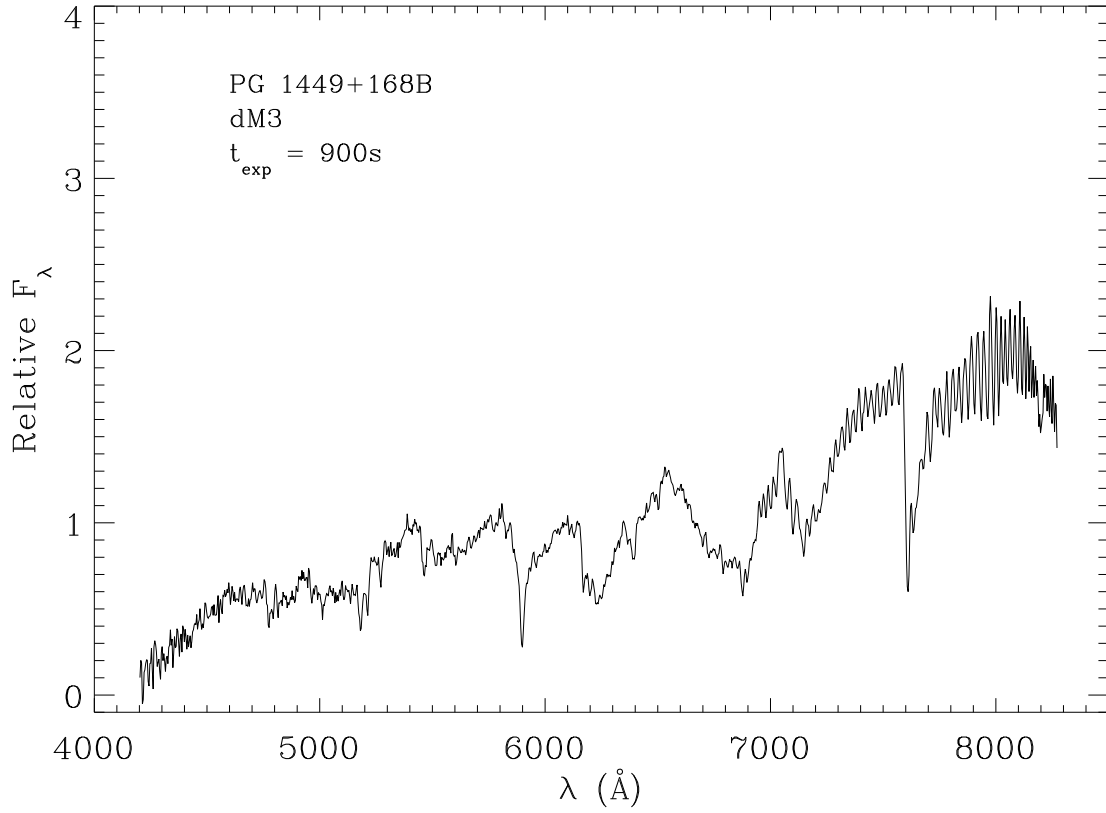


Fig. 35.— Optical spectrum of PG 1449+168B taken with the Boller & Chivens Spectrograph on the Bok 2.3 meter in April 2003.

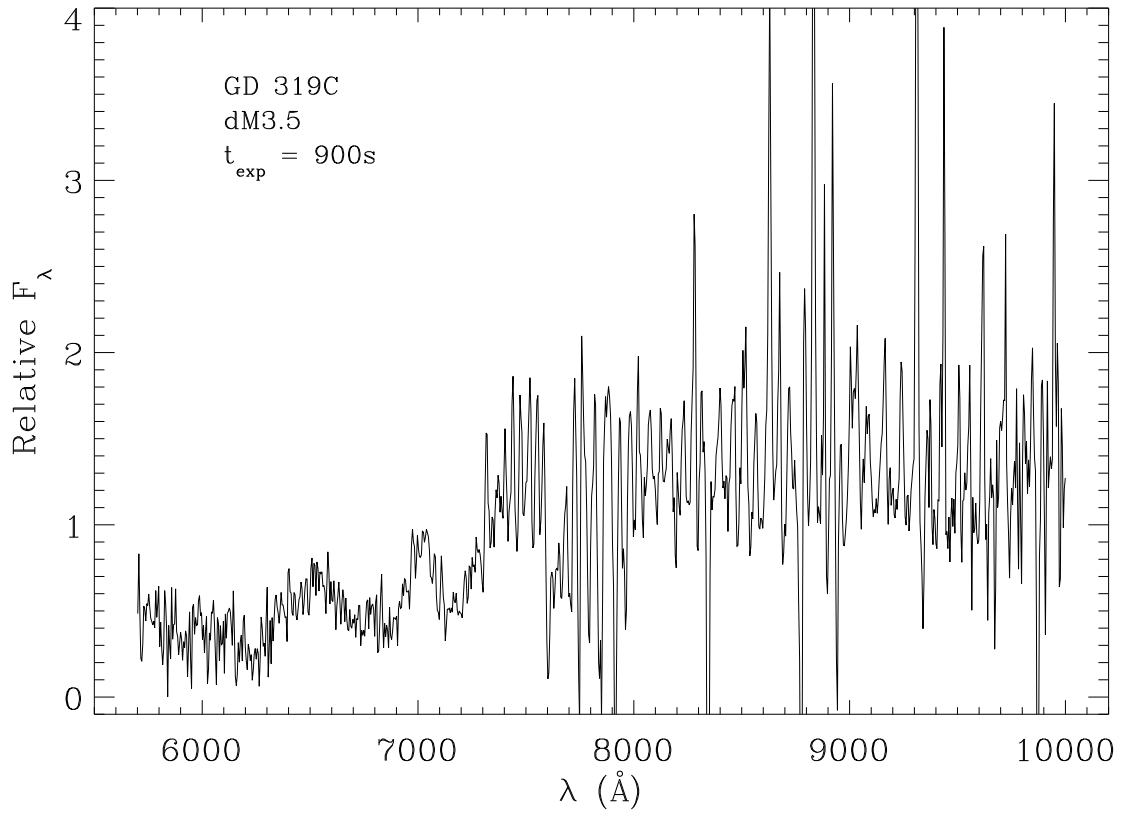


Fig. 36.— Red optical spectrum of GD 319C taken with the Kast Spectrograph on the Shane 3 meter telescope in August 2002.

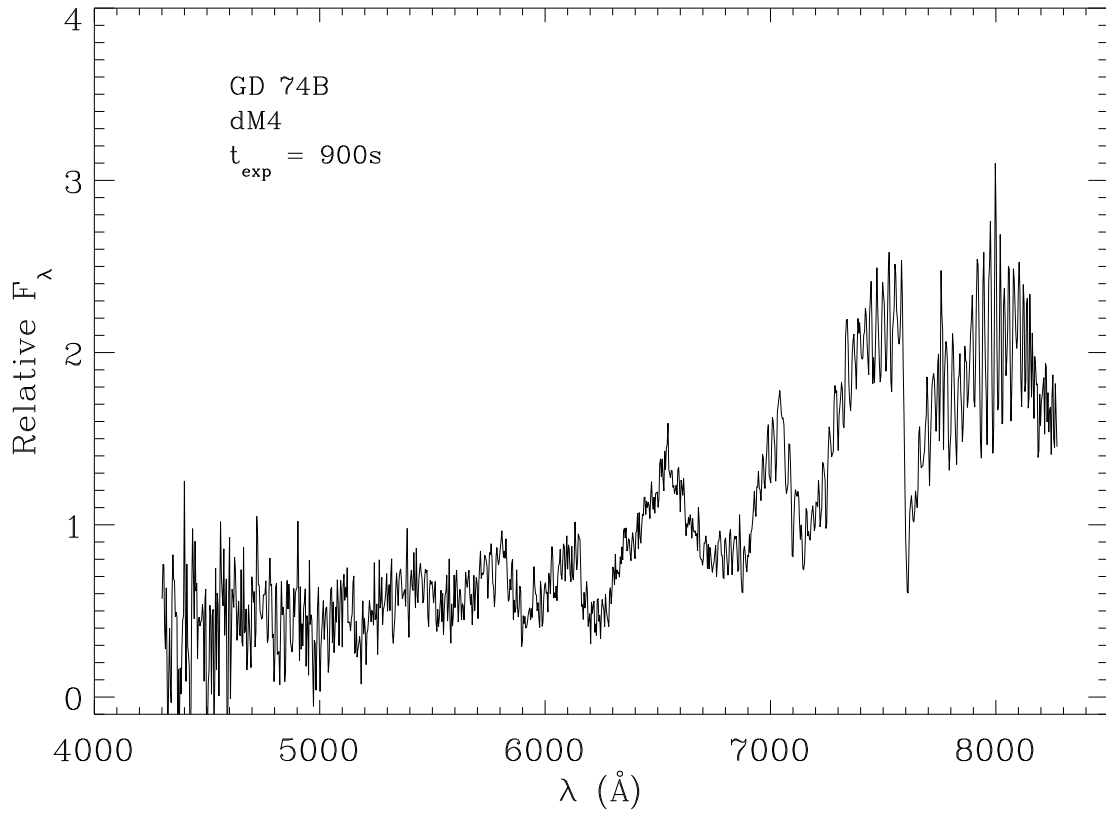


Fig. 37.— Optical spectrum of GD 74B taken with the Boller & Chivens Spectrograph on the Bok 2.3 meter in April 2003.



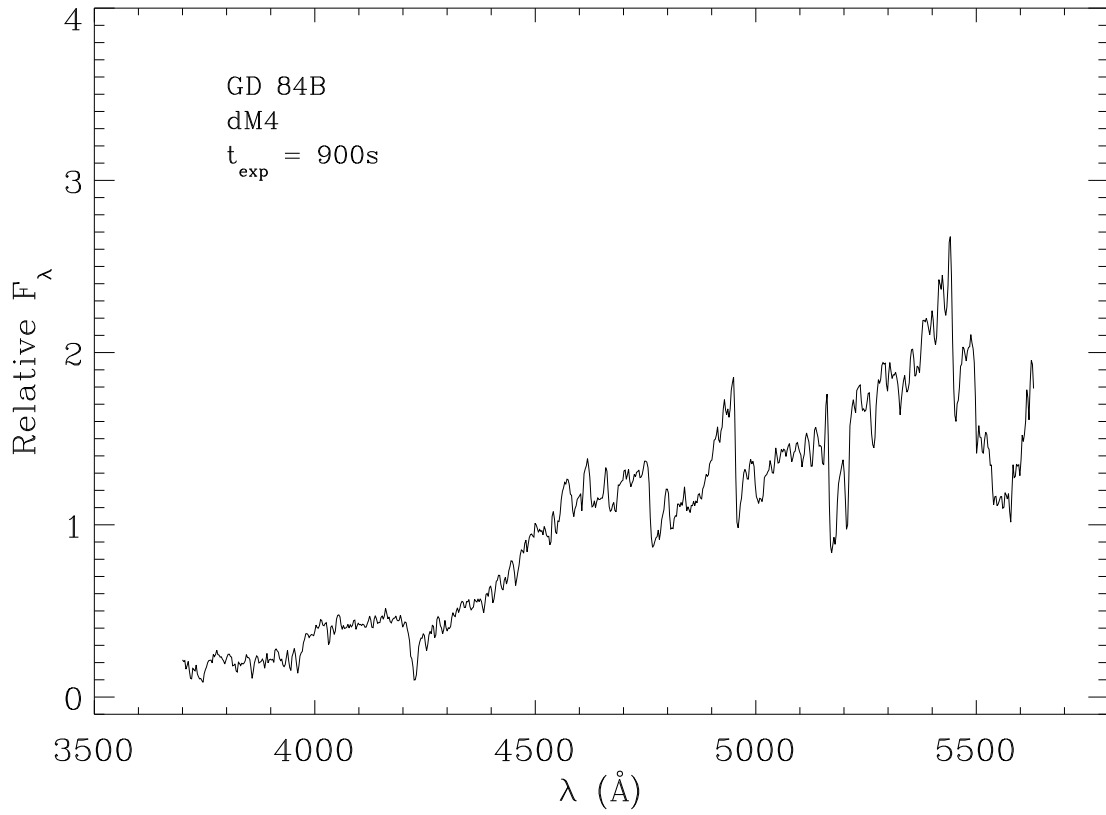


Fig. 38.— Blue optical spectrum of GD 84B taken with the Kast Spectrograph on the Shane 3 meter telescope in February 2002.

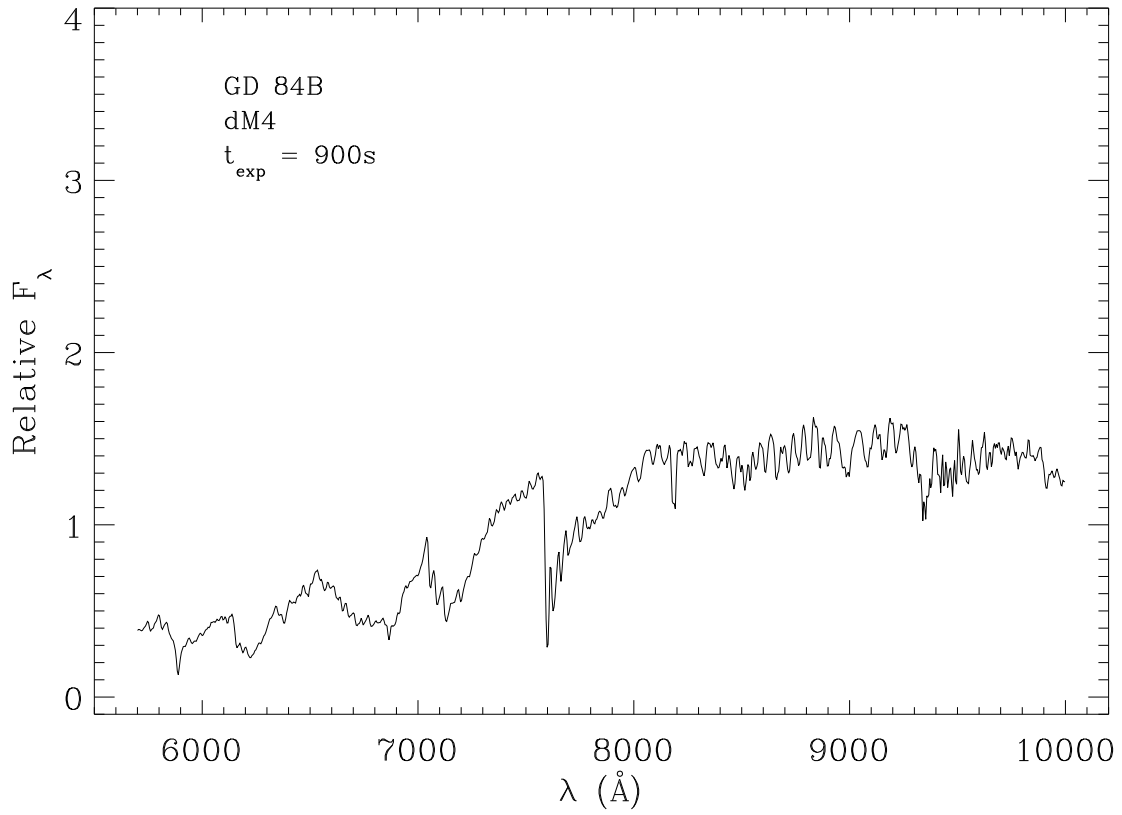


Fig. 39.— Red optical spectrum of GD 84B taken with the Kast Spectrograph on the Shane 3 meter telescope in February 2002.

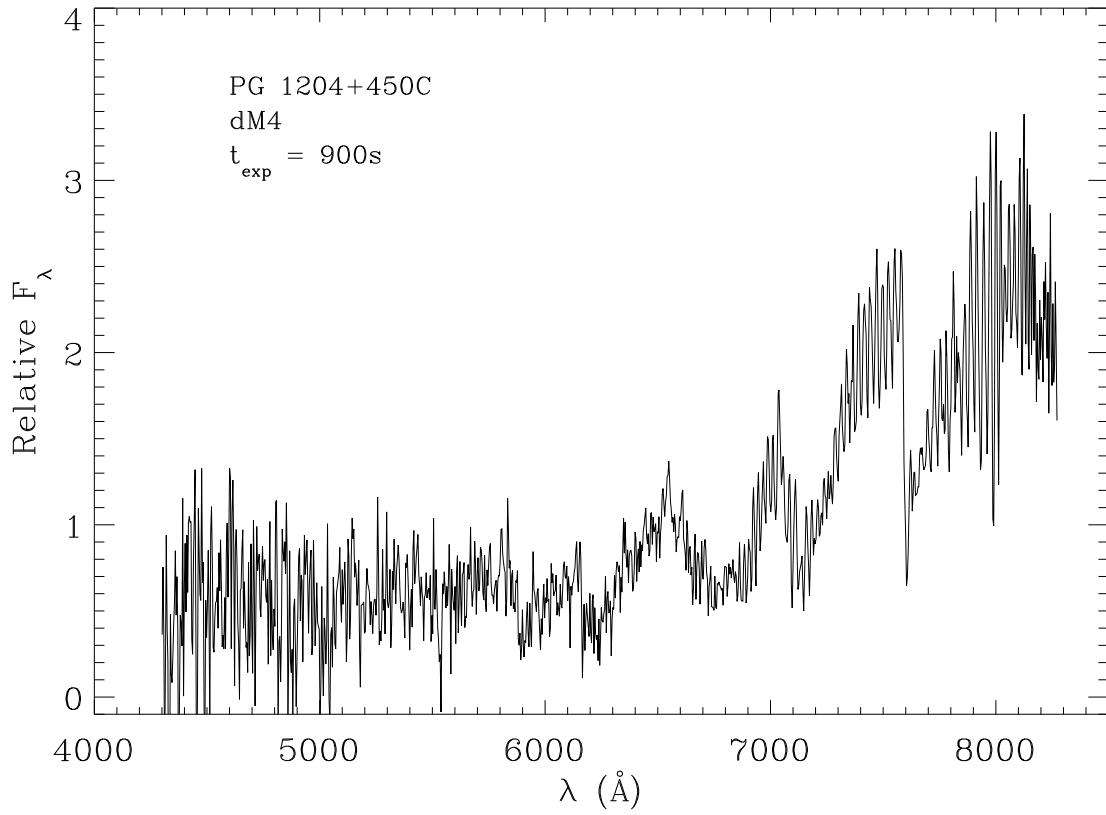


Fig. 40.— Optical spectrum of PG 1204+450C taken with the Boller & Chivens Spectrograph on the Bok 2.3 meter in April 2003.

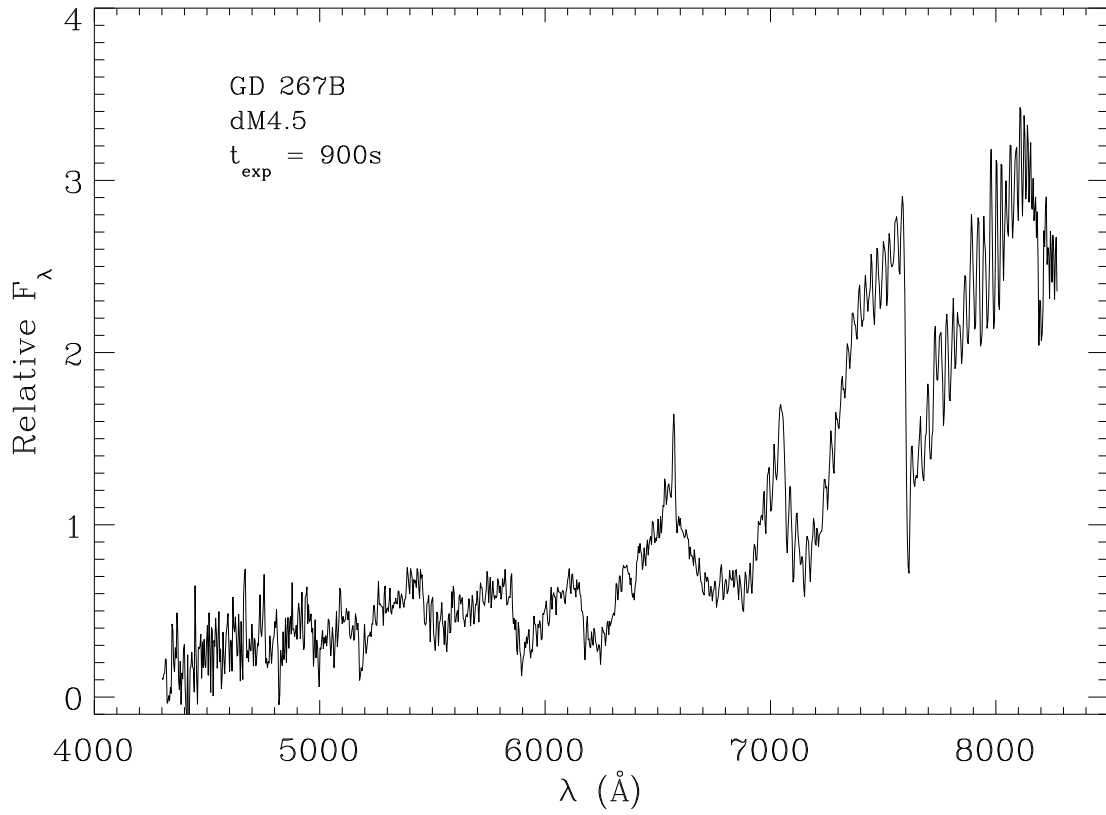


Fig. 41.— Optical spectrum of GD 267B taken with the Boller & Chivens Spectrograph on the Bok 2.3 meter in April 2003.

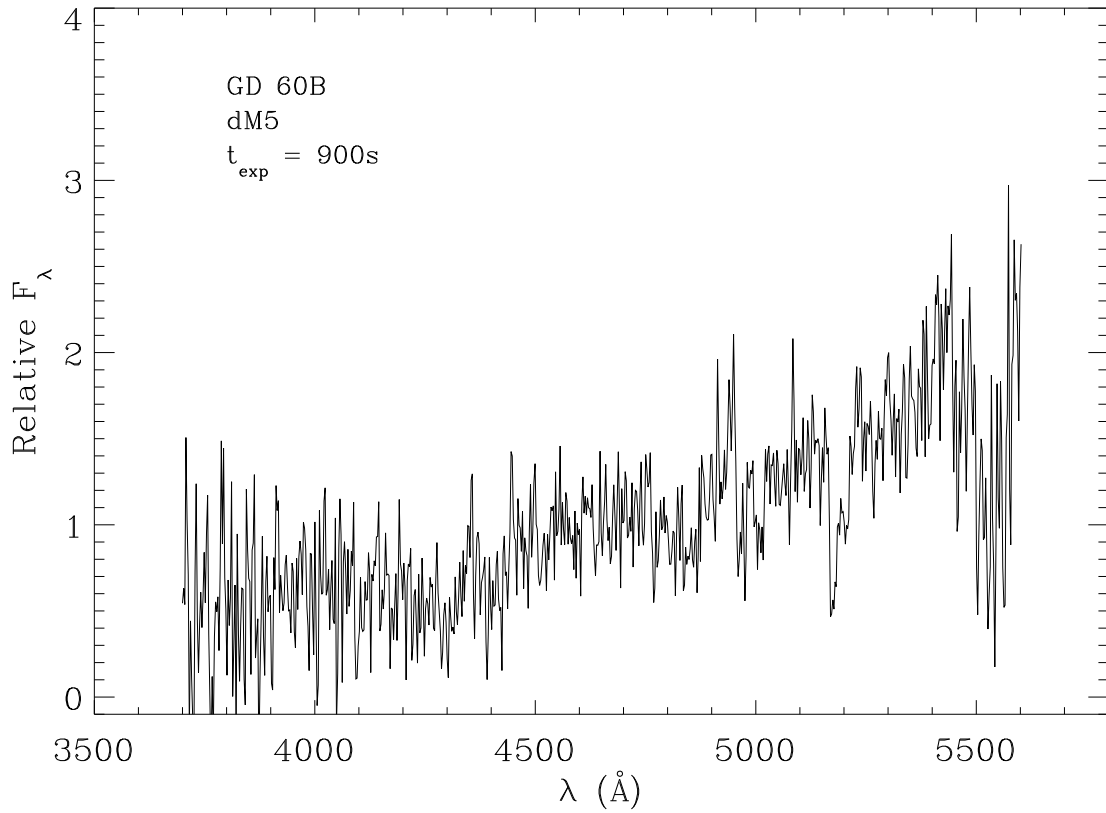


Fig. 42.— Blue optical spectrum of GD 60B taken with the Kast Spectrograph on the Shane 3 meter telescope in February 2002.

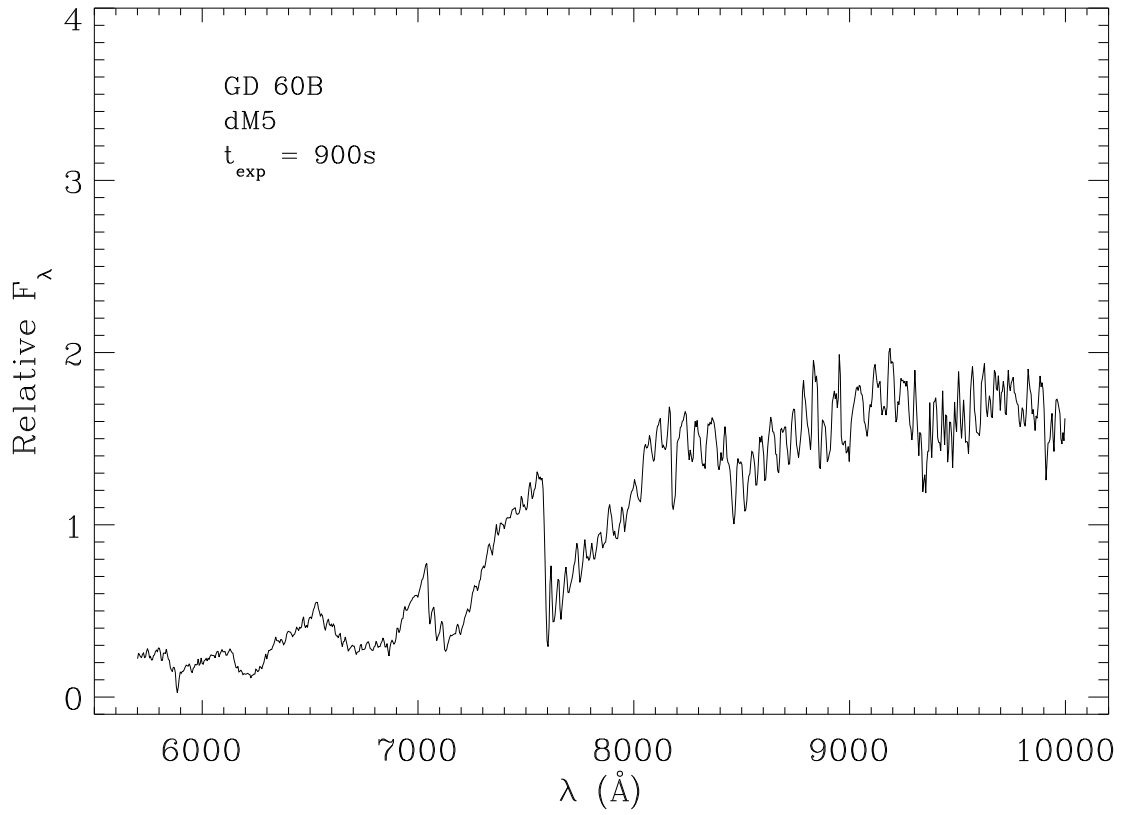


Fig. 43.— Red optical spectrum of GD 60B taken with the Kast Spectrograph on the Shane 3 meter telescope in February 2002.

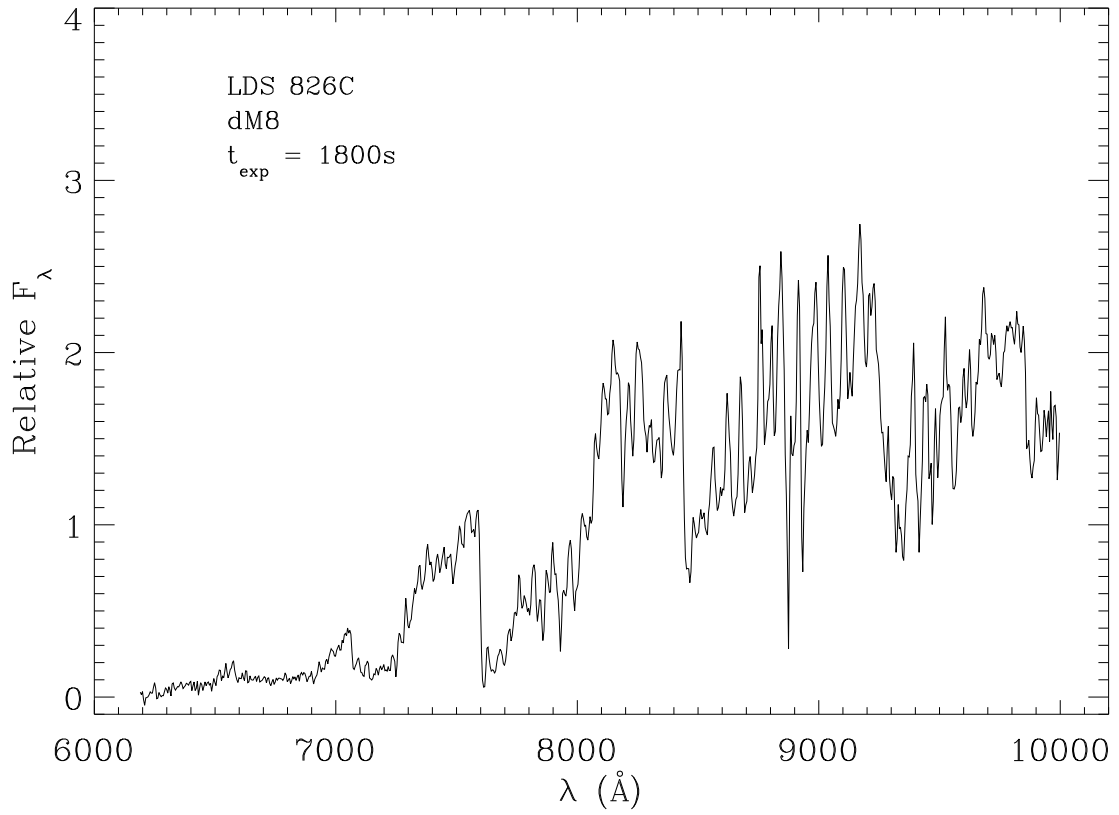


Fig. 44.— Optical spectrum of LDS 826C taken with the Kast Spectrograph on the Shane 3 meter telescope in August 2003.

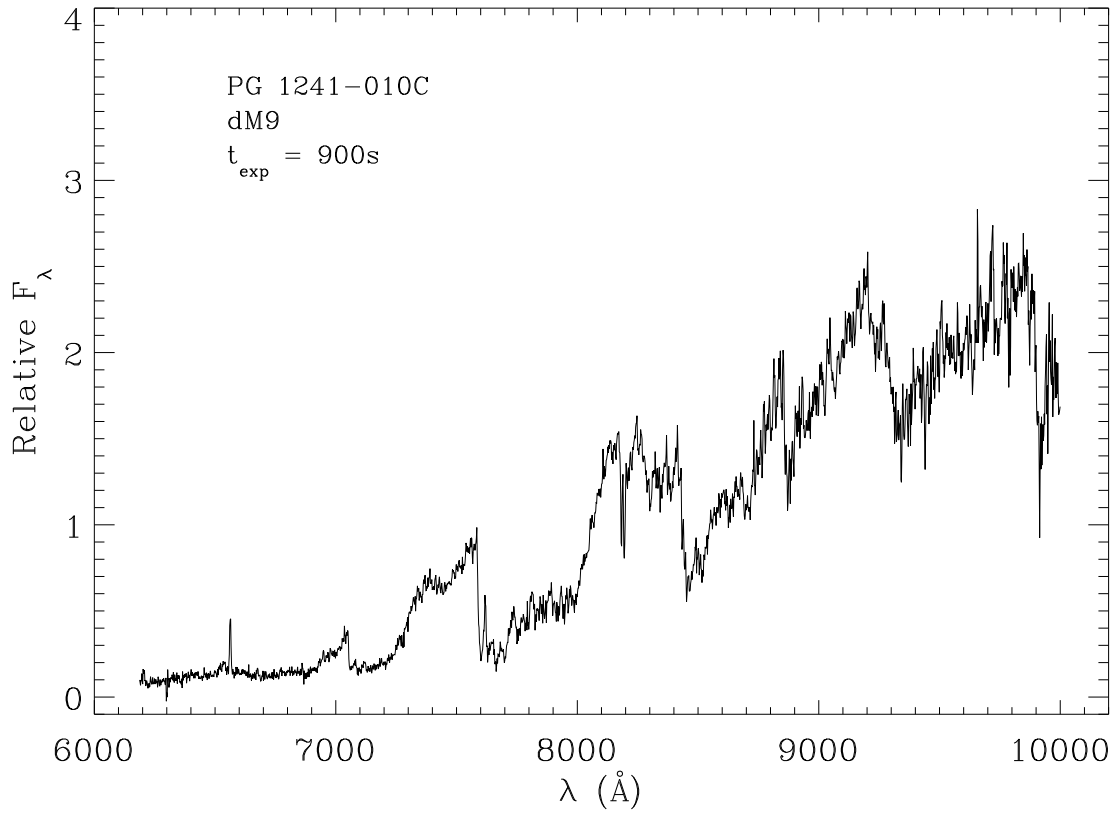


Fig. 45.— Optical spectrum of PG 1241-010C taken with the Low Resolution Imaging Spectrograph on the Keck I 10 meter telescope in May 2003.



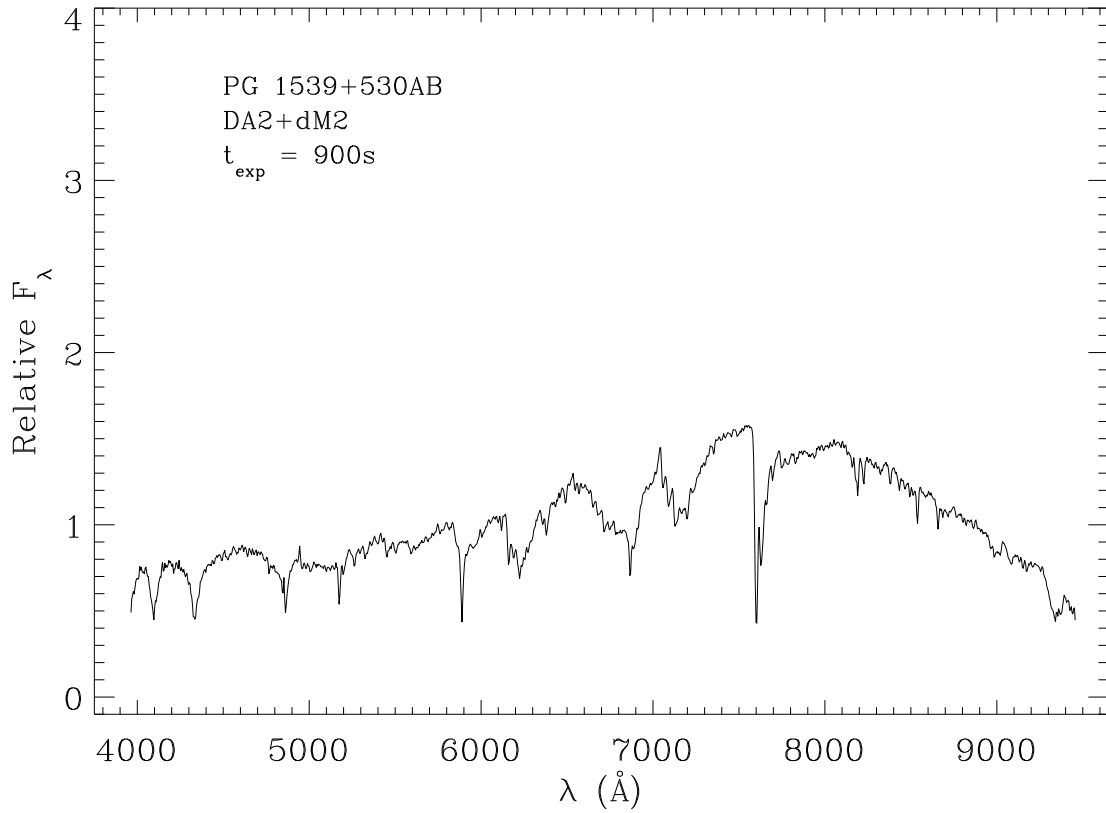


Fig. 46.— Optical spectrum of PG 1539+530AB taken with the Kast Spectrograph on the Shane 3 meter telescope in August 2003.

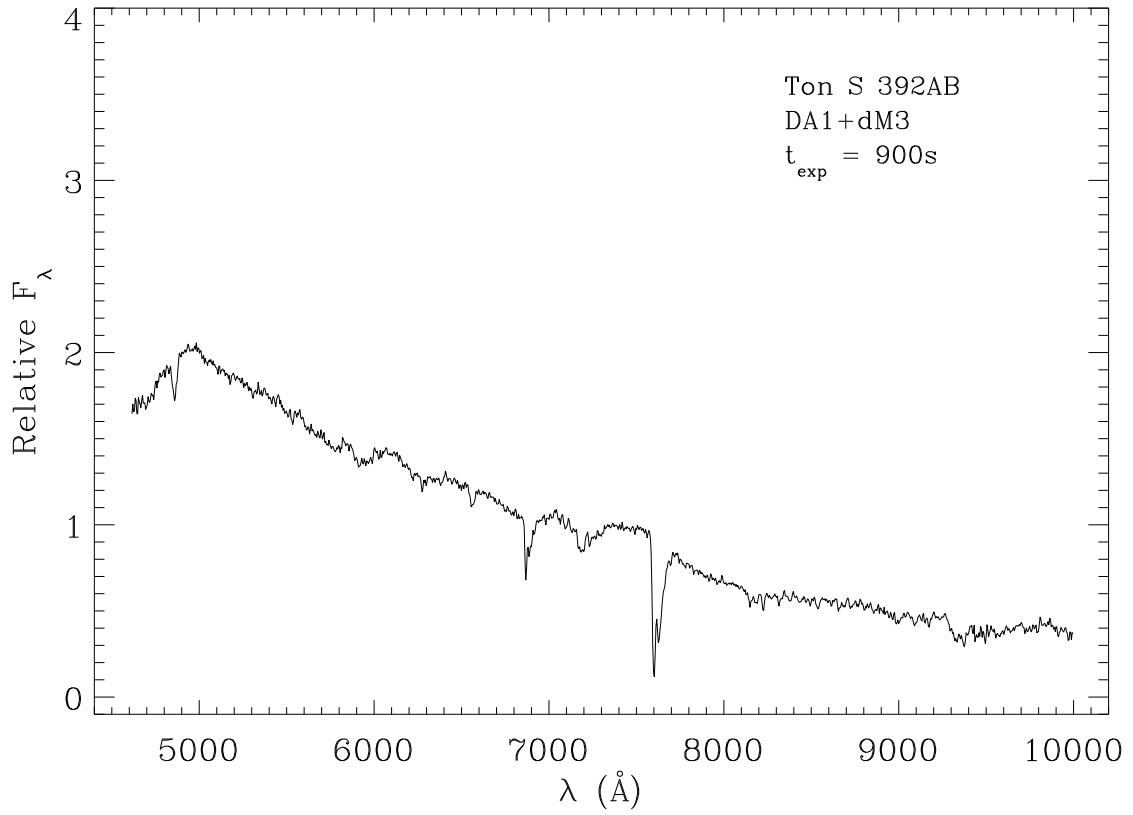


Fig. 47.— Optical spectrum of Ton S 392AB taken with the Kast Spectrograph on the Shane 3 meter telescope in August 2003.

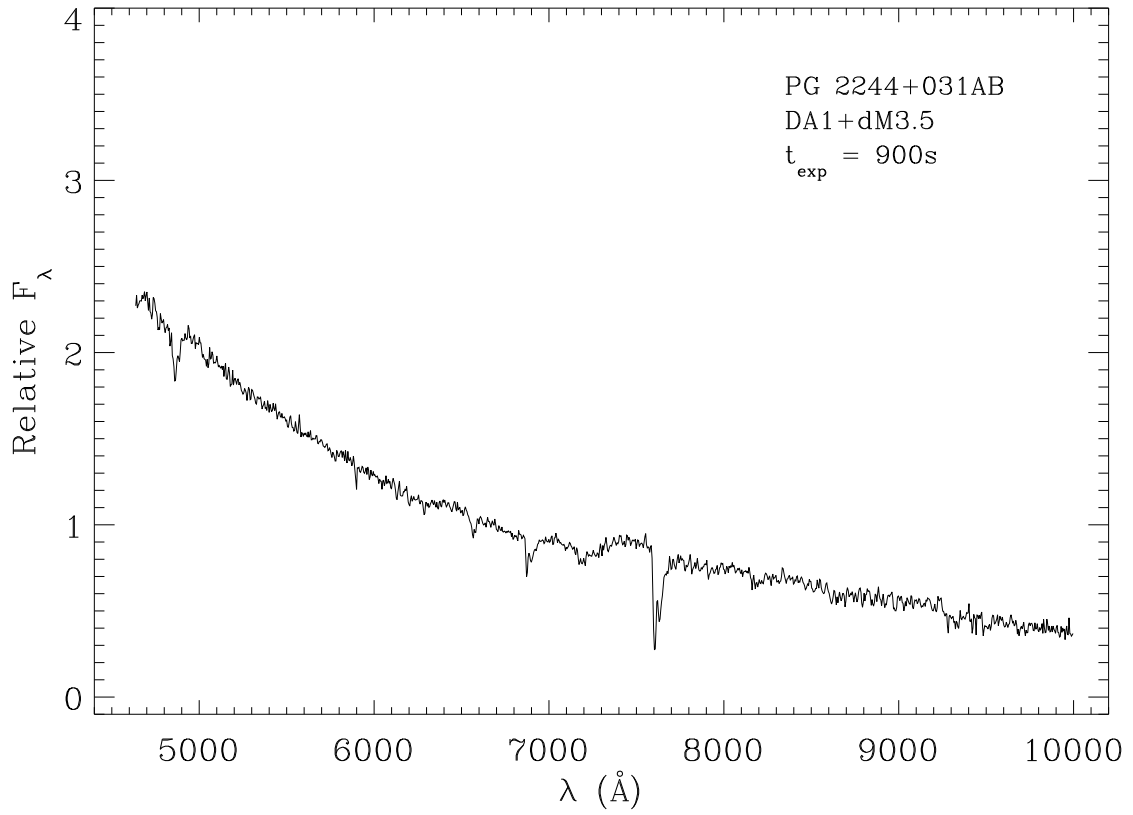


Fig. 48.— Optical spectrum of PG 2244+031AB taken with the Kast Spectrograph on the Shane 3 meter telescope in August 2003.

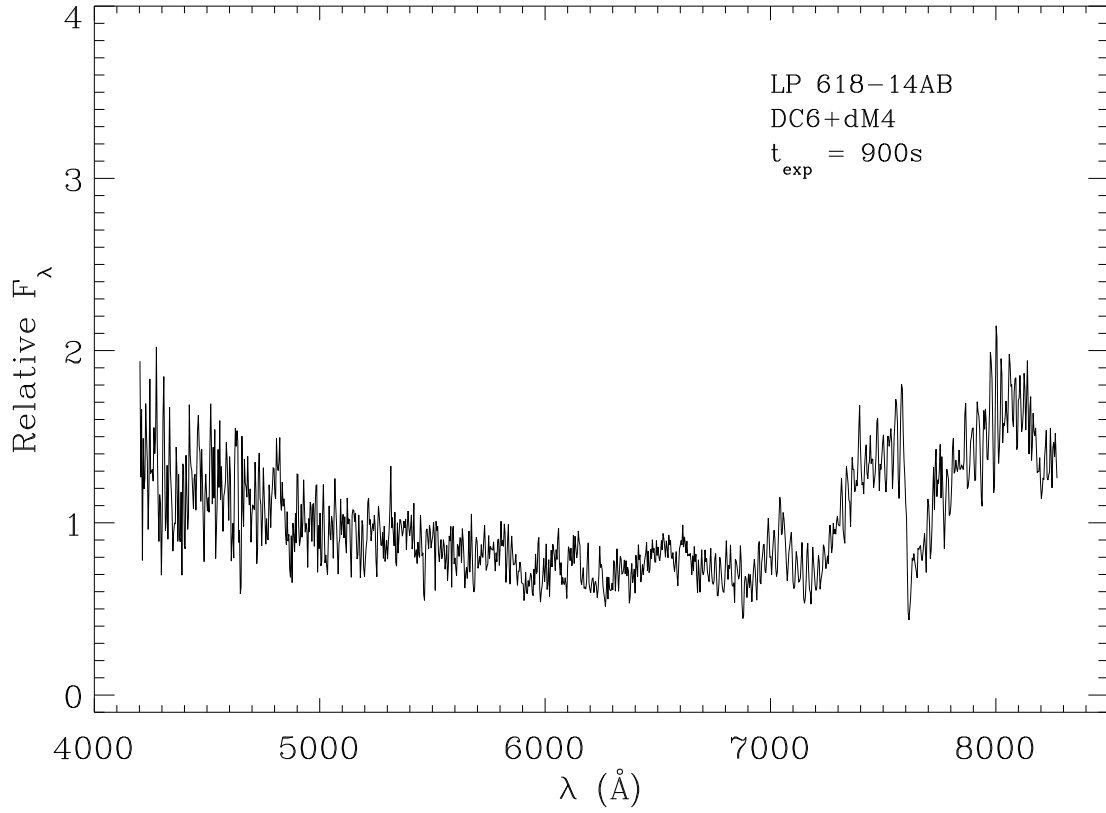


Fig. 49.— Optical spectrum of LP 618-14AB taken with the Boller & Chivens Spectrograph on the Bok 2.3 meter in April 2003.

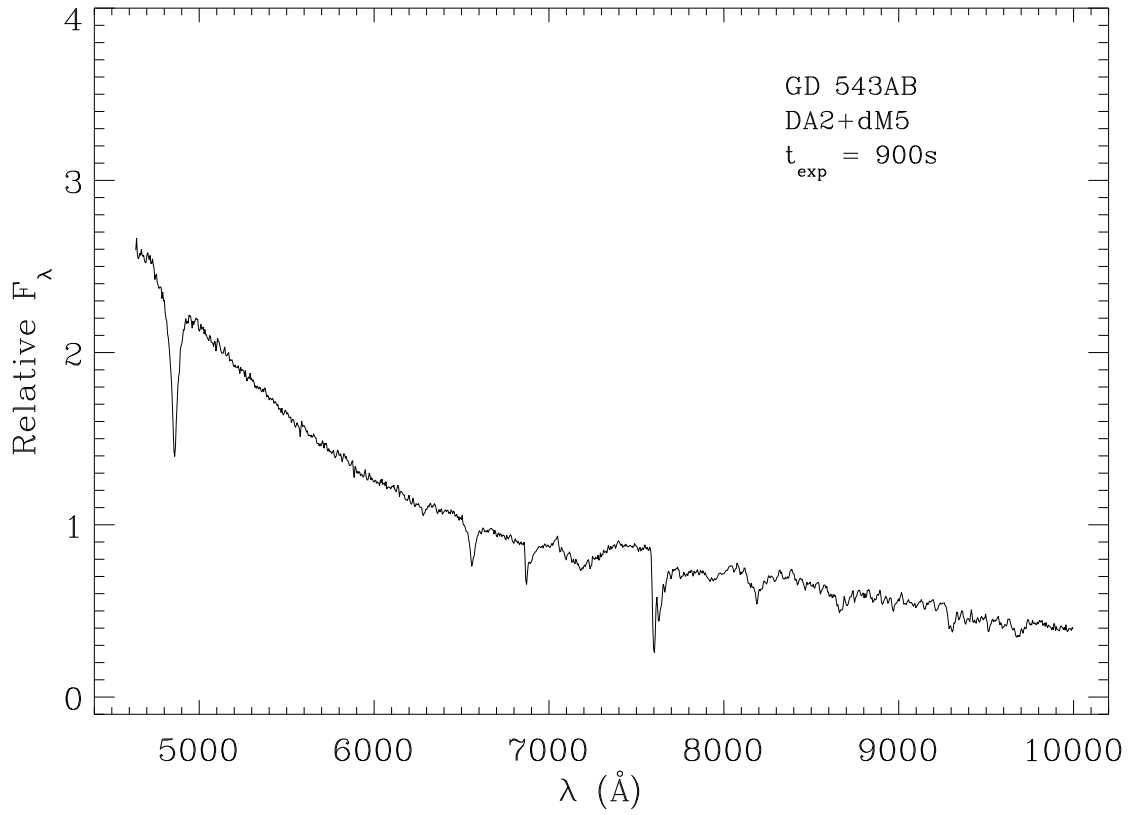


Fig. 50.— Optical spectrum of GD 543AB taken with the Kast Spectrograph on the Shane 3 meter telescope in August 2003.

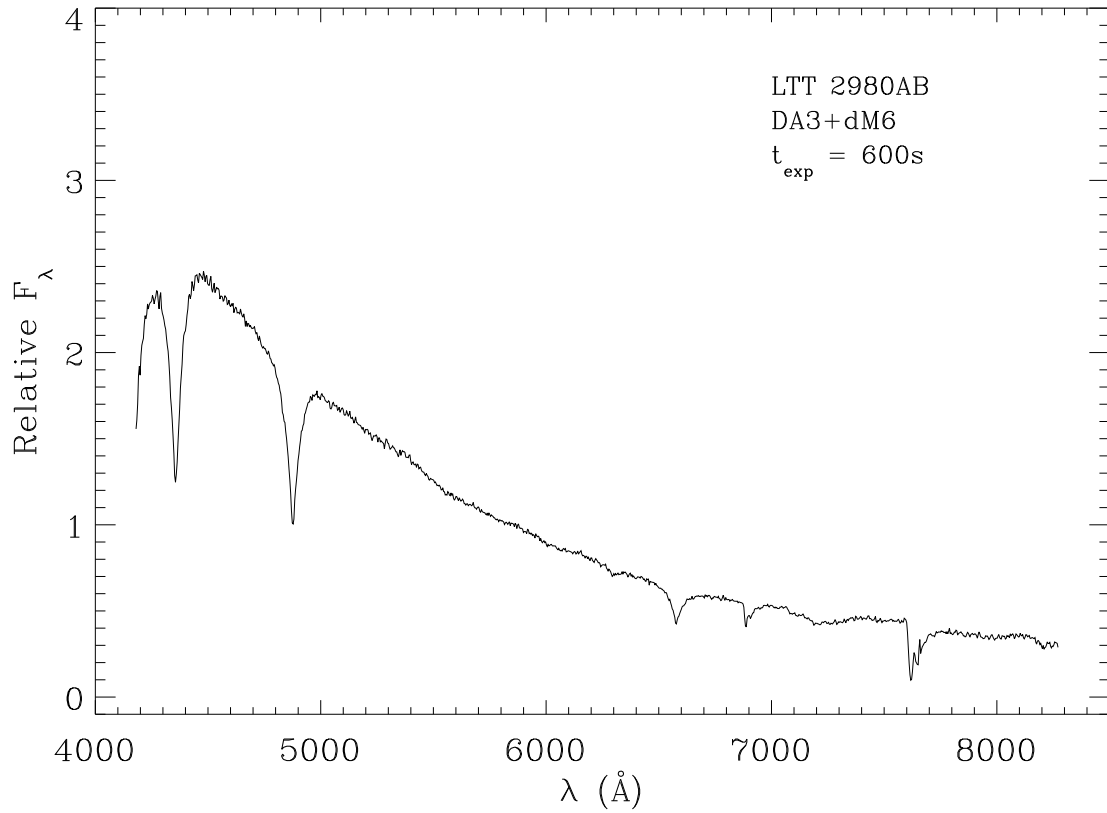


Fig. 51.— Optical spectrum of LTT 2980AB taken with the Boller & Chivens Spectrograph on the Bok 2.3 meter in April 2003.

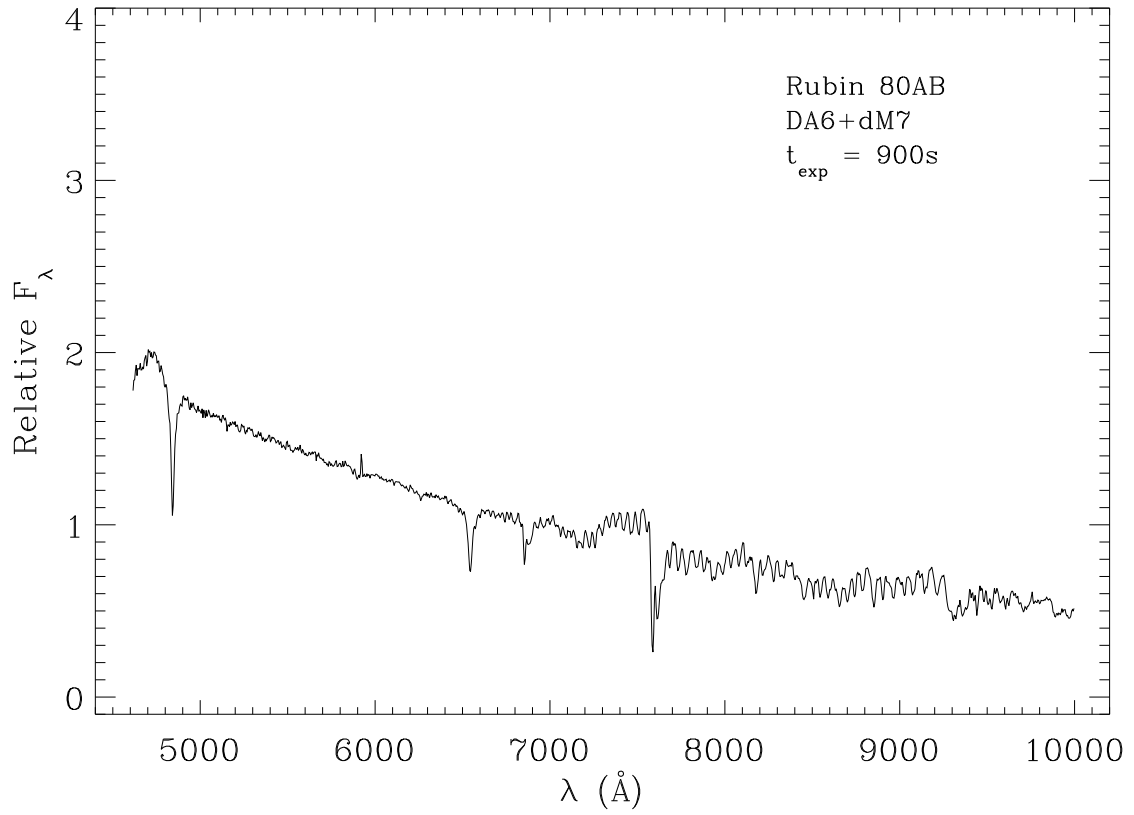


Fig. 52.— Optical spectrum of Rubin 80AB taken with the Kast Spectrograph on the Shane 3 meter telescope in August 2003.

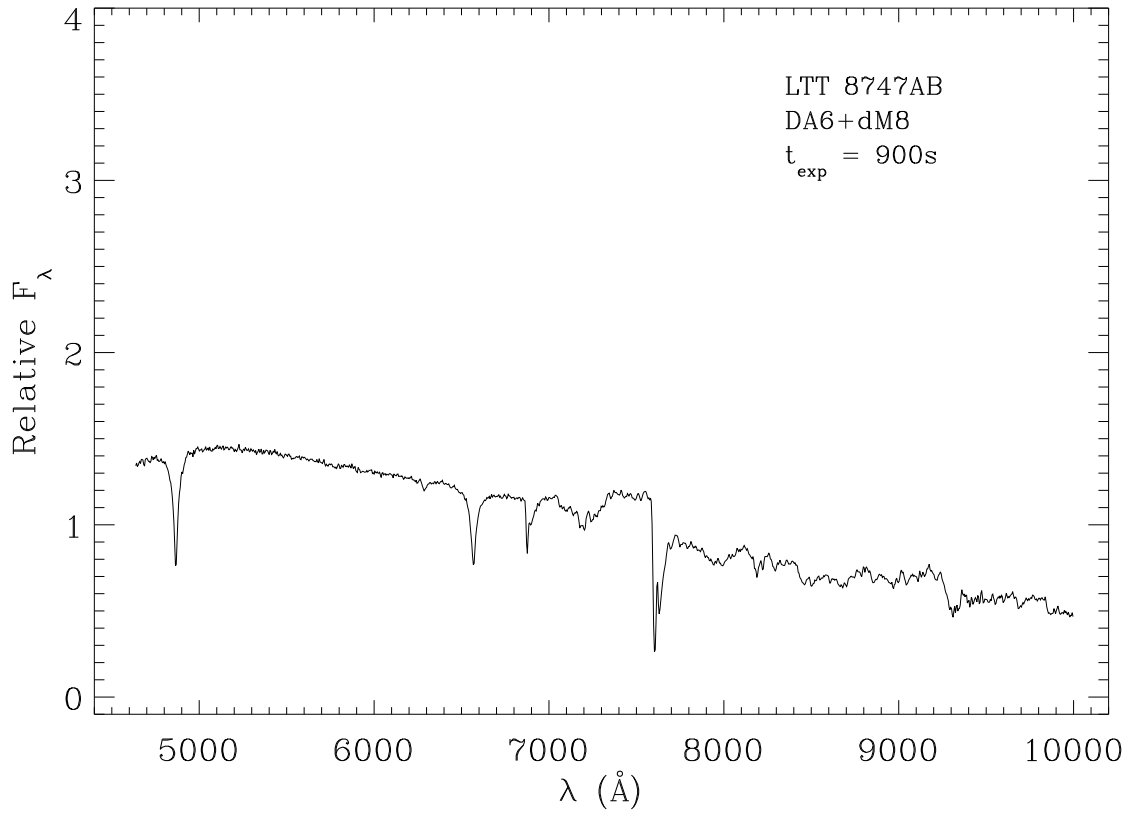


Fig. 53.— Optical spectrum of LTT 8747AB taken with the Kast Spectrograph on the Shane 3 meter telescope in August 2003.



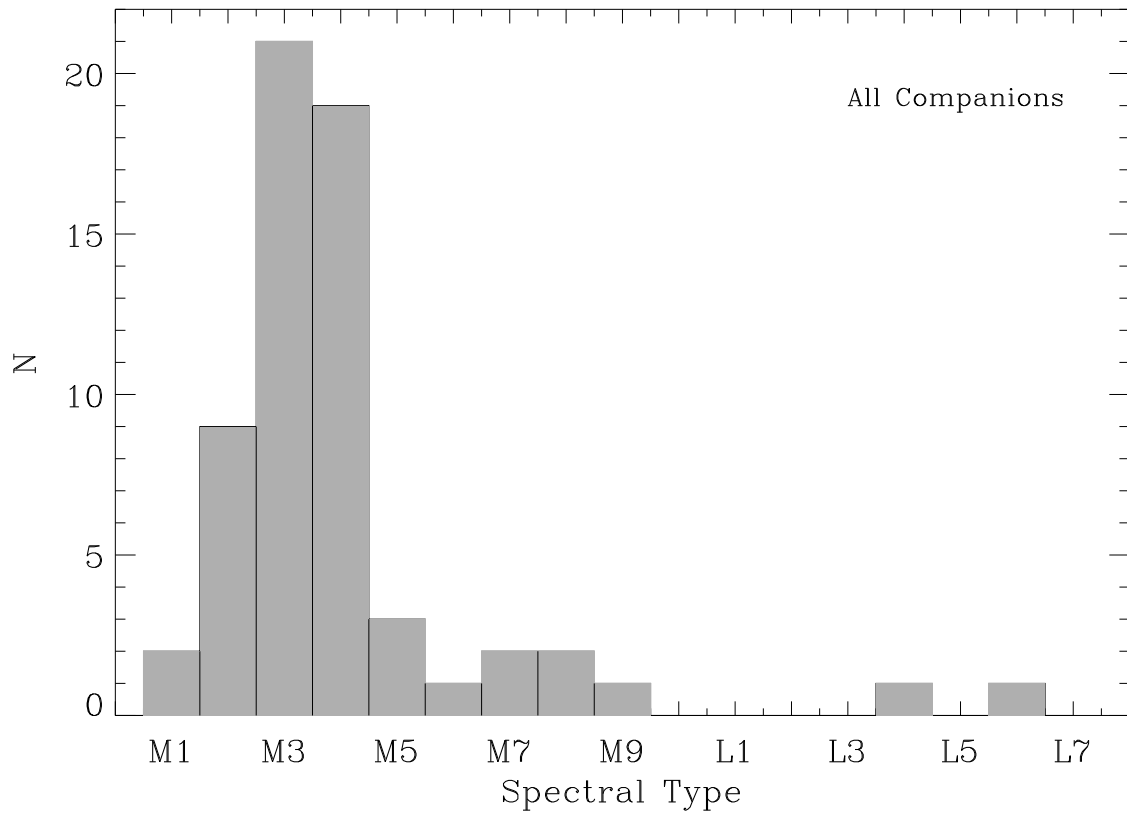


Fig. 54.— The number of cool dwarf companions versus spectral type for objects discovered and studied in this work.

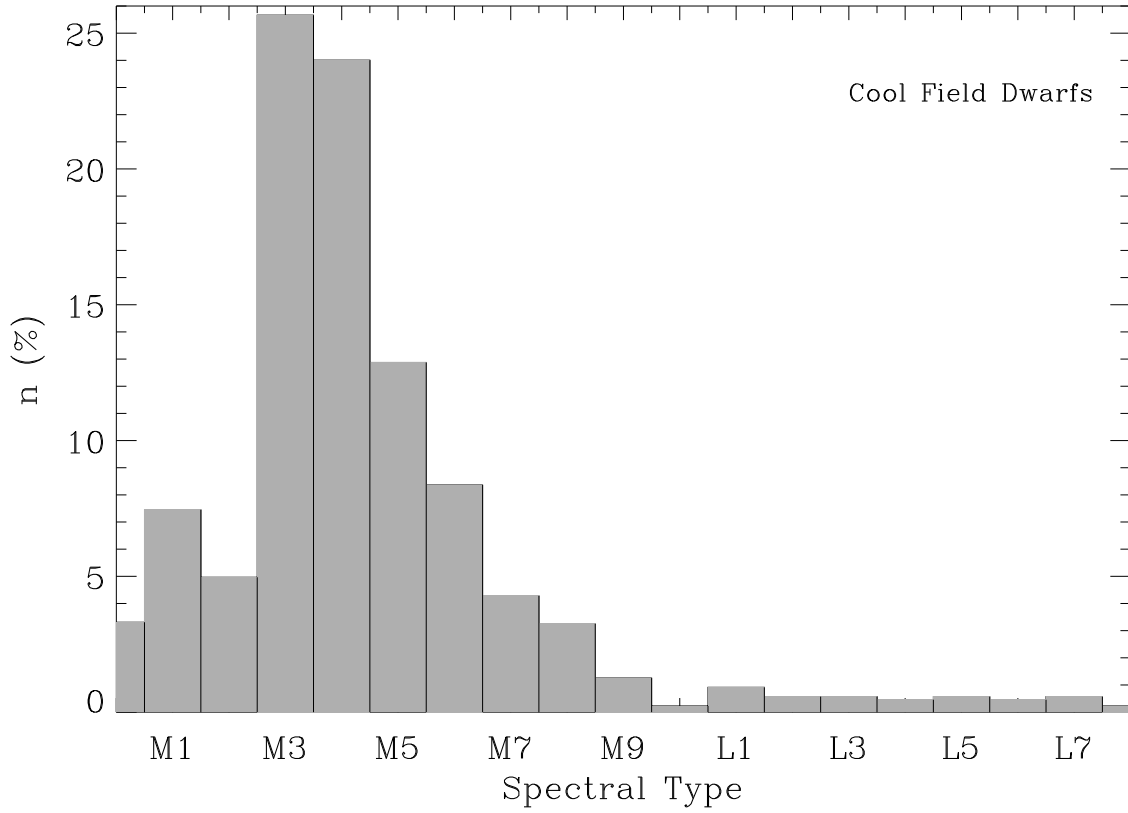


Fig. 55.— The frequency of cool field dwarfs within  $d = 20$  pc versus spectral type (Reid & Hawley 2000; Cruz et al. 2003). The data have been corrected for volume, sky coverage, and estimated completeness.

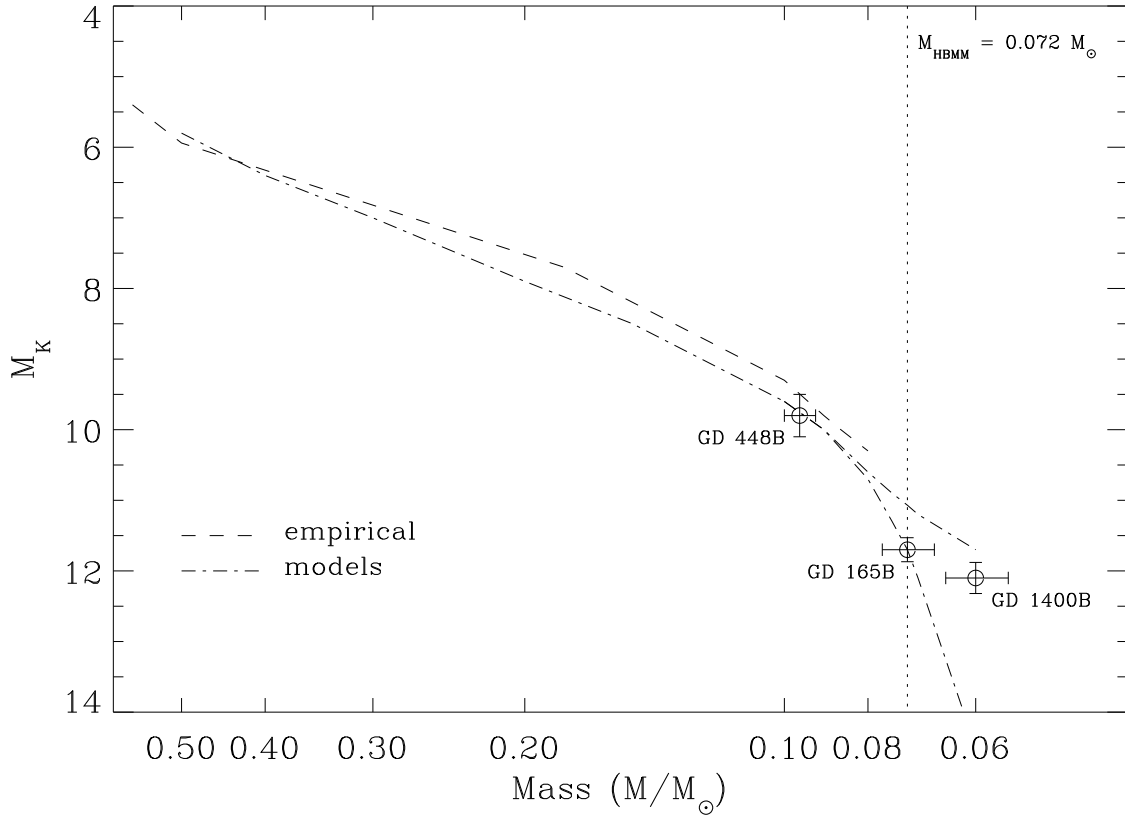


Fig. 56.— Empirical and model relations between absolute  $K$  band magnitude and mass. Three very cool companions to white dwarfs with mass estimates are shown along with 1 and 5 Gyr brown dwarf model cooling tracks.

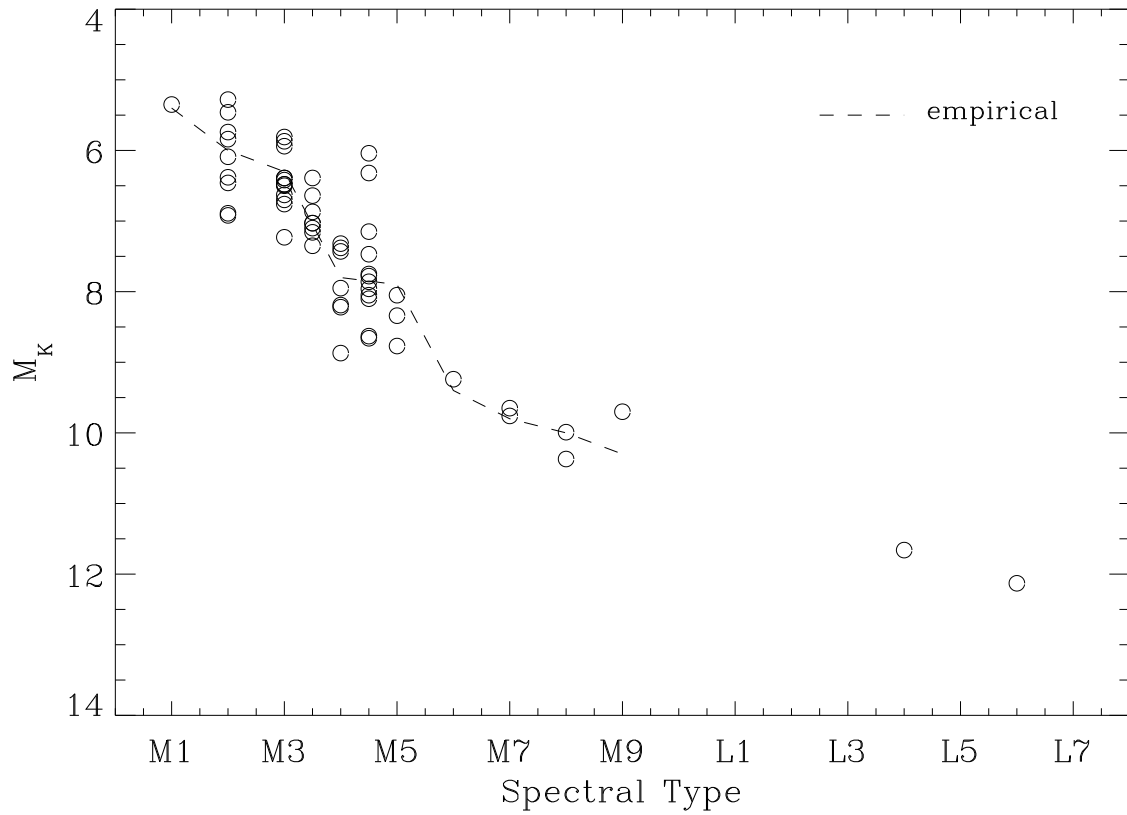


Fig. 57.— Absolute  $K$  magnitude versus spectral type for all low mass companions based on the white dwarf distance. The dashed line is the relation of Kirkpatrick & McCarthy (1994).

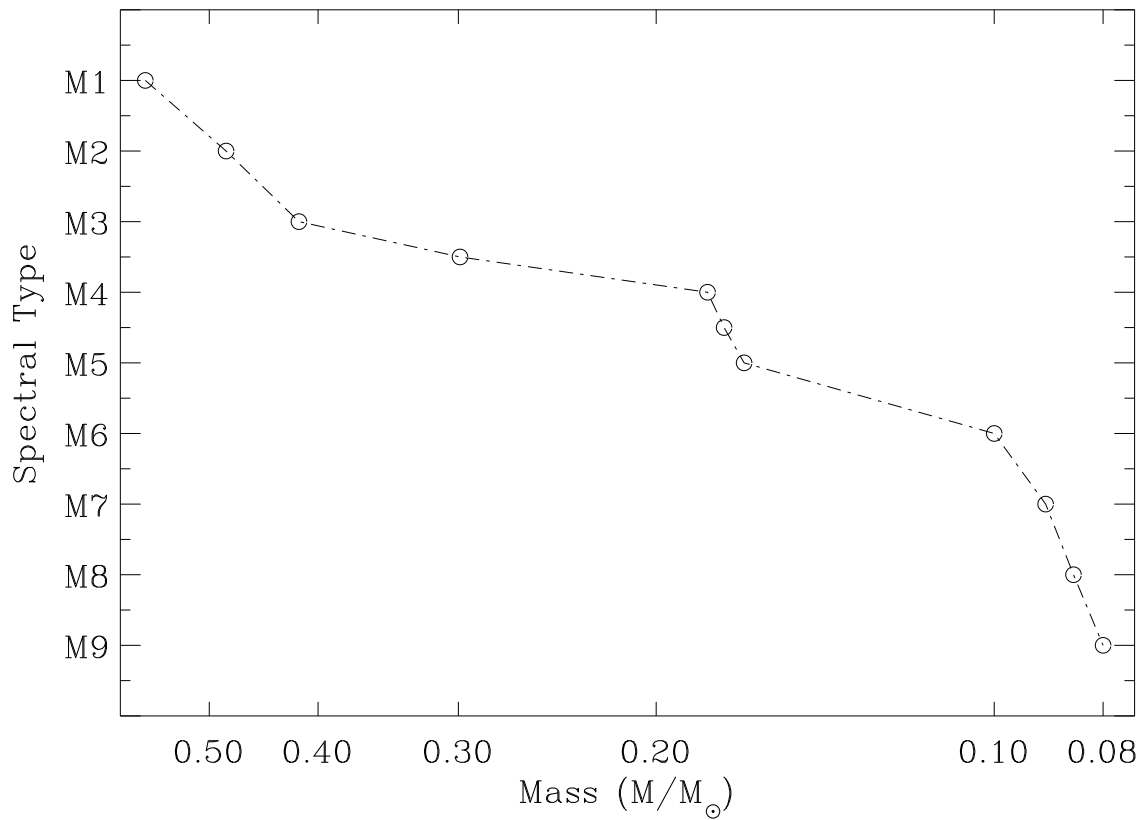


Fig. 58.— Spectral type correlation with mass used for constructing the companion mass function. Data points represent the nodes in the constructed correlation function. These points are from the empirical and semiempirical relations of Henry & McCarthy (1993); Kirkpatrick & McCarthy (1994); Dahn et al. (2002), corrected for progress in the field and the best available models (Burrows et al. 1997; Chabrier et al. 2000).

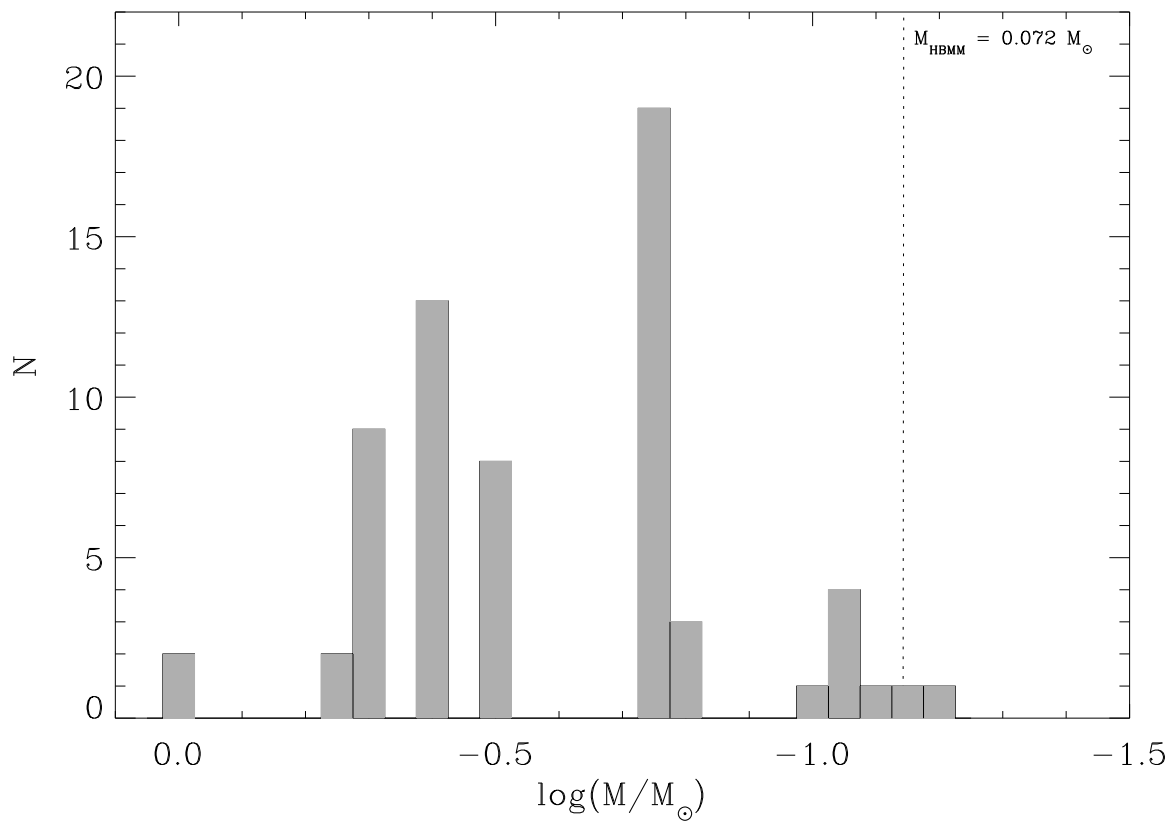


Fig. 59.— Detected companion mass function. The two wide G dwarf companions are included. The empty bins are, for the most part, an artifact of the discrete relations used between spectral type and mass.

Table 1. Observed Targets

WD#	Name	SpT	$d$ (pc)	$\mu$ ( $''$ yr $^{-1}$ )	$\theta$ ( $^\circ$ )	$(U, V, W)^*$ (km s $^{-1}$ )	Telescope
0000-170	G266-32	DB4	39.6	0.246	91.0	(31, -10, -2)	K,I
0000-345	LHS 1008	DAH7	13.2	0.772	169.2	(-22, -35, 11)	S
0002+729	GD 408	DBZ4	34.7	0.253	57.4	(19, -7, 21)	S
0009+191 <sup>†</sup>	PG	sdB	...	...	...	...	S
0009+501	LHS1038	DAP7	11.0	0.713	219.8	(-36, 20, -17)	S
0011+000	G31-35	DA5	30.4	0.457	114.2	(30, -36, -14)	S
0013-241	Ton 147	DA3	70.5	0.149	276.9	(-49, 41, 14)	S
0016-220	GD 597	DA4	72.8	0.085	230.1	(-38, 7, 8)	S,K
0017+061	PHL 790	DA2	133.0	0.049	243.4	(-39, 16, 3)	I
0018-339	GD 603	DA3	57.5	0.198	88.8	(38, -13, 1)	S
0028-274 <sup>†</sup>	GD 617	sdO	...	...	...	...	S,K
0031-274	GD 619	DA1	53.5	0.004	223.9	(-10, 12, 7)	S,K,I
0032-175	G266-135	DA5	30.9	0.608	90.0	(67, -33, 2)	S
0033+016	G1-7	DA4	29.8	0.393	202.1	(-51, -15, -17)	S
0034-211	LTT 0329	DA3	63.4	0.348	227.8	(-112, -7, 4)	I
0037-006	PG	DA4	39.2	0.017	93.1	(-6, 10, 7)	S
0038-226	LHS 1126	DQ9	9.9	0.600	231.2	(-37, 9, 6)	S
0041-102	Feige 7	DAP2	49.5	0.196	226.9	(-54, 5, -1)	S
0046+051	LHS 7	DZ7	4.4	2.975	155.5	(-13, -42, -24)	S
0048-202 <sup>†</sup>	GD 656	sdB	...	...	...	...	S
0050-332	GD 659	DA1	59.9	0.045	300.8	(-15, 23, 6)	S,K
0058-044	GD 9	DAP3	69.2	0.111	69.9	(26, 3, 13)	S,I
0100-068	G270-124	DB3	39.4	0.187	166.7	(-20, -19, -5)	S,K

Table 1—Continued

WD#	Name	SpT	$d$ (pc)	$\mu$ ( $''$ yr $^{-1}$ )	$\theta$ ( $^\circ$ )	$(U, V, W)^*$ (km s $^{-1}$ )	Telescope
0101+048	G1-45	DA5	13.5	0.395	54.1	(15, 11, 16)	S,K
0102+095	PHL 972	DA2	71.1	0.049	258.4	(-24, 19, 4)	S
0103-278	G269-93	DA4	58.3	0.261	105.1	(38, -43, 11)	S
0106+372	GD 11	DA2	127.1	0.152	108.4	(57, -49, -13)	S
0106-358	GD 683	DA2	95.5	0.028	194.4	(-19, 4, 9)	S
0107+267	GD 12	DA4	59.8	0.264	124.9	(29, -45, -23)	S
0107-342 <sup>†</sup>	GD 687	sdB	...	...	...	...	S,K
0113-243	GD 693	DA6	29.8	0.006	111.0	(-9, 11, 7)	S
0112+104	PG	DB2	75.9	0.049	211.8	(-23, 7, -3)	S
0115+159	G33-49	DQ5	15.4	0.651	181.8	(-28, -17, -26)	S
0115+521	GD 275	DA5	50.4	0.164	260.2	(-40, 33, -4)	S
0125-236	G274-39	DB5	41.1	0.296	78.3	(43, -12, 16)	S
0126+101	G2-40	DA6	35.6	0.408	200.7	(-54, -17, -36)	S
0126+422	GD 13	DA2	82.8	0.102	124.6	(15, -16, -9)	I
0131-163	GD 984	DA1	120.2	0.038	50.3	(12, 13, 12)	I
0133-116	G271-106	DAV4	31.5	0.480	104.2	(35, -44, 14)	S
0134+833	GD 419	DA3	25.6	0.147	311.8	(-24, 19, 14)	S,K
0136+768	GD 420	DA3	67.6	0.198	141.2	(36, -8, -32)	S
0142+312	G72-31	DA6	35.5	0.339	114.8	(26, -32, -2)	S
0143+216	G94-9	DA5	40.0	0.217	235.1	(-41, 19, -18)	S
0148+467	GD 279	DA4	15.9	0.124	0.6	(-9, 15, 16)	S,K
0155+069	GD 20	DA2	83.2	0.093	288.1	(-30, 42, 5)	S,I
0156+155	PG	DC6	46.1	0.082	265.8	(-23, 22, 1)	S



Table 1—Continued

WD#	Name	SpT	$d$ (pc)	$\mu$ ( $''$ yr $^{-1}$ )	$\theta$ ( $^\circ$ )	$(U, V, W)^*$ (km s $^{-1}$ )	Telescope
0210+168 <sup>†</sup>	PG	sdG	...	...	...	...	S
0213+396	GD 25	DA6	25.1	0.180	237.5	(-22, 18, -9)	S
0213+427	LHS 153	DA9	19.9	1.010	125.2	(45, -62, -17)	S
0227+050	Feige 22	DA3	24.3	0.075	109.1	(-5, 5, 9)	S
0230-144	LHS 1415	DA9	15.6	0.680	177.8	(-38, -27, -5)	S
0231+570	GD 283	DA5	21.5	0.204	97.9	(5, -2, 12)	S
0231-054	GD 31	DA3	29.5	0.256	69.0	(20, 0, 35)	S
0232+525	G174-5	DA3	28.2	0.245	134.0	(10, -12, -4)	S
0250-026	KUV	DA3	36.3	0.042	295.3	(-11, 19, 5)	K,I
0253+508	KPD	DAP2	78.7	0.034	305.5	(-17, 22, 9)	S,I
0257+080	G76-48	DAP8	27.8	0.181	129.7	(-4, -11, 7)	S
0302+027	GD 41	DA1	132.4	0.154	198.9	(-68, -35, -54)	S,K
0308+096	PG	DA2	100.9	0.091	158.0	(-15, -29, -8)	I
0308+188	PG	DA4	34.1	0.182	170.5	(-13, -12, -10)	S
0319+055 <sup>†</sup>	PG	sdB	...	...	...	...	S
0322-019	LHS 1547	DAZ10	17.5	0.903	163.8	(-34, -55, 13)	S
0339-035	GD 47	DA4	61.7	0.230	79.9	(27, -23, 52)	S
0346-011	GD 50	DA1	29.6	0.173	158.3	(-16, -11, 3)	K
0347-137	GD 51	DA2	83.6	0.186	70.1	(36, -15, 57)	S,I
0348+339	GD 52	DA4	66.1	0.181	118.1	(13, -39, 19)	I
0349+247	LB 1497	DA2	141.3	0.054	164.9	(-9, -19, -11)	S,I
0352+096	HZ 4	DA4	45.7	0.168	88.6	(6, -11, 31)	I
0354+463	Rubin 80	DA6	41.1	0.135	276.0	(-20, 31, -8)	S,I

Table 1—Continued

WD#	Name	SpT	$d$ (pc)	$\mu$ ( $''$ yr $^{-1}$ )	$\theta$ ( $^\circ$ )	$(U, V, W)^*$ (km s $^{-1}$ )	Telescope
0357–233	Ton S 392	DA1	278.0	0.018	358.4	(9, 27, 11)	S
0401+250	G8-8	DA4	27.0	0.253	148.6	(–5, –19, 0)	S
0406+169	LB 227	DA3	57.2	0.107	103.0	(0, –11, 22)	K,I
0407+179	HZ 10	DA3	38.2	0.111	139.4	(–8, –8, 7)	K,I
0408–041	GD 56	DA3	67.3	0.126	177.3	(–30, –19, –8)	S,K
0410+117	HZ 2	DA3	37.7	0.098	150.8	(–11, –5, 4)	S,K
0413–077	40 Eri B	DA3	4.9	4.079	213.3	(–73, –11, –59)	I
0416+272	V411 Tau	DAV4	47.2	0.098	137.5	(–5, –10, 7)	S,I
0416+334	GD 60	DA3	60.8	0.190	155.1	(1, –39, –11)	S
0416+701	GD 429	DA4	44.7	0.168	135.5	(14, –15, 8)	S
0421+162	VR 7	DA3	47.0	0.113	103.3	(–3, –8, 21)	I
0423+120	G83-10	DC8	16.2	0.249	201.3	(–16, 3, –8)	S
0425+168	VR 16	DA2	41.7	0.082	111.5	(–6, –2, 14)	I
0431+126	HZ 7	DA2	47.3	0.099	97.6	(–4, –4, 22)	I
0435–088	LHS 194	DQ7	9.5	1.520	171.2	(–47, –42, –11)	S
0435+410	GD 61	DBAZ3	54.5	0.102	184.5	(–5, –6, –12)	I
0437+138	EGGR 316	DA3	33.1	0.096	100.8	(–6, 1, 16)	K,I
0438+108	HZ 14	DA2	50.8	0.091	96.9	(–5, –3, 22)	I
0453+418	GD 64	DA4	37.6	0.220	174.8	(0, –20, –15)	S
0516+365	KPD	DA2	95.9	0.027	208.6	(–8, 7, –4)	S
0517+307	GD 66	DAV4	57.8	0.132	155.8	(–7, –23, 0)	S
0532+414	GD 69	DA7	18.3	0.146	285.9	(–10, 21, –1)	S
0543+579	GD 290	DA5	50.6	0.136	107.1	(–5, –11, 29)	S

Table 1—Continued

WD#	Name	SpT	$d$ (pc)	$\mu$ ( $''$ yr $^{-1}$ )	$\theta$ ( $^\circ$ )	$(U, V, W)^*$ (km s $^{-1}$ )	Telescope
0549+158	GD 71	DA1	49.7	0.187	155.9	(−19, −31, 2)	S,K
0612+177	G104-27	DA2	36.1	0.358	190.2	(−20, −35, −31)	S
0625+415	GD 74	DA3	83.2	0.111	186.2	(1, −25, −15)	S,I
0627+299	KUV	DA5	22.9	0.018	3.9	(−9, 14, 8)	I
0631+107	KPD	DA2	56.5	0.110	199.7	(−16, −7, −15)	I
0637+477	GD 77	DAP5	40.0	0.171	185.4	(1, −16, −7)	S,I
0644+375	G87-7	DA2	15.4	0.965	193.8	(4, −44, −33)	S,K,I
0710+741	GD 448	DA3	92.0	0.132	129.5	(−1, −30, 45)	S,I
0710+216	GD 83	DA5	40.7	0.179	221.9	(−6, −5, −23)	S
0713+584 <sup>†</sup>	GD 294	sdB	...	...	...	...	S,K
0714+458	GD 84	DQ6	33.1	0.201	213.2	(3, −7, −15)	S,I
0716+404	GD 85	DBA3	57.8	0.171	127.4	(−18, −27, 32)	S,K
0730+487	GD 86	DA3	38.5	0.231	217.3	(10, −13, −21)	S,K
0743+442	GD 89	DA4	39.6	0.182	208.3	(4, −13, −12)	S
0751+578	G193-78	DC5	31.9	0.438	189.2	(20, −46, −4)	I
0752−146	LTT 2980	DA3	35.0	0.320	191.9	(−36, −13, −26)	I
0802+386	G111-54	DZ5	46.6	0.304	186.8	(0, −52, −12)	S
0802+413	KPD	DA1	139.3	0.037	221.1	(1, −3, −9)	S
0811+644	GD 457	DA4	61.4	0.193	262.9	(24, 15, −39)	I
0816+376	GD 90	DAP4	47.4	0.150	228.2	(5, −6, −17)	S,K
0817+386	PG	DA2	113.8	0.105	228.1	(16, −19, −33)	S
0824+288	PG	DA1	119.1	0.050	272.9	(7, 17, −16)	S
0826+455	GD 91	DA5	47.6	0.147	132.1	(−20, −13, 26)	S,K

Table 1—Continued

WD#	Name	SpT	$d$ (pc)	$\mu$ ( $''$ yr $^{-1}$ )	$\theta$ ( $^\circ$ )	$(U, V, W)^*$ (km s $^{-1}$ )	Telescope
0836+404	KUV	DA3	38.4	0.136	267.5	(6, 13, -13)	S
0840+262	Ton 10	DB3	48.3	0.122	248.9	(5, 4, -16)	S,K
0843+358	GD 95	DZ6	23.1	0.169	245.7	(1, 6, -7)	S
0846+346	GD 96	DA7	28.3	0.121	275.7	(1, 15, -5)	S
0853+163	PG	DBA2	91.6	0.041	227.0	(-4, 2, -7)	S
0856+331	G47-18	DQ5	20.5	0.322	270.7	(12, 14, -17)	I
0858+363	GD 99	DAV4	35.0	0.206	209.7	(1, -17, -8)	S,K
0859-039	RE	DA2	38.7	0.016	304.6	(-7, 13, 6)	S,K
0900+554 <sup>†</sup>	PG	sdB	...	...	...	...	S,K
0901+140	PG	DA5	52.2	0.113	260.9	(9, 9, -16)	S,K
0912+536	G195-19	DC7	10.3	1.553	224.1	(35, -42, -23)	S
0913+442	G116-16	DA6	30.5	0.265	177.6	(-9, -26, 10)	S
0913+103	LP 487-21	DC6	39.8	0.191	116.0	(-38, -1, 25)	S
0914+547 <sup>†</sup>	SBSS	sdOB	...	...	...	...	S
0915+526	PG	DC6	74.5	0.025	166.0	(-9, 4, 10)	S,K
0922+162	PG	DA2	118.7	0.066	266.0	(17, 8, -20)	S
0930+294	G117-25	DA6	32.1	0.236	221.0	(3, -16, -12)	S
0933+025	PG	DA2	133.7	0.062	181.9	(-26, -18, -11)	I
0933+729	PG	DA3	96.4	0.075	228.2	(17, -9, 0)	S
0938+286	Ton 20	DA4	75.2	0.154	315.5	(28, 47, -14)	S
0938+550	PG	DA3	53.5	0.068	256.4	(4, 7, -3)	S,K
0939+071	PG	DA2	18.9	0.014	273.3	(-8, 12, 6)	S
0943+441	G116-52	DA4	34.0	0.290	0.0	(-7, 58, 2)	I

Table 1—Continued

WD#	Name	SpT	$d$ (pc)	$\mu$ ( $''$ yr $^{-1}$ )	$\theta$ ( $^\circ$ )	$(U, V, W)^*$ (km s $^{-1}$ )	Telescope
0945+245	PG	DA3	41.4	0.119	211.3	(−5, −8, −4)	K,I
0946+534	G195-42	DA6	23.0	0.262	263.9	(13, 6, −10)	S
0947+325	Ton 458	DA1	72.1	0.068	269.1	(9, 9, −8)	K
0947+639 <sup>†</sup>	PG	sdB	...	...	...	...	I
0950+185	PG	DA2	201.4	0.010	210.1	(−8, 4, 2)	I
0955+247	G49-33	DA6	24.4	0.415	220.3	(5, −27, −17)	S
0956+045	PG	DA3	112.7	0.146	169.8	(−55, −47, −16)	I
0959+149	G42-33	DC7	22.2	0.339	272.1	(20, 8, −14)	S,I
1000+220	Ton 1145	DA6	38.9	0.0	0.0	(−9, 12, 7)	S
1001+203	Ton 1150	DA2	117.5	0.095	247.8	(23, −14, −26)	S,I
1005+642	GD 462	DA3	44.9	0.131	232.4	(11, −7, 1)	K
1011+570	GD 303	DBZ4	44.7	0.132	135.6	(−24, −3, 24)	S,K
1013−010	G53-38	DA7	26.2	0.515	273.6	(45, 3, −27)	S
1013−050	RE	DAO1	108.1	0.095	276.1	(33, 7, −17)	S
1015+161	PG	DA2	83.9	0.126	239.4	(−16, −19, −23)	S,K
1015+076	PG	DA2	179.5	0.037	220.6	(−3, −12, −13)	S
1017+125	PG	DA2	111.7	0.029	215.8	(−7, 0, −1)	S
1017+366	GD 116	DAH3	64.6	0.126	193.8	(−9, −26, 4)	I
1019+129	PG	DA3	85.5	0.084	238.6	(8, −9, −14)	K,I
1019+637	G235-67	DA7	16.5	0.377	53.2	(−29, 33, 12)	S
1026+002	PG	DA3	38.2	0.090	141.3	(−23, 5, 7)	S
1026+023	LP 550-292	DA4	34.5	0.123	232.9	(−1, −1, −6)	K,I
1031−114	EGGR 70	DA2	31.0	0.344	265.5	(31, −2, −21)	K,I

Table 1—Continued

WD#	Name	SpT	$d$ (pc)	$\mu$ ( $"$ yr $^{-1}$ )	$\theta$ ( $^{\circ}$ )	$(U, V, W)^*$ (km s $^{-1}$ )	Telescope
1033+464	GD 123	DA2	84.7	0.074	184.6	(-11, -17, 12)	I
1034+492	GD 304	DA2	78.7	0.063	97.4	(-29, 15, 19)	K
1038+633	PG	DA2	57.3	0.090	233.1	(7, -6, 4)	K
1039+747	PG	DA2	165.2	0.067	233.5	(30, -24, 6)	S
1042-690	LTT 3943	DA3	36.5	0.176	269.4	(17, 4, -8)	I
1046-017	GD 124	DBZ5	56.2	0.117	186.9	(-21, -11, -10)	S
1046+281	Ton 547	DA4	42.7	0.059	222.3	(-5, 1, 3)	K
1049+103	PG	DA2	109.1	0.097	199.2	(-16, -32, -15)	I
1052+273	GD 125	DA3	37.5	0.143	257.9	(10, 0, -4)	S,K
1055-072	LHS 2333	DA7	12.2	0.821	276.3	(34, 2, -10)	S
1056+345	G119-47	DB5	49.0	0.291	219.6	(12, -50, -8)	S
1057+719	PG	DA1	132.4	0.050	246.5	(16, -7, 3)	S
1101+385 <sup>†</sup>	PG	BLL	...	...	...	...	I
1102+748	GD 466	DA3	51.5	0.120	258.5	(16, -2, -1)	S,K
1104+602	G197-4	DA3	43.9	0.249	228.9	(21, -31, 8)	K
1105-048	G163-50	DA3	25.8	0.451	189.0	(-29, -28, -25)	S,K
1108+475	GD 129	DA5	43.7	0.137	232.1	(6, -12, 4)	S
1115-029	G10-11	DQ5	38.0	0.582	292.7	(95, 7, -7)	S
1115+166	PG	DA2	132.4	0.021	270.0	(2, 7, 2)	S
1116+026	GD 133	DA4	49.4	0.097	288.1	(13, 10, 2)	K,I
1119+385	PG	DA3	85.5	0.088	313.2	(21, 25, -5)	I
1121+216	LHS 304	DA7	13.4	1.039	268.9	(48, -13, -15)	S
1123+189	PG	DA1	114.8	0.029	236.3	(-1, -1, 1)	I

Table 1—Continued

WD#	Name	SpT	$d$ (pc)	$\mu$ ( $''$ yr $^{-1}$ )	$\theta$ ( $^\circ$ )	$(U, V, W)^*$ (km s $^{-1}$ )	Telescope
1125−025	PG	DA2	109.6	0.045	271.7	(12, 4, 0)	I
1126+185 <sup>†</sup>	PG	sdG	...	...	...	...	S
1129+155	PG	DA3	36.3	0.069	131.5	(−20, 9, 8)	K
1133+293	Feige 45	DA2	88.7	0.050	216.9	(−5, −8, 4)	S,I
1134+300	GD 140	DA2	15.3	0.148	265.8	(0, 7, 4)	S,K,I
1143+321	G148-7	DA3	31.6	0.283	202.0	(−11, −30, 5)	S
1154+186	G57-29	DZ5	29.9	0.328	276.0	(34, −4, −2)	S,K
1159+803	G255-2	DAV4	63.1	0.201	255.0	(39, −24, 8)	S
1201−001	PG	DA2	60.3	0.099	254.8	(11, −6, −1)	K
1202−232	EC	DA6	11.2	0.228	9.1	(−6, 19, 17)	K
1202+308	Ton 75	DA2	110.7	0.048	182.4	(−20, −11, 8)	I
1204+450	PG	DA2	92.9	0.064	257.3	(12, −6, 4)	S
1208+576	G197-47	DA9	20.0	0.629	132.0	(−61, 1, 34)	S
1210+464	PG	DA2	139.3	0.051	159.4	(−32, −9, 19)	I
1210+533	PG	DAO1	103.3	0.035	166.8	(−19, 0, 15)	I
1214+267	PG	DA1	211.8	0.030	246.9	(9, −12, 3)	I
1220+234	Ton 610	DAP2	44.7	0.064	262.9	(2, 4, 5)	S
1225−079	PG	DZ5	26.3	0.125	250.4	(1, 1, 3)	S
1230+417	GD 317	DA3	102.3	0.102	280.2	(37, −5, 1)	S
1232+479	GD 148	DA3	45.5	0.162	145.0	(−39, −1, 18)	S
1234+481	PG	DA1	134.9	0.101	236.3	(20, −45, 17)	S
1237−028	LP 615-183	DA5	37.8	0.213	284.7	(27, 0, 10)	S
1240+754	LB 261	DA3	81.7	0.190	262.7	(50, −32, 11)	I

Table 1—Continued

WD#	Name	SpT	$d$ (pc)	$\mu$ ( $''$ yr $^{-1}$ )	$\theta$ ( $^\circ$ )	$(U, V, W)^*$ (km s $^{-1}$ )	Telescope
1241–010	PG	DA2	88.7	0.186	196.9	(–25, –54, –29)	I
1241+235	PG	DA2	110.2	0.020	101.3	(–19, 16, 7)	I
1242–105 $\ddagger$	LP 736-4	DA6	18.0	0.348	257.7	(13, –8, 2)	S
1244–125	EC	DA4	43.9	0.206	277.9	(29, –7, 10)	K
1247+553 $\dagger$	GD 319	sdB	...	...	...	...	K
1254+233	GD 153	DA1	67.0	0.196	188.2	(–35, –44, 2)	S,K
1257+037	LHS 2661	DC9	16.1	0.966	206.6	(–14, –57, –18)	S
1257+047	GD 267	DA2	78.3	0.123	215.8	(–6, –30, –6)	I
1257+278	G149-28	DA6	34.6	0.328	283.0	(41, –7, 9)	S
1258+593	GD 322	DA3	60.3	0.087	28.9	(–8, 34, –5)	S
1307+354	GD 154	DAV5	44.3	0.228	275.8	(33, –11, 10)	I
1309+853	G256-7	DC9	18.1	0.324	140.5	(–31, 13, 24)	S
1310+583	PG	DA5	21.1	0.210	112.4	(–29, 18, 9)	S,I
1314–153	LHS 2712	DA3	58.6	0.709	198.2	(–30, –142, –114)	S
1319+466	G177-34	DA3	38.0	0.258	289.1	(35, –3, 7)	S,K
1327–083	LHS 354	DA4	18.0	1.207	246.9	(48, –73, –2)	S
1328+343	PG	DA3	75.5	0.062	209.1	(–12, –9, 11)	S,I
1330+473	PG	DA2	92.5	0.028	262.9	(0, 3, 9)	I
1333+005 $\ddagger$	LP 618-14	DC6	86.3	0.307	244.1	(52, –98, 2)	S
1334+039	LHS 46	DZ9	8.2	3.880	252.8	(80, –110, 14)	S
1335+700	PG	DA2	92.9	0.084	298.4	(26, 1, 1)	S,K,I
1337+705	G238-44	DA2	24.8	0.405	266.3	(26, –19, 18)	S,K
1344+106	G63-54	DA7	20.0	0.906	261.6	(48, –50, 22)	S



Table 1—Continued

WD#	Name	SpT	$d$ (pc)	$\mu$ ( $''$ yr $^{-1}$ )	$\theta$ ( $^\circ$ )	$(U, V, W)^*$ (km s $^{-1}$ )	Telescope
1344+572	G223-24	DA4	24.0	0.273	315.9	(21, 12, 1)	K,I
1345+238	LHS 361	DC9	12.1	1.490	274.9	(60, -35, 26)	S
1349+144	PG	DA3	85.5	0.094	266.3	(18, -14, 15)	K,I
1349+545	SBSS	DAP5	77.3	0.090	270.0	(-34, 33, -1)	S
1350-090	LP 907-37	DA3	14.7	0.512	134.7	(-38, 10, -14)	S
1353+409	PG	DA2	136.1	0.050	130.1	(-41, 13, 5)	I
1407+425	PB 1549	DA5	31.2	0.015	256.7	(-8, 10, 8)	S
1408+323	GD 163	DA3	39.5	0.243	176.2	(-42, -19, 9)	S
1422+095	GD 165	DAV4	31.5	0.255	233.9	(-1, -25, 11)	S,K,I
1424+240 <sup>†</sup>	PG	BLL	...	...	...	...	I
1428+373	PG	DA5	96.8	0.086	169.2	(-42, -9, 9)	S
1430+427 <sup>†</sup>	PG	sdB	...	...	...	...	I
1433+538	GD 337	DA2	150.7	0.141	284.8	(74, -38, 35)	I
1444-096	PG	DB3	63.4	0.170	164.3	(-36, -15, -28)	I
1449+003 <sup>†</sup>	G66-36	sdM	...	...	...	...	I
1449+168	PG	DA2	101.4	0.057	10.1	(6, 35, 11)	I
1450+432 <sup>†</sup>	PG	BHB	...	...	...	...	I
1501+032	PG	DA4	71.1	0.069	312.0	(9, 12, 22)	I
1503-070	GD 175	DAH7	25.9	0.205	264.4	(4, -6, 18)	S
1507+220	PG	DA3	78.3	0.071	248.5	(-2, -11, 18)	I
1507-105	GD 176	DA5	50.8	0.150	278.5	(12, -8, 28)	S
1508+637	GD 340	DA4	32.4	0.129	220.6	(-14, -2, 20)	S,K,I
1509+322	GD 178	DA4	47.6	0.180	290.9	(23, -4, 26)	S,K

Table 1—Continued

WD#	Name	SpT	$d$ (pc)	$\mu$ ( $''$ yr $^{-1}$ )	$\theta$ ( $^\circ$ )	$(U, V, W)^*$ (km s $^{-1}$ )	Telescope
1521+310	Ton 229	DA2	100.9	0.058	136.4	(−34, 12, −4)	S
1531−022	GD 185	DA3	31.6	0.141	206.9	(−13, −8, 3)	S,K
1537+651	GD 348	DA5	27.2	0.205	324.9	(17, 7, 7)	S,K
1539−035	GD 189	DA5	34.5	0.106	105.4	(−18, 20, −5)	S,I
1539+530 <sup>‡</sup>	PG	DA2	173.0	0.0	0.0	(−9, 12, 7)	S
1542−275	LP 916-27	DB4	52.2	0.246	235.9	(10, −45, 14)	S
1542+182	GD 190	DB2	53.5	0.118	177.1	(−30, −7, −1)	S,K,I
1548+149	PG	DA2	80.2	0.052	184.4	(−21, −3, 2)	I
1550+183	GD 194	DA4	40.0	0.192	309.5	(19, 9, 30)	S,K
1553+353	PG	DA2	87.5	0.046	145.6	(−27, 11, 0)	S,I
1554+215	PG	DA2	121.9	0.060	158.6	(−38, −1, −8)	I
1606+422	C2	DA5	26.3	0.170	314.0	(10, 9, 16)	S
1607−251 <sup>‡</sup>	LTT 6451	DA5	38.2	0.194	312.5	(2, 13, 40)	S,I
1608+118	PG	DA2	89.9	0.040	135.0	(−21, 11, −5)	I
1609+044	PG	DA2	116.9	0.026	240.9	(−8, −1, 13)	I
1609+135	LHS 3163	DA5	18.3	0.546	178.7	(−40, −20, −8)	S
1612−111	GD 198	DB2	69.8	0.110	158.6	(−24, −5, −21)	I
1614+136	PG	DA2	131.2	0.040	180.0	(−25, −5, −1)	I
1614+270 <sup>†</sup>	PG	sdO	...	...	...	...	I
1615−154	G153-41	DA2	48.8	0.236	226.8	(−5, −42, 13)	S,K
1619+123	PG	DA3	58.6	0.098	135.8	(−27, 11, 13)	S
1620−391	EGGR 274	DA2	12.8	0.074	88.1	(−10, 15, 4)	K,I
1625+093	G138-31	DA7	23.4	0.468	189.3	(−38, −29, −6)	S

Table 1—Continued

WD#	Name	SpT	$d$ (pc)	$\mu$ ( $"$ yr $^{-1}$ )	$\theta$ ( $^{\circ}$ )	$(U, V, W)^*$ (km s $^{-1}$ )	Telescope
1626+368	G180-57	DZ6	15.9	0.893	326.7	(51, 15, 37)	S,K,I
1630+618 <sup>†</sup>	GD 354	sdB	...	...	...	...	I
1631+396	KUV	DA3	43.8	0.061	172.4	(-21, 8, 5)	I
1631+781	RE	DA1	57.3	0.067	247.2	(-11, 2, 22)	S,I
1632+177	PG	DA5	15.1	0.089	108.4	(-12, 14, 2)	S,K,I
1633+433	G180-63	DA8	15.1	0.378	144.0	(-33, 14, -4)	S,I
1636+160	GD 202	DA4	49.7	0.072	155.6	(-22, 6, -3)	I
1636+351	PG	DA1	115.3	0.036	289.4	(1, 4, 21)	I
1637+335	G180-65	DA5	28.6	0.470	182.5	(-63, -21, 2)	S,I
1639+153	G138-56	DA7	29.8	0.672	178.8	(-75, -49, -24)	S
1639+537	GD 356	DAEH6	21.1	0.220	212.4	(-24, 0, 18)	S
1641+387	GD 357	DA4	29.9	0.167	9.5	(11, 24, 5)	S,I
1643+143	PG	DA2	150.0	0.036	34.4	(2, 35, 3)	S,I
1644+198	PG	DB4	50.1	0.108	150.1	(-28, 6, -9)	I
1645+325	GD 358	DBV2	36.6	0.162	178.0	(1, -3, 29)	S,K
1647+375	PG	DA2	78.7	0.061	287.2	(2, 2, 24)	S
1647+591	G226-29	DAV4	11.0	0.328	155.6	(-26, 14, 4)	S,K
1654+160	PG	DBV2	166.0	0.047	320.2	(15, 16, 35)	I
1654+637	GD 515	DA4	90.8	0.150	233.3	(-37, -22, 54)	I
1655+215	LHS 3254	DA5	23.3	0.577	177.4	(-58, -24, -12)	S,K,I
1658+440	PG	DAP2	24.2	0.106	344.6	(3, 14, 10)	S
1659+303 <sup>‡</sup>	PG	DA5	53.5	0.063	170.8	(-23, 6, 2)	S
1705+030	G139-13	DZ7	17.5	0.386	180.0	(-26, -11, -7)	S,I

Table 1—Continued

WD#	Name	SpT	$d$ (pc)	$\mu$ ( $''$ yr $^{-1}$ )	$\theta$ ( $^\circ$ )	$(U, V, W)^*$ (km s $^{-1}$ )	Telescope
1708−147	LTT 6847	DQ5	27.4	0.409	134.4	(−23, 4, −44)	S,I
1709+230	GD 205	DB2	59.2	0.164	176.5	(−45, −12, −8)	I
1713+332	GD 360	DA2	85.5	0.170	142.2	(−62, 12, −37)	I
1713+695	G240-51	DA3	27.7	0.345	189.4	(−52, 10, 21)	S,K,I
1748+708	G240-72	DQ8	6.1	1.678	311.3	(22, −12, 36)	S
1756+827	LHS 56	DA7	15.6	3.610	336.7	(217, −122, 54)	S
1809+284	GD 375	DA4	59.2	0.168	347.0	(−47, −3, −17)	I
1820+609	G227-28	DA11	12.8	0.710	168.0	(−50, 19, −6)	S
1822+410	GD 378	DBAZ4	41.9	0.138	359.2	(16, 18, 15)	S,I
1824+040	G21-15	DA4	54.9	0.378	220.0	(−60, −69, 29)	S
1826−045	G21-16	DA6	28.7	0.298	178.1	(−26, −19, −13)	I
1827−106	G155-19	DA3	35.6	0.282	141.9	(−16, −6, −36)	I
1829+547	G227-35	DQ7	15.0	0.392	317.7	(8, 4, 28)	S
1840+042	GD 215	DA6	24.9	0.128	299.0	(−8, 12, 22)	I
1844−223	RE	DA2	58.1	0.090	119.4	(−5, 10, −17)	S
1855+338	G207-9	DAV4	32.8	0.353	7.5	(40, 32, 22)	S,I
1858+393	G205-52	DA6	34.7	0.234	169.6	(−41, 6, −13)	I
1900+705	G260-15	DAP5	13.0	0.510	9.1	(22, 5, 8)	S,K
1910+047	WD	DA2	157.0	0.112	185.1	(−57, −48, −25)	I
1914+094	KPD	DA2	148.6	0.050	196.3	(−33, −13, 0)	I
1917−077	EGGR 131	DBQA5	11.2	0.174	200.6	(−13, 4, 6)	S
1917+386	G125-3	DC8	11.7	0.250	174.7	(−21, 9, 0)	S
1918+110	GD 218	DA3	133.7	0.107	159.2	(−40, −20, −44)	I

Table 1—Continued

WD#	Name	SpT	$d$ (pc)	$\mu$ ( $"$ yr $^{-1}$ )	$\theta$ ( $^{\circ}$ )	$(U, V, W)^*$ (km s $^{-1}$ )	Telescope
1935+276	G185-32	DAV4	18.0	0.442	87.7	(8, 23, -25)	S,I
1936+327	GD 222	DA2	34.8	0.153	207.0	(-32, 2, 6)	S,I
1940+374	EGGR 133	DB3	49.3	0.222	356.6	(34, 22, 35)	S,I
1950+250	GD 385	DAV4	38.0	0.150	1.5	(12, 23, 20)	S,I
1952-206	LTT 7873	DA4	51.8	0.392	165.8	(-16, -69, -45)	S,I
1953-011	LHS 3501	DAH6	11.4	0.833	212.0	(-38, -22, 10)	S,K,I
2006+481 <sup>†</sup>	KPD	sdO	...	...	...	...	I
2007-219	LTT 7983	DA5	18.2	0.331	161.7	(-9, -12, -9)	S,I
2007-303	LTT 7987	DA4	15.4	0.428	233.5	(-23, -10, 24)	S,K
2009+622	GD 543	DA2	134.3	0.164	202.2	(-112, 27, -6)	I
2025+554	GD 546	DA2	115.4	0.107	51.8	(47, 14, -10)	S,I
2028+390	GD 391	DA2	41.7	0.176	59.4	(22, 19, -7)	S,I
2032+248	G186-31	DA3	14.8	0.693	215.7	(-54, -7, 7)	S,I
2032+188	GD 231	DA3	107.7	0.145	182.2	(-60, -25, -32)	I
2039-202	EGGR 141	DA3	21.1	0.368	105.4	(10, 6, -24)	S,K,I
2047+372	G210-36	DA4	18.4	0.213	44.3	(9, 15, 5)	S,I
2048+263	G187-8	DC9	20.1	0.518	234.1	(-55, -1, 20)	S
2055+221 <sup>†</sup>	G187-9	sdM	...	...	...	...	S
2058+181	GD 232	DA4	54.0	0.112	108.8	(3, 8, -19)	K
2058+342	GD 392	DB4	57.8	0.168	42.6	(36, 21, 5)	S,I
2058+506	GD 393	DA5	34.0	0.114	208.4	(-27, 12, 3)	S,I
2059+316	G187-15	DQ5	34.5	0.399	214.9	(-72, -4, 1)	I
2111+261	G187-32	DA6	31.9	0.395	165.0	(-37, -10, -41)	I

Table 1—Continued

WD#	Name	SpT	$d$ (pc)	$\mu$ ( $''$ yr $^{-1}$ )	$\theta$ ( $^\circ$ )	$(U, V, W)^*$ (km s $^{-1}$ )	Telescope
2115+010	PG	DA2	122.5	0.028	12.4	(1, 24, 12)	S
2116+736	KPD	DA1	161.4	0.061	218.4	(−53, 28, 5)	S
2117+539	G231-40	DA3	19.7	0.213	336.4	(−2, 10, 25)	S
2123−229	LP 873-45	DA4	58.6	0.201	141.9	(5, −31, −26)	I
2126+734	G261-43	DA3	21.2	0.289	168.8	(−22, 24, −16)	S,K
2131+066	PG	DO1	398.1	0.018	210.4	(−37, −6, 3)	I
2134+218	GD 234	DA3	47.0	0.100	274.6	(−24, 14, 23)	K,I
2136+229	G126-18	DA5	42.0	0.292	65.3	(46, 18, −12)	S,I
2140+207	G126-27	DQ6	12.5	0.690	197.5	(−42, −5, −10)	S,I
2144−079	G26-31	DB4	69.4	0.285	117.1	(37, −32, −62)	S
2147+280	G188-27	DB4	35.3	0.262	108.1	(14, 3, −29)	I
2149+021	G93-48	DA3	25.1	0.301	177.3	(−26, −14, −11)	K,I
2151−015	LTT 8747	DA6	19.6	0.404	180.3	(−27, −17, −9)	I
2154+408	KPD	DA2	92.5	0.045	237.7	(−29, 13, 9)	I
2200+085 <sup>†</sup>	PG	sdK	...	...	...	...	I
2207−303	RE	DA2	108.1	0.066	142.4	(1, −17, −6)	S
2207+142	G18-34	DA6	25.5	0.361	44.8	(33, 24, 8)	S
2244+031	PG	DA1	407.4	0.008	113.2	(0, 4, −3)	I
2246+223	G67-23	DA5	19.0	0.528	83.3	(34, 2, −10)	S,I
2246+154 <sup>†</sup>	PG	sdB	...	...	...	...	S
2249−105	LP 761-114	DC8	53.2	0.192	146.9	(−4, −30, −17)	S
2251−070	LHS 69	DZ11	8.1	2.576	105.3	(60, −36, −44)	S
2253−062	GD 243	DBA4	54.7	0.073	99.5	(6, 4, −2)	S,K

Table 1—Continued

WD#	Name	SpT	$d$ (pc)	$\mu$ ( $"$ yr $^{-1}$ )	$\theta$ ( $^{\circ}$ )	$(U, V, W)^*$ (km s $^{-1}$ )	Telescope
2256+249	GD 245	DA2	51.3	0.152	119.0	(10, -5, -20)	I
2303+242	PG	DAV4	52.5	0.088	129.5	(-1, 1, -10)	S
2307+636	G241-46	DA2	53.8	0.368	171.9	(-29, 25, -84)	S
2309+105	GD 246	DA1	69.8	0.142	94.0	(30, -6, -13)	S,K
2309+258	KUV	DA4	34.8	0.007	167.0	(-9, 11, 6)	I
2311-068	G157-34	DQ6	25.1	0.381	243.3	(-54, 9, 14)	S,I
2316+123	KUV	DAP4	53.3	0.102	95.6	(12, 1, -4)	S,I
2316-173	LP 822-50	DBQA4	27.7	0.238	93.4	(19, 3, -3)	S,K
2317-185 <sup>‡</sup>	GD 1295	DA4	32.9	0.013	344.0	(-9, 14, 8)	I
2319+691	GD 559	DA3	63.9	0.134	265.7	(-43, 26, 17)	S
2322-181	G273-40	DA2	88.1	0.240	87.6	(80, -21, -25)	S
2323+157	GD 248	DC5	37.3	0.116	201.3	(-25, 4, -3)	S
2324+060	PB 5379	DA4	70.8	0.120	164.6	(-19, -19, -18)	S,I
2326+049	G29-38	DAV4	13.6	0.482	237.0	(-40, 10, 6)	K,I
2328+107	KPD	DA2	109.6	0.068	245.7	(-44, 15, 8)	S,I
2328+510	GD 406	DB2	50.4	0.173	67.6	(30, -2, 10)	S
2329+267	G128-72	DAH5	38.6	0.444	86.4	(64, -17, -14)	S
2329+407	G171-2	DA3	34.1	0.280	110.9	(22, -7, -20)	S
2329-291	GD 1669	DA2	45.0	0.019	95.3	(-6, 10, 6)	I
2333-049	G157-82	DA5	50.1	0.240	235.5	(-66, 5, 8)	S
2341+322	G130-5	DA3	17.6	0.229	252.2	(-27, 17, 7)	S,K
2342+806	GD 561	DAO1	64.0	0.028	278.1	(-16, 15, 10)	S,K
2349+286	PG	DA1	234.4	0.062	215.8	(-67, 6, -29)	I

Table 1—Continued

WD#	Name	SpT	$d$ (pc)	$\mu$ ( $''$ yr $^{-1}$ )	$\theta$ ( $^\circ$ )	$(U, V, W)^*$ (km s $^{-1}$ )	Telescope
2351–335	LHS 4040	DA5	20.0	0.500	216.5	(−46, −8, 16)	S
2352+401	G171-27	DQ5	25.8	0.566	158.2	(−9, −15, −57)	S
2357+296	PG	DA1	191.4	0.061	131.0	(13, −21, −31)	I
2359–434	LHS 1005	DA6	7.8	1.020	135.2	(4, −24, 9)	K,I

\* $U, V, W$  calculated assuming  $v_r = 0$  with respect to the local standard of rest (§3.2).

†Not a white dwarf.

‡Not listed in McCook & Sion (1999). The WD number is unofficial.



Table 2. Sample Kinematics

All 371 Stars	330 Stars with $\mu < 0.5'' \text{ yr}^{-1}$
$\langle U \rangle = -5 \text{ km s}^{-1}$	$\langle U \rangle = -6 \text{ km s}^{-1}$
$\langle V \rangle = -6 \text{ km s}^{-1}$	$\langle V \rangle = -3 \text{ km s}^{-1}$
$\langle W \rangle = 0 \text{ km s}^{-1}$	$\langle W \rangle = 1 \text{ km s}^{-1}$
$\langle T \rangle = 37 \text{ km s}^{-1}$	$\langle T \rangle = 33 \text{ km s}^{-1}$
$\langle \mu \rangle = 0.27'' \text{ yr}^{-1}$	$\langle \mu \rangle = 0.16'' \text{ yr}^{-1}$
$\langle d \rangle = 56.6 \text{ pc}$	$\langle d \rangle = 61.7 \text{ pc}$
$\sigma_U = 32 \text{ km s}^{-1}$	$\sigma_U = 26 \text{ km s}^{-1}$
$\sigma_V = 24 \text{ km s}^{-1}$	$\sigma_V = 20 \text{ km s}^{-1}$
$\sigma_W = 20 \text{ km s}^{-1}$	$\sigma_W = 18 \text{ km s}^{-1}$
$\sigma_T = 44 \text{ km s}^{-1}$	$\sigma_T = 38 \text{ km s}^{-1}$
$\sigma_\mu = 0.45'' \text{ yr}^{-1}$	$\sigma_\mu = 0.11'' \text{ yr}^{-1}$
$\sigma_d = 47.1 \text{ pc}$	$\sigma_d = 47.6 \text{ pc}$

Table 3. Summary of All Companion Systems

Companion	SpT	Primary	SpT	$a_s^1$ (")	PA (°)	$d$ (pc)	$a$ (AU)	$M_{abs}^2$ (mag)	References
GD 360B	DA	1713+332	DA2	close	...	85.5	< 0.1	...	8
G1-45B	DC	0101+048	DA5	close	...	13.5	< 0.1	...	5,9
G21-15B	DC	1824+040	DA4	close	...	54.9	< 0.1	...	5,13
GD 429B	DC	0416+701	DA4	close	...	44.7	< 0.1	...	9
PG 1241-010B	DC	1241-010	DA2	close	...	88.7	< 0.1	...	8
PG 1428+373B	DC	1428+373	DA5	close	...	96.8	< 0.1	...	14
PG 0922+162B	DA2	0922+162	DA2	4.4	287.0	118.7	522	11.93	1,22
PG 1204+450B	DA3	1204+450	DA2	close	...	92.9	< 0.1	...	5,12
PG 0945+245B	DAXP3	0945+245	DA3	< 0.03	...	41.4	< 1.2	...	23,24
PG 1115+166B	DB3	1115+166	DA2	close	...	132.4	< 0.1	...	19,20
PG 1017+125B	DA4	1017+125	DA2	48.8	336.1	111.7	5450	11.59	1
GD 420B	DA5	0136+768	DA3	close	...	67.6	< 0.1	...	12,13
PG 0901+140B	DA6	0901+140	DA5	3.6	173.6	41.3	149	13.40	1
GD 559B	DC6	2319+691	DA3	28.7	180.8	63.9	1834	13.16	1,25
GD 322B	DC7	1258+593	DA3	15.6	235.6	60.3	941	13.65	1
G261-43B	DC10	2126+734	DA3	1.4	167.9	21.2	30	14.80	1,26
G21-15C	DC11	1824+040	DA4	58.6	124.4	54.9	3217	15.30	1
GD 392B	DC14	2058+342	DB4	45.8	103.9	57.8	2647	15.69	1,27
HD 147528	dG0	1619+123	DA3	63.3	130.6	58.6	3709	3.00	1
HD 147513	dG2	1620-391	DA2	432.4	72.3	12.8	5535	3.39	1,28
PG 0824+288B	dC	0824+288	DA1	< 0.5	...	119.1	< 60	6.50	29
GD 319B	dM	1247+553	sdB	close	...	436.5	< 0.1	...	1,5,31,32
RE 1016-053C	dM1	1013-050	DAO1	3.2	19.0	108.1	346	5.35	1,10

Table 3—Continued

Companion	SpT	Primary	SpT	$a_s^1$ (")	PA (°)	$d$ (pc)	$a$ (AU)	$M_{abs}^2$ (mag)	References
RE 1016–053D	dM1	1013–050	DAO1	3.2	19.0	108.1	346	5.35	1,10
GD 683B <sup>†</sup>	dM2	0106–358	DA2	111.5	173.4	95.5	10648	6.38	1
GD 984B	dM2	0131+163	DA1	< 0.5	...	120.2	< 60	6.92	1,3
LP 761-113	dM2	2249–105	DC8	7.7	327.7	53.2	410	5.74	1,25
PG 0933+729B <sup>†</sup>	dM2	0933+729	DA3	80.9	81.8	96.4	7797	6.46	1
PG 0950+185B	dM2	0950+185	DA2	1.1	100.3	201.4	222	5.28	1,2,4,17
PG 1210+464B	dM2	1210+464	DA2	< 0.5	...	139.3	< 70	5.46	1,2,3,4
PG 1539+530B	dM2	1539+530	DA2	2.7	68.1	173.0	467	5.84	1
PG 1643+143B	dM2	1643+143	DA2	< 0.5	...	150.0	< 75	6.09	1,3
PG 1659+303B	dM2	1659+303	DA4	154.8	326.5	53.5	8275	6.89	1
G130-6	dM3	2341+322	DA3	174.7	9.8	17.6	3075	5.81	1,6
G163-51	dM3	1105–048	DA3	279.1	159.2	25.8	7201	5.87	1,6
GD 51B	dM3	0347–137	DA2	< 0.5	...	83.6	< 42	6.70	1,3
LB 261B	dM3	1240–754	DA3	6.1	127.2	81.7	498	6.39	1,2
LTT 0329B	dM3	0034–211	DA3	< 0.5	...	63.4	< 32	6.63	1,3,15
PG 1015+076B	dM3	1015+076	DA2	47.8	36.9	179.5	8580	6.48	1
PG 1123+189B	dM3	1123+189	DA1	1.3	336.1	114.8	149	6.76	1,2,4
PG 1449+168B	dM3	1449+168	DA2	78.3	55.1	101.4	7939	5.94	1
PG 1608+118B	dM3	1608+118	DA2	3.0	291.1	89.9	270	6.50	1,2
PG 2131+066B	dM3	2131+066	DO1	0.3	21.0	398.1	119	6.48	1,3,4,35
RE 1629+780B	dM3	1631+781	DA1	< 0.5	...	57.3	< 29	6.39	1,3,34
Ton 1150B	dM3	1001+103	DA2	< 0.5	...	117.5	< 59	6.42	1,3,4
Ton S 392B	dM3	0357–233	DA1	1.2	3.5	278.0	334	7.23	1

Table 3—Continued

Companion	SpT	Primary	SpT	$a_s^1$ (")	PA (°)	$d$ (pc)	$a$ (AU)	$M_{abs}^2$ (mag)	References
G148-6	dM3.5	1143+321	DA3	10.4	272.2	31.6	329	6.64	1,7
GD 319C	dM3.5	1247+553	sdB	125.8	101.7	436.5	54914	6.39	1
KPD 2154+408B	dM3.5	2154+408	DA2	close	...	92.5	< 0.1	7.35	1,3
LDS 678B	dM3.5	1917-077	DBQA5	27.3	306.7	11.2	306	7.16	1,7
LDS 826B	dM3.5	2351-335	DA5	6.6	358.8	20.0	132	7.10	1,18
PG 0824+288C	dM3.5	0824+288	DA1	3.3	121	119.1	393	7.03	1,36
PG 0933+025B	dM3.5	0933+025	DA2	< 0.5	...	133.7	< 67	6.87	1,3,4
PG 2244+031B	dM3.5	2244+031	DA1	2.4	58.0	407.4	978	7.03	1
GD 74B	dM4	0625+415	DA3	99.9	248.9	83.2	8309	8.19	1
GD 84B <sup>†</sup>	dM4	0714+458	DQ6	73.7	264.9	33.1	2440	7.95	1
GD 245B	dM4	2256+249	DA2	close	...	51.3	< 0.1	7.38	1,2,3,30
LP 618-014B	dM4	1333+005	DA?6	< 1	...	86.3	< 86	8.87	1
PG 1049+103B	dM4	1049+103	DA2	< 0.5	...	109.1	< 55	7.32	1,2,4
PG 1204+450C	dM4	1204+450	DA2	83.4	279.5	92.9	7748	8.22	1
PHL 790B	dM4	0017+061	DA2	2.0	89.3	133.0	266	7.43	1,2,3
GD 13B	dM4.5	0126+422	DA2	4.7	216.7	82.4	387	8.63	1,2
GD 123B	dM4.5	1033+464	DA2	< 0.5	...	84.7	< 42	7.15	1,2,3
GD 267B	dM4.5	1257+047	DA2	8.9	52.5	75.5	672	7.78	1
GD 337B	dM4.5	1433+538	DA2	< 0.5	...	150.7	< 75	8.10	1,2,3,15
LHS 353	dM4.5	1327-083	DA4	503.3	198.9	18.0	9064	7.47	1,7
LP 916-26	dM4.5	1542-275	DB4	53.6	326.6	52.2	2800	6.32	1,18
LTT 3943B	dM4.5	1042-690	DA2	close	...	36.5	< 0.1	7.75	1,2,8
PG 0308+096B	dM4.5	0308+096	DA2	close	...	100.9	< 0.1	7.96	1,2,3,16

Table 3—Continued

Companion	SpT	Primary	SpT	$a_s^1$ (")	PA (°)	$d$ (pc)	$a$ (AU)	$M_{abs}^2$ (mag)	References
PG 0956+045B	dM4.5	0956+045	DA3	2.0	32.6	112.7	225	8.66	1,2,4
PG 1026+002B	dM4.5	1026+002	DA3	close	...	38.2	< 0.1	8.05	1,2,3,16
PG 1654+160B	dM4.5	1654+160	DB2	3.5	131.0	166.0	581	6.04	1,2
RE 1016–053B	dM4.5	1013–050	DAO1	close	...	108.1	< 0.1	7.86	1,10,33
GD 60B	dM5	0416+334	DA3	68.2	132.8	60.8	4147	8.34	1
GD 543B	dM5	2009+622	DA2	close	...	134.3	< 0.1	8.05	1,2,6,14
LHS 362	dM5	1345+238	DC9	198.5	51.9	12.1	2394	8.77	1,37
LTT 2980B	dM6	0752–146	DA3	close	...	35.0	< 0.1	9.24	1,2,3,9
GD 448B	dM7	0710+741	DA3	close	...	92.0	< 0.1	9.65	1,2,21
Rubin 80B	dM7	0354+463	DA6	< 0.5	...	41.1	< 21	9.76	1,3,11
LDS 826C	dM8	2351–335	DA5	102.7	93.9	20.0	2054	10.37	1,38
LTT 8747B	dM8	2151–015	DA6	< 0.5	...	19.6	< 10	9.99	1,3,11
PG 1241–010C	dM9	1241–010	DA2	3.2	252.7	88.7	284	9.70	1,2
GD 165B	dL4	1422+095	DA4	3.7	191.5	31.5	117	11.66	2,39,40
GD 1400B <sup>‡</sup>	dL6	0145–221	DA4	< 0.3	...	39.3	< 12	12.13	41

<sup>1</sup> $a_s$  is the separation on the sky, where a designation of “close” indicates a known radial velocity variable.

<sup>2</sup>The absolute magnitude,  $M_{abs}$ , is  $M_V$  for white dwarf companions and  $M_K$  for low mass stellar or substellar companions. These are generally not measured quantities, but are based upon the photometric distance for the white dwarf primary. In a few cases, there exists a trigonometric parallax.

<sup>†</sup>Candidate companion.

<sup>‡</sup>Discovered independently of the full survey.

References. — (1) This work; Farihi 2004b; (2) Zuckerman & Becklin 1992; (3) Schultz et al. 1996; (4) Green et al. 1986; (5) Saffer et al. 1998; (6) Greenstein 1984; (7) Eggen & Greenstein 1965; (8) Marsh et al. 1995; (9) Maxted et al. 2000; (10) Vennes et al. 1999; (11) Greenstein 1986a; (12) Maxted et al. 2002b; (13) Maxted & Marsh 1999; (14) Marsh 2000; (15) Probst 1983; (16) Saffer et al. 1993; (17) Greenstein 1986b; (18) Oswalt et al. 1988; (19) Maxted et al. 2002a; (20) Bergeron & Liebert 2002; (21) Maxted et al. 1998; (22) Finley & Koester 1997; (23) Liebert et al. 1993; (24) Schmidt et al. 1998; (25) McCook & Sion 1999; (26) Zuckerman et al. 1997; (27) Farihi 2004a; (28) Alexander & Lourens 1969; (29) Heber et al. 1993; (30) Schmidt & Smith 1995; (31) McAlister et al. 1996; (32) Maxted et al. 2000c; (33) Tweedy et al. 1993; (34) Cooke et al. 1992; (35) Reed et al. 2000; (36) Green & Margon 1994; (37) Dahn & Harrington 1976; (38) Scholz et al. 2004; (39) Becklin & Zuckerman 1988; (40) Kirkpatrick et al. 1999b; (41) Farihi & Christopher 2004

Table 4. Measured Proper Motions

Star	$\mu_\alpha$ (yr <sup>-1</sup> )	$\mu_\delta$ (yr <sup>-1</sup> )	Reference
G21-15AB	-0.25''	-0.28''	1
G21-15C	-0.27''	-0.28''	1
GD 60A	+0.08''	-0.17''	1
GD 60B	+0.08''	-0.17''	1
GD 74A	-0.01''	-0.11''	1
GD 74B	-0.01''	-0.08''	1
GD 84A	-0.11''	-0.16''	1
GD 84B <sup>†</sup>	-0.06''	-0.21''	1
GD 267A	-0.08''	-0.10''	1
GD 267B	-0.07''	-0.10''	1
GD 319AB	-0.07''	-0.01''	1
GD 319C	-0.06''	-0.01''	1
GD 322A	+0.03''	+0.07''	1
GD 322B	+0.04''	+0.07''	1
GD 392A	+0.12''	+0.13''	1
GD 392B	+0.12''	+0.12''	1
GD 559A	-0.13''	-0.01''	2
GD 559B	-0.13''	-0.01''	2
GD 683A	+0.00''	-0.06''	3
GD 683B <sup>†</sup>	+0.00''	-0.06''	3
LDS 826AB	-0.32''	-0.33''	5
LDS 826C	-0.32''	-0.35''	1
PG 0901+140A	-0.11''	-0.01''	1
PG 0901+140B	-0.11''	-0.01''	1

Table 4—Continued

Star	$\mu_\alpha$ (yr <sup>-1</sup> )	$\mu_\delta$ (yr <sup>-1</sup> )	Reference
PG 0922+162A	−0.05''	−0.02''	1
PG 0922+162B	−0.05''	−0.02''	1
PG 0933+729A	−0.06''	−0.04''	1
PG 0933+729B <sup>†</sup>	−0.06''	−0.05''	1
PG 1015+076A	−0.00''	−0.03''	3
PG 1015+076B	−0.02''	−0.03''	2
PG 1017+125A	−0.03''	−0.02''	1
PG 1017+125B	−0.03''	−0.02''	1
PG 1204+450AB	−0.06''	−0.01''	1
PG 1204+450C	−0.06''	−0.02''	1
PG 1449+168A	+0.00''	+0.06''	1
PG 1449+168B	+0.01''	+0.06''	1
PG 1659+303A	+0.02''	−0.07''	1
PG 1659+303B	+0.02''	−0.07''	1
PG 1619+123	+0.07''	−0.08''	1
HD 147528	+0.07''	−0.07''	4

Note. — Uncertainties are generally  $\sim 0.01''$  yr<sup>-1</sup> (§4.3).

<sup>†</sup>Candidate companion.

References. — (1) This work; Farihi 2004b; (2) USNO B1.0 Catalog (Monet et al. 2003); (3) UCAC Catalogs (Zacharias et al. 2000, 2004); (4) Tycho 2 Catalog (Høg et al. 2000); (5) Reylé et al. 2002.



Table 5. Optical & Near-infrared Photometry of Resolved Pairs

Star	<i>B</i>	<i>V</i>	<i>R</i>	<i>I</i>	<i>J</i>	<i>H</i>	<i>K</i>	Reference
G21-15AB	14.03	13.92	13.94	13.96	14.10	14.16	14.16	1,5
G21-15C	20.05	19.00	18.44	17.82	17.53	17.05	16.88	1
G130-5	13.06	12.92	...	...	13.17	13.20	13.18	2,4
G130-6	13.25	11.69	10.59	9.21	7.86	7.25	7.04	2,3
G148-7	13.69	13.64	...	...	14.01	13.98	14.03	2,4
G148-6	15.72	14.09	...	...	9.96	9.39	9.14	2,3
G163-50	13.10	13.06	13.15	13.15	13.41	13.45	13.54	2,6
G163-51	14.10	12.58	11.50	10.14	8.80	8.14	7.93	2,6
GD 13A	14.83	14.94	15.06	15.18	15.42	15.47	15.61	1
GD 13B	20.15	18.75	17.61	15.49	13.99	13.41	13.21	1
GD 60A	15.19	15.16	15.28	15.43	15.46	15.54	15.59	1
GD 60B	19.54	18.05	16.85	14.67	12.91	12.50	12.15	1
GD 74A	14.96	14.93	15.09	15.20	15.53	15.60	15.72	1
GD 74B	19.21	17.74	16.70	14.95	13.57	13.03	12.79	1,2
GD 84A	15.27	15.19	15.12	15.12	15.10	15.04	14.89	1,4
GD 84B	16.96	15.53	14.46	12.79	11.48	10.87	10.55	1
GD 267A	14.76	14.93	15.08	15.17	15.54	15.63	...	1,2
GD 267B	19.13	17.76	16.62	14.51	13.04	12.45	12.17	1,2
GD 319AB	...	12.70	...	...	13.36	13.36	13.50	1,7
GD 319C	20.77	19.36	18.38	16.61	15.38	14.84	14.59	1
GD 322A	15.22	15.02	14.97	15.31	15.67	15.66	15.79	1
GD 322B	18.25	17.68	17.25	17.16	17.04	16.83	16.83	1
GD 392A	15.75	15.68	15.62	15.66	15.75	15.80	15.87	1,8
GD 392B	20.82	19.50	18.80	18.06	17.73	18.16	18.51	1,8

Table 5—Continued

Star	<i>B</i>	<i>V</i>	<i>R</i>	<i>I</i>	<i>J</i>	<i>H</i>	<i>K</i>	Reference
GD 559A	...	14.63	...	...	15.14	...	15.32	1,4
GD 559B	...	17.20	...	...	16.98	...	16.88	1,4
GD 683A	14.54	14.72	14.84	15.11	15.42	...	...	1,2,9
GD 683B	16.88	15.49	14.58	13.29	12.09	11.48	11.28	1,2
LB 261A	...	...	...	...	15.66	...	15.82	1
LB 261B	...	...	...	...	11.83	11.24	10.95	2
LDS 678A	12.36	12.32	12.28	12.24	12.35	12.36	12.42	2,3
LDS 678B	13.76	12.13	11.09	9.82	8.22	7.66	7.41	2,3,10
LDS 826A	...	14.42	14.34	14.22	...	...	...	1,3
LDS 826B	...	13.54	12.25	10.78	9.48	8.91	8.61	1,2,3
LDS 826C	...	...	18.41	15.89	13.05	12.37	11.88	1,2
LHS 354	12.40	12.33	12.38	12.38	12.62	12.68	12.74	2,3
LHS 353	15.89	14.23	12.91	11.21	9.60	9.05	8.75	2,3
LHS 361	16.75	15.65	15.08	14.53	13.92	13.67	13.62	2,3
LHS 362	17.29	15.33	13.84	11.90	10.08	9.51	9.18	2,3
LP 761-114	18.38	17.83	17.56	17.10	16.66	16.42	16.49	1
LP 761-113	14.84	13.57	12.59	11.29	10.18	9.62	9.37	1,2
LP 916-27	15.53	15.49	15.40	15.37	15.28	15.32	15.41	1,2
LP 916-26	16.77	15.33	14.17	12.26	10.79	10.20	9.91	1,2
PG 0824+288AB	...	14.22	...	...	12.74	...	11.84	1,4
PG 0824+288C	...	...	...	...	13.24	...	12.41	1
PG 0901+140A	16.27	15.93	15.87	15.85	15.87	15.82	15.80	1
PG 0901+140B	16.86	16.48	16.33	16.24	16.13	15.98	15.96	1

Table 5—Continued

Star	<i>B</i>	<i>V</i>	<i>R</i>	<i>I</i>	<i>J</i>	<i>H</i>	<i>K</i>	Reference
PG 0922+162A	...	16.26	...	...	16.82	16.94	17.07	1,11
PG 0922+162B	...	17.30	...	...	17.72	17.78	17.87	1,11
PG 0933+729A	...	15.71	...	...	16.11	...	...	2,4
PG 0933+729B <sup>†</sup>	...	...	...	...	12.22	11.61	11.38	2
PG 0956+045A	15.86	15.88	16.02	16.10	16.39	16.42	16.46	1
PG 0956+045B	...	19.42	18.50	16.26	14.74	14.18	13.92	1
PG 1015+076A	16.45	16.60	16.69	16.84	...	...	...	1
PG 1015+076B	18.50	17.30	16.26	14.73	13.60	12.96	12.75	1,2
PG 1017+125A	15.73	15.74	15.78	15.99	16.34	16.41	16.52	1
PG 1017+125B	17.03	16.83	16.79	16.88	17.08	17.11	17.15	1
PG 1204+450AB	14.85	15.04	15.14	15.34	15.70	15.85	16.03	1
PG 1204+450C	19.40	18.22	17.11	15.30	13.91	13.30	13.06	1,2
PG 1241–010AB	13.86	14.00	...	14.26	14.51	14.60	14.58	1,4
PG 1241–010C	...	...	...	18.56	15.60	14.92	14.44	1
PG 1449+168A	15.34	15.44	15.54	15.66	16.01	...	...	1,2
PG 1449+168B	16.83	15.49	14.44	12.94	11.77	11.25	10.97	1,2
PG 1539+530A	16.40	16.52	16.67	16.82	...	...	...	1
PG 1539+530B	17.54	16.25	15.25	13.98	12.03	12.21	12.90	1,2
PG 1619+123	14.67	14.66	14.74	14.82	15.00	14.99	15.01	1,2
HD 1457218	8.71	8.19	...	...	7.56	6.89	6.84	2,12
PG 1659+303A	15.07	14.99	15.06	15.12	15.33	15.32	15.36	1,2
PG 1659+303B	16.06	14.81	13.85	12.48	11.39	10.69	10.53	1,2
PG 1654+160A	16.42	16.55	16.61	16.56	...	...	...	1
PG 1654+160B	19.17	17.74	16.57	14.50	13.09	12.43	12.14	1,2

Table 5—Continued

Star	<i>B</i>	<i>V</i>	<i>R</i>	<i>I</i>	<i>J</i>	<i>H</i>	<i>K</i>	Reference
PG 1608+118A	15.25	15.29	15.38	15.50	...	...	...	1
PG 1608+118B	17.32	15.85	14.80	13.26	12.10	11.50	11.27	1,2
PG 2244+031A	16.15	16.46	16.57	16.73	17.02	17.09	17.27	1
PG 2244+031B	...	19.82	18.73	17.18	15.83	15.24	15.08	1
PHL 790A	15.09	15.32	15.37	15.54	15.93	16.06	16.21	1
PHL 790B	...	18.10	16.88	15.11	13.83	13.25	13.05	1,2
RE 1016–053AB	13.93	14.14	14.19	14.19	13.74	13.12	12.90	1,13
RE 1016–053CD	15.08	13.58	12.66	11.63	10.61	9.99	9.77	2,13

Note. — All entries are in magnitudes. Uncertainties for photometry are 5% or less with a few exceptions (§4.5).

†Candidate companion.

References. — (1) This work; Farihi 2004b; (2) 2MASS Catalog (Cutri et al. 2003); (3) ARICNS (Gliese & Jahrei 2000); (4) McCook & Sion 1999; (5) Bergeron et al. 2001.

Table 6. Optical & Near-infrared Photometry of Composite Pairs

Star	<i>B</i>	<i>V</i>	<i>R</i>	<i>I</i>	<i>J</i>	<i>H</i>	<i>K</i>	Reference
GD 51AB	15.27	14.99	14.64	13.32	12.05	11.57	11.30	1,2
WD	15.62	15.67	15.77	15.90	16.24	16.31	16.42	3,9
RD	...	...	...	13.43	12.07	11.58	11.31	
GD 123AB	14.21	14.40	14.42	13.76	12.56	12.03	11.75	1,2
WD	14.22	14.41	14.54	14.71	15.13	15.23	15.36	3,4
RD	...	...	...	14.35	12.67	12.09	11.79	
GD 245AB	13.67	13.68	13.57	12.83	11.66	11.20	10.89	1,2,3
WD	13.70	13.78	13.80	13.94	14.36	14.43	14.54	10,11
RD	...	...	...	13.31	11.75	11.26	10.93	
GD 337AB	16.04	16.11	16.13	15.61	14.67	14.22	13.92	1,2
WD	16.04	16.12	16.23	16.36	16.71	16.78	16.89	3,4
RD	...	...	...	16.37	14.85	14.33	13.99	
GD 448AB	14.91	14.97	...	...	14.71	14.43	14.16	2,3
WD	14.96	15.01	15.10	15.22	15.51	15.58	15.67	7,12
RD	...	...	...	...	15.42	14.89	14.47	
GD 543AB	15.15	15.26	15.32	15.06	14.28	13.92	13.58	1,2
WD	15.14	15.26	15.38	15.53	15.91	15.99	16.11	1,7
RD	...	...	...	16.20	14.55	14.09	13.69	
GD 984AB	13.69	13.89	13.95	13.63	12.96	12.45	12.24	1,2
WD	13.83	14.11	14.25	14.45	14.90	15.02	15.15	3,13
RD	...	...	...	14.32	13.16	12.56	12.32	
KPD 2154+408AB	15.24	15.21	14.97	14.02	12.88	12.38	12.15	1,2
WD	15.24	15.33	15.44	15.57	15.93	16.00	16.12	5,14
RD	...	...	...	14.32	12.95	12.42	12.18	
LP 618-14AB	17.68	17.23	16.74	15.64	14.26	13.74	13.51	1,2,6
WD	17.68	17.46	17.30	17.16	17.17	17.14	17.14	1
RD	...	...	...	15.89	14.34	13.79	13.55	

Table 6—Continued

Star	<i>B</i>	<i>V</i>	<i>R</i>	<i>I</i>	<i>J</i>	<i>H</i>	<i>K</i>	Reference
LTT 0329AB	14.85	14.44	13.95	12.63	11.43	10.91	10.64	1,2
WD	15.05	15.03	15.11	15.21	15.49	15.54	15.63	8,15
RD	...	...	14.41	12.74	11.46	10.93	10.65	
LTT 2980AB	13.54	13.59	13.66	13.48	12.63	12.14	11.83	1,2
WD	13.59	13.60	13.69	13.80	14.09	14.15	14.25	16
RD	...	...	...	14.96	12.94	12.33	11.96	
LTT 3943AB	13.05	13.09	...	12.39	11.24	...	10.44	3,6
WD	13.10	13.17	13.27	13.40	13.73	13.80	13.90	8,17
RD	...	...	...	12.93	11.36	...	10.49	
LTT 8747AB	14.76	14.54	14.39	13.97	12.46	11.79	11.36	1,2,6
WD	14.76	14.54	14.39	14.24	14.16	14.06	14.09	1,5
RD	...	...	...	15.61	12.71	11.93	11.45	
PG 0308+096AB	15.25	15.31	15.33	14.79	13.72	13.18	12.93	1,2
WD	15.25	15.39	15.51	15.66	16.05	16.14	16.26	1,4
RD	...	...	...	15.44	13.86	13.25	12.98	
PG 0933+025AB	16.12	15.97	15.66	14.44	13.27	12.73	12.48	1,2
WD	16.12	16.22	16.33	16.47	16.83	16.90	17.01	3,4
RD	...	...	...	14.63	13.31	12.75	12.50	
PG 0950+185AB	15.59	15.40	14.98	13.78	12.69	12.01	11.79	1,2
WD	15.59	15.81	15.94	16.11	16.54	16.64	16.77	3,4
RD	...	...	15.56	13.92	12.72	12.03	11.80	
PG 1026+002AB	13.88	13.82	13.68	12.90	11.77	11.22	10.92	1,2
WD	13.88	13.86	13.95	14.04	14.32	14.38	14.46	3,4
RD	...	...	...	13.37	11.88	11.28	10.96	
PG 1049+103AB	...	15.65	...	...	13.27	12.83	12.48	2,3
WD	15.69	15.74	15.83	15.95	16.28	16.34	16.44	3,4

Table 6—Continued

Star	<i>B</i>	<i>V</i>	<i>R</i>	<i>I</i>	<i>J</i>	<i>H</i>	<i>K</i>	Reference
RD	...	...	...	...	13.34	12.87	12.51	
PG 1123+189AB	13.83	14.11	14.09	13.58	12.78	12.23	12.00	2,18
WD	13.87	14.16	14.30	14.49	14.95	15.07	15.20	4,18
RD	...	...	...	14.20	12.94	12.31	12.06	
PG 1210+464AB	15.53	14.94	14.19	13.05	12.08	11.41	11.17	1,2
WD	15.53	15.59	15.71	15.88	16.28	16.37	16.49	3,4
RD	...	...	14.50	13.13	12.10	11.42	11.18	
PG 1643+143AB	15.76	15.45	14.90	13.79	12.77	12.10	11.96	1,2
WD	15.76	15.91	16.03	16.19	16.59	16.68	16.80	3,4
RD	...	...	15.37	13.92	12.80	12.12	11.97	
PG 2131+066AB	16.35	16.56	16.49	16.06	15.19	14.64	14.43	1
WD	16.33	16.65	16.80	17.00	17.47	17.60	17.73	19,20
RD	...	...	...	16.65	15.33	14.71	14.48	
RE 1016–052AB	13.93	14.14	14.19	14.19	13.74	13.12	12.90	1,21
WD	13.93	14.23	14.37	14.57	15.02	15.14	15.27	21
RD	...	...	...	15.51	14.14	13.30	13.03	
RE 1629+780AB	12.95	13.03	12.83	12.05	11.00	10.38	10.15	2,22
WD	12.95	13.21	13.34	13.53	13.98	14.10	14.22	23
RD	...	...	...	12.37	11.07	10.42	10.18	
Rubin 80AB	15.86	15.57	15.37	14.88	13.59	13.08	12.73	1,2
WD	15.86	15.62	15.51	15.38	15.36	15.28	15.33	1,5
RD	...	...	...	15.96	13.83	13.23	12.83	
Ton 1150AB	15.80	15.21	14.75	13.75	12.64	12.02	11.76	1,2
WD	15.84	15.91	16.02	16.14	16.48	16.55	16.66	1,4
RD	...	...	15.15	13.88	12.67	12.04	11.77	
Ton S 392AB	15.64	15.77	15.85	15.58	14.96	14.59	14.26	1,2

Table 6—Continued

Star	<i>B</i>	<i>V</i>	<i>R</i>	<i>I</i>	<i>J</i>	<i>H</i>	<i>K</i>	Reference
WD	15.64	15.93	16.07	16.26	16.72	16.84	16.96	1,24
RD	...	...	...	16.41	15.20	14.74	14.35	

Note. — All entires are in magnitudes. Uncertainties for photometry are 5% or less with a few exceptions (§4.5).

References. — (1) This work; Farihi 2004b; (2) 2MASS Catalog (Cutri et al. 2003); (3) McCook & Sion 1999; (4) Liebert et al. 2005; (5) Zuckerman et al. 2003; (6) DENIS Catalog; (7) Bergeron et al. 1992; (8) Bragaglia et al. 1995; (9) Koester et al. 2001; (10) Schwartz 1972; (11) Schmidt et al. 1995; (12) Hintzen & Jensen 1979; (13) Finley et al. 1997; (14) Downes 1986; (15) Greenstein 1974; (16) Eggen & Greenstein 1965; (17) Kawka et al. 2000; (18) Marsh et al. 1997; (19) Bond et al. 1984; (20) Kawaler et al. 1995; (21) Vennes et al. 1999; (22) Schwartz et al. 1995; (23) Napiwotzki et al. 1999; (24) Greenstein 1979.



Table 7. Survey Completeness for  $d = 57$  pc,  $\tau = 3$  Gyr

Survey	$a_{in}$ (AU)	$a_{out}$ (AU)	$m_{abs}$ (mag)	SpT	$M$ ( $M_{\odot}$ )	N
IRTF	0	700	$M_K = 12.2$	L6	0.065	84
Steward	110	4700	$M_J = 14.2$	L7	0.060	261
Keck	55	1100	$M_J = 17.2$	T9 <sup>†</sup>	0.030	86
All	0	110	$M_H = 13.5$	L8	0.058	371

Note. — This table presents only average separations and sensitivities. The actual values depend on each individual white dwarf distance and age. The “All” entry refers to detection in 2MASS of an  $H$  band excess above a white dwarf photosphere (§5.3).

<sup>†</sup>No objects are known with spectral type later than T8. However, the average limiting magnitude of the Keck survey probed  $\sim 1.5$  magnitudes deeper than that of any known brown dwarf (Vrba et al. 2004; Leggett et al. 2002).

Table 8. Median Spectral Type for Low Mass Companions

Subgroup	Description	Median SpT	N
0	All	M3.5	62
1	Resolved	M3.5	38
2	Close	M4.5	9
3	Unresolved / not close	M3.5	15
4	Groups 1 + 3	M3.5	47
5	Groups 2 + 3	M4.5	24

Table 9. High Velocity Background Star Data

Object	$a$	PA	$V$ (mag)	$V - K$ (mag)	$\mu_\alpha$ (yr $^{-1}$ )	$\mu_\delta$ (yr $^{-1}$ )	SpT
GD 248			15.1	+0.0	-0.05''	-0.11''	DC5
background star	93''	9°	19.6	+3.4	-0.06''	-0.13''	sdK/M
GD 304			15.3	-0.8	+0.06''	-0.01''	DA2
background star	104''	33°	20.5	+4.7	+0.05''	-0.01''	dM
PG 1038+633			14.8	-1.0	-0.08''	-0.04''	DA2
background star	37''	37°	18.9	+3.2	-0.08''	-0.04''	dK/M
PG 1026+002			13.8	+2.9	+0.06''	-0.08''	DA3+dM
background star	114''	21°	19.7	+3.5	+0.05''	-0.07''	sdK/M

Table 10. Candidate Binary Proper Motions

Object	$\mu_\alpha$ (yr <sup>-1</sup> )	$\mu_\delta$ (yr <sup>-1</sup> )
GD 84A	$-0.11 \pm 0.02''$	$-0.16 \pm 0.02''$
GD 84B	$-0.06 \pm 0.02''$	$-0.21 \pm 0.02''$
GD 683A	$-0.04 \pm 0.01''$	$-0.06 \pm 0.01''$
GD 683B	$-0.03 \pm 0.01''$	$-0.06 \pm 0.01''$
PG 0933+729A	$-0.06 \pm 0.01''$	$-0.04 \pm 0.01''$
PG 0933+729B	$-0.06 \pm 0.01''$	$-0.05 \pm 0.01''$

Table 11. Possible Parameters for Rubin 80AB

Object	$T_{\text{eff}}$ (K)	$\log g$	$V$	$I$	$J$	$K$	$d$ (pc)
WD	9000	8.0	15.62	15.38	15.36	15.33	41.1
RD	...	...	...	15.96	13.83	12.83	40.7
WD	8000	8.0	15.58	15.21	15.08	14.97	32.6
RD	...	...	...	16.33	13.91	12.88	41.7
WD	8000	7.6	15.58	15.21	15.08	14.97	41.7
RD	...	...	...	16.33	13.91	12.88	41.7

Note. —  $V I J K$  in magnitudes.